The *cyp21a2* mutant medaka, a novel cortisol-deficiency disease model, reveals a new role of cortisol in reproduction

(コルチゾル欠損病因モデルのメダカ *cyp21a2* 変異体を用いた生殖におけるコルチゾルの役割の解析)

CARRANZA LUNA José Alexander

Department of Biological Science, Graduate School of Science
Nagoya University

Nagoya, Japan

March, 2024

To my family for their endless love and support

ACKNOWLEDGMENTS

First of all, I would like to express my sincere gratitude to my advisor Dr. Tanaka Minoru Prof. He has happened to be not only a thesis advisor but also a great mentor during these 6 years of my graduate studies in Nagoya. Thank you for allowing me to be part of your Lab. Your continue support and guidance are the reason for the completion of this work, as part of my professional career. Thank you for helping me to grow as a scientist, for trusting me, and for encouraging me to achieve this goal. I would also like to say thank you to Dr. Fukami Maki and Dr. Hibi Masahiko for their reviews of this thesis.

A special thank you to the former members of the Tanaka Lab. Thank you for being such an amazing senpai and friend, Dr. Nishimura Toshiya. I have learned a lot from you. Likewise, thank you to my colleagues and friends MSc. Yamada Kazuki and Dr. Sakae Yuta, who have made significant contributions to my research. To all the current lab members (Kikuchi Mariko, Kameyama Shiyu, Maeno Isamu, Ogisawa Karen, Minami Yuzuki, and Williams Alexandria), thank you for your support, encouragement, and advice to my work. Thank you to Mrs. Fujisho for all of your administrative support, and for making my stay in Nagoya simpler. Thank you, Mrs. Miyoshi, for your great work at maintaining fish medakas.

Furthermore, I would like to express my gratitude to Dr. Choi Man Ho and the Dr.(c) Noh Jongsung (KIST, Korea), Dr. Shibata Yasushi (Teikyo University of Science), Dr. Ogiwara Katsueki and Dr. Kotani Tomoya (Hokkaido University), Dr. Kanda Shinji and Dr. Okubo Kataaki (The University of Tokyo). Some of them have actively collaborated with my study and others have been part of my training in techniques described in this work.

Life in Nagoya was not easy. This time has been of many ups and downs. However, the people I met in Nagoya have contributed to overcoming all kinds of challenges I have faced during these 6 years. To all my friends a special thank you.

Last, but not least, I would like to express my gratitude to the people who although thousands of kilometers away from Nagoya, they have been just a phone call away when I needed them. Thank you, my lovely and amazing family, *José, Rosario* and *Ximena*. YOU are the force that pushes me every day to be a better version of myself.

TABLE OF CONTENTS

LIST OF FIGURES

LIST OF TABLES

ABSTRACT

CYP21A2 is a key enzyme for the synthesis of cortisol, which is considered the main glucocorticoid in teleost fish. Besides its well-known role as a stress-response hormone, cortisol also plays essential roles in osmoregulation, immune response, and reproduction. However, much of what we know about the roles of cortisol, specifically in teleost fish remains at the physiological level. Therefore, in Chapter 1, I present a molecular characterization of the steroidogenic enzyme CYP21A2 in medaka, in which a single copy of the *cyp21a2* gene was retained on chromosome 16 during evolution. A frameshift mutation (by CRISPR/Cas9) resulting in a truncated protein that lacks about 97% of its single domain, compromised the survivability of medaka after hatching. Only 10% of the homozygous mutants reached adulthood. A mass spectrometry analysis confirmed cortisol deficiency as well as a complex hormonal imbalance in 13 dph mutant larvae. In addition, *cyp21a2* mutant medakas showed upregulation of the adrenocorticotropic hormone or ATCH (encoded on the mRNA called *pomca*) and interrenal gland (mammalian adrenal gland-equivalent in teleosts) hyperplasia, typical phenotypes of the human Congenital Adrenal Hyperplasia (CAH) condition. Importantly, cortisol administration successfully rescued these phenotypes. Finally, I show that two populations of *pomca*-expressing cells (on located at the *rostral pars distalis*: RPD and the other at the *pars intermedia*: PI) identified in the pituitary of medaka, have different responsiveness to cortisol levels. Cells from the RPD are the main cells involved in the quick response mechanism (upregulation of ACTH and increase in cell number) to changes in cortisol levels.

In Chapter 2, I outline that the lack of CYP21A2 does not result in sex reversal phenotypes in contrast to the virilization phenotype observed in women with 21-

hydroxylase deficiency (21OHD). Nonetheless, mutant females were infertile and never spawned eggs. Notably, males were fertile. On the other hand, although medaka germ cells express *cyp21a2*, a cell transplantation experiment revealed that systemic cortisol is critical for oogenesis. In this regard, systemic cortisol deficiency leads to changes in gonadotropin secretion dynamics, a polycystic ovary syndrome (PCOS)-like phenotype –a simultaneous development of multiple follicles-, aberrant expression of maturation and ovulation-related genes, morphological defects in granulose cells, and failure in ovulation. Moreover, high levels of androgens and maturation inducing hormone was also observed in homozygous mutant follicles. However, significantly, here I show that mutant follicles likely fail to establish a proper meiotic arrest, due to the parthenogenetic activation observed in vitro and in vivo.

In Chapter 3, I present preliminary observations about the action of cortisol in oogenesis. Unlike in Nile tilapia and rainbow trout, an in vitro maturation of medaka oocytes showed that maturation could be completed in the absence of cortisol, however, further studies are needed to confirm any role for cortisol in oocyte hydration and ovulation in medaka. Nevertheless, the expression analysis of MR and GR receptors in early vitellogenic oocytes and RNAseq data of immature oocytes raises the possibility that cortisol may act on early oocytes, perhaps as a competence factor for a successful maturation.

PUBLISHED WORK STATEMENT

Chapter 1 is a copyedited of a manuscript accepted for publication in *Zoological Science* on December of 2023: José Carranza, Kazuki Yamada, Yuta Sakae, Jongsung Noh, Man Ho Choi, and Minoru Tanaka (2024) Genetic disruption of *cyp21a2* leads to systemic glucocorticoid deficiency and tissues hyperplasia in the teleost fish medaka (*Oryzias latipes*). *Zoological Science* (*in press*).

Data related to secondary sex characteristics, fertility, and gonadal morphology of the *cyp21a2* described in Chapter 2 are also part of the manuscript accepted for publication in *Zoological Science* described lines above. All remaining data in Chapters 2 and 3 are part of a manuscript under preparation.

CHAPTER 1. The *cyp21a2* mutant medaka as a novel cortisol-deficiency disease model

Collaborative work statement

This chapter describes a collaborative effort of José Carranza, Yuta Sakae, Kazuki Yamada, Jongsung Noh, and Man Ho Choi, under the supervision of Dr. Minoru Tanaka. Yuta Sakae prepared the protocol for mutagenesis. Kazuki Yamada established the *cyp21a2+9* mutant line and performed the WISH of *cyp17a1* and *cyp17a2* in gonads. Jongsung Noh and Man Ho Choi performed the mass spectrometry analysis. All other experiments were conducted by José Carranza.

1.1 Introduction

Congenital adrenal hyperplasia (CAH) is an autosomal recessive disorder, resulting in adrenal insufficiency. This leads to an increased level of adrenocorticotropic hormone (ACTH) in the pituitary gland, which occurs due to a failure in the negative feedback on the hypothalamus-pituitary-adrenal axis. A high level of ACHT then drives multiple complex hormonal imbalances, and eventually adrenal hyperplasia (White and Speiser, 2000; Speiser et al., 2018; Merke and Auchus, 2020; Auer et al., 2023). Mutations in several steroidogenic enzymes could leads to CAH, nevertheless mutations in the *p450 21-hydroxylase* (*cyp21a2*) gene resulting in 21-hydroxylase deficiency (21OHD) is known to be the genetic cause with the highest prevalence (Miller, 2018; Speiser et al., 2018; Auer et al., 2023).

CYP21A2 has a single P450 domain with a 21-hydroxylase activity. It mediates the synthesis of 11-deoxycorticosterone and 11-deoxycortisol which are metabolic precursors

of aldosterone and cortisol, respectively (Zhao et al., 2012). The latter, cortisol, is an important glucocorticoid since it regulates a wide range of vital processes in all vertebrates. Loss-of-function mutations in the human *cyp21a2* gene diminish cortisol production, leading to severe systemic consequences, in some cases even being life-threatening (Simonetti et al., 2018; Speiser et al., 2018; Merke and Auchus, 2020; Auer et al., 2023).

In teleosts like medaka cortisol is the major glucocorticoid being mainly produced in the interrenal gland (evolutionally equivalent to the mammalian adrenal gland) (Murata et al, 2020), and is regulated by the hypothalamus-pituitary-interrenal (HPI) axis (Takahashi et al., 2016). The scope of the cortisol activity includes osmoregulation by adaptation to water salinity and early ionocyte development (McCormick, 2001; Trayer et al., 2013), in response to stress due to fluctuations in environmental factors such as temperature, salinity, and likely light (Sakamoto et al., 2001; Adolfi et al., 2019; Hayasaka et al., 2019), and also in growth and reproduction (Mommsen et al., 1999; Faught and Vijayan, 2018). However, understanding of these phenomena still remains at physiological levels.

Here, the c*yp21a2* gene was genetically disrupted with the CRISPR/Cas9 system to generate a cortisol-deficient medaka model and to determine the roles of medaka cortisol. Homozygous mutant medakas recapitulates several aspects of the human 21OHD condition such as such as interrenal insufficiency with a compromised cortisol biosynthesis, upregulation of ACTH, complex steroid hormones imbalances, and interrenal gland hyperplasia. It is anticipated, therefore, that the *cyp21a2* mutant medaka presented here is a valuable disease model for understanding the clinical symptoms of the CAH. Besides, it will be a useful resource to study the systemic complications of

glucocorticoid deficiency and steroid hormones as well as to depict the steroidogenic metabolic pathway in non-mammalian vertebrates.

1.2 Materials and methods

1.2.1 Ethics statement

All animal experiments were conducted by following the Nagoya University guidelines on the Animal Care and Use committee (S230007-001).

1.2.2 Fish strain and maintenance

The medaka (*Oryzias latipes*) Cab strain was used in all experiments. Medakas were raised at 29ºC during the embryonic stage. After hatching, larvae were raised in freshwater at 25 ± 0.5ºC under a 14 h light and 10 h dark photoperiod.

1.2.3 Synteny, sequence-conservation and relative expression of *cyp21a2*

The human CYP21A2 protein (ENSP00000415043, Ensembl) (Table 1.1) was used as a reference sequence to search for vertebrates *cyp21a2* orthologs and paralogs by the BLAST tool on Ensembl genomic assemblies for human (*H. sapiens,* GRCh38.p14), mouse (*M. musculus,* GRCm39), tropical clawed frog (*X. tropicalis*, UCB_Xtro_10.0), coelacanth (*L. chalumnae,* LatCha1), medaka (*O. latipes,* ASM223467v1), stickleback (*G. aculeatus,* Broad S1), nile tilapia (*O. niloticus,* O_niloticus_UMD_NMBU), and fugu (*T. rubripes,* fTakRub1.2). Besides, the identified medaka CYP21A2 protein (ENSORLP00000008663) on chromosome 16 was subsequently BLASTED against the medaka whole-genome to search for any duplicated copy.

Next, the degree of sequence conservation or homology at the amino acid level of CYP21A2 proteins among vertebrates was evaluated with the software GENETYX v.14. All protein sequences except for fugu (*cyp21a12* is currently annotated as a pseudogene on Ensemble release 110) were retrieved from Ensembl. The gene and protein IDs of all sequences used in the analysis are described in Table 1.1. The percentages of sequence similarity are reported on Table 1.2.

For *cyp21a2* relative expression in multiple tissues, total RNA was purified with TriPure Isolation Reagent (ROCHE, 11667165001) from a total of six tissues of a 5.5 months old wild-type medaka. Dissected tissues were flash-frozen in liquid nitrogen before the RNA was extracted. Complementary DNA (cDNA) was synthesized from 400 ng/mL of total RNA with ReverTra Ace (TOYOBO, FSQ-301) and used as a template for RT-qPCR with the KOD SYBR qPCR Mix (TOYOBO, QKD-201). The expression was normalized with *β*-actin and the liver biological replicate 1 was used as standard control. The relative expression was analyzed by the 2^-ΔΔCt method. Primers set are listed in Table 1.5.

1.2.4 Generation of loss-of-function *cyp21a2* mutant by CRISPR/Cas9

A CRISPR gRNA target site was selected with the online target predictor tool CCTop (https://cctop.cos.uni-heidelberg.de) (Stemmer et al., 2015) by targeting the first exon after the third methionine of the *cyp21a2* gene (Fig. 1.4A).

The DNA template was prepared as previously reported (Liang et al., 2015). Briefly, two oligonucleotides that recreate the target sequence, a T7 promoter-tag forward (cyp21a2-gRNA-F2) and a reverse that contains 15 bases of the 80 bp cr/tracr constant region (cyp21a2-gRNA-R2) were designed. These oligos were mixed in a PCR reaction at a concentration of 3μM together with the 80bp cr/tracr oligos (0.3μM) and the T7-

forward and tracr-reverse universal primers (0.3μM). PCR products were then used as template for IVT with MEGAscript T7 (Invitrogen, AM1333). The gRNA and *Cas9* mRNA were synthesized with the MEGAscript T7 (Invitrogen, AM1333) and the mMESSAGE mMACHINE SP6 (Invitrogen, AM1340) IVT kits, respectively.

Purified gRNA and *Cas9* mRNA were co-microinjected into 1-cell stage wild-type medaka embryos with a micromanipulator FemtoJet (Eppendorf, 5247). F0 founders were crossed with wild-type medakas and the mutant allele $cyp21a2^{+9}$ was identified and isolated during F1 screening by sequence analysis with the cyp21a2-qPCR-F/R primer sets (Table 1.5).

1.2.5 Genotyping

Genomic DNA was purified from the caudal fin (fin-clip) by freezing at -80ºC and heating at 96ºC for 5 and 10min, respectively. The gDNA was then diluted and used for real-time PCR (qPCR) with primers set specific to the male sex-determining gene *dmy* and the autosomic gene *cyp19a1* (control) combined with TaqMan probes (TaqMan MGB probes, Applied Biosystems, 4324034) targeting the *dmy* (FAM) and *cyp19a1* (VIC) genes. The qPCR was performed with a TaqMan Fast Advanced Master Mix on a StepOnePlus real-time PCR (Thermo Fisher Scientific, 4444557) with 40 cycles of 95ºC for 3 s > 60ºC for 20 s.

Mutant allele genotyping was performed by designing primers specific to the wild-type (cyp21a2-WT_check-F) and the mutant (cyp21a2-+9_check-F) alleles combined with a single reverse primer cyp21a2-+9_check-R (Table 1.5). The genomic location of the primers as well as examples of PCR amplification plots are shown in Fig. A.1. All real-time PCRs were conducted with the KOD SYBR qPCR Mix (TOYOBO, QKD-201) on a StepOnePlus (Applied Biosystems) with initial denaturation at 95ºC for 10 m,

followed by 40 cycles of 95ºC for 15 s > 60ºC for 20 m, and a final melting curve step at 95ºC for 15 s > 60ºC for 1 m > 95ºC for 15 s.

1.2.6 Whole-mount (WISH) and fluorescent in situ hybridization (FISH)

For whole-mount in situ hybridization (WISH) probes, cDNAs of *cyp21a2* (ENSORLG00000006896), *cyp17a1* (ENSORLG00000019226), *cyp17a2* (ENSORLG00000002242), and *pomca* (ENSORLG00000025908) genes were PCR-amplified from wild-type gonad or pituitary cDNA libraries followed by gel purification. Primers are listed in Table 1.5. Purified PCR products were used as templates to prepare DIG-labeled antisense RNA probes synthesized in vitro with the DIG RNA labeling mix (ROCHE, 11277073910) and the T7 RNA polymerase (ROCHE, 10881775001).

A medaka embryos-pre-absorbed anti-DIG-AP Fab fragments (ROCHE, 11093274910) primary antibody was used to detect hybridized probes. Briefly, medaka embryos around 3 dpf: days post-fertilization were fixed in 4% PFA for 4 h at room temperature, rinsed 3 times in 1xPTW, and then preserved in 100% MeOH until use. Fixed embryos were then rinsed in 1xPTW, smashed, and incubated in a solution of 1 mL 1xPTW and 10µL of anti-DIG-AP at 4°C overnight gently on shaker. The next day, the pre-absorbed antibody was recovered by centrifugation at 15 000 rpm (5 min at 4 °C) and filtration with a 0.22 µm Millex-GP filter unit (Merck, SLGPR 33RS), for a total of four times. Finally, a stock solution of 20 mL was prepared by adding 15 mL of 1xPTW, 1 mL of Normal Sheep Serum (Sigma Aldrich, S2263), and 200µL of 3%NaN3. The final concentration of the pre-absorbed anti-DIG-AP was 1:20 000. The NBT/BCIP Stock Solution (ROCHE, 11681451001) was used to develop the signal for about 3 h at room temperature.

After the WISH signal developed, samples were refixed in 4% PFA for at least 20 min before a serial dehydration steps with ethanol. The Technovit kit 8100 (Heraus Kulzer, 64709012) was used for making resin-based sectioning blocks from gonadal samples, which were sectioned to a 4 μm thickness.

The TSA Biotin System (Perkin Elmer, NEL700A001KT) was used for *pomca*-FISH experiment. DIG-labeled RNA probe was detected with an anti-DIG-POD Fab fragments (1:100, ROCHE-1426346) primary antibody. Signal was then amplified with tyramide-biotin (TSA Biotin Kit) and streptavidin-Alexa Fluor 488 conjugated (1:100, Invitrogen-S11223). Nuclei were stained with DAPI (1:200, Thermo Fischer Scientific-D1306).

1.2.7 WISH and FISH images quantification

Pituitary and interrenal WISH images in Fig. 1.8, 1.11B were all captured with an Olympus DP74 and the total area of the positive signals were measured and quantified in terms of pixels with Fiji software.

FISH images of *pomca* were captured with a scanning confocal microscope (Olympus, FLUOVIEW FV1000) at 1μm of step size. To measure and quantify the *pomca* area in Fig. 1.11A, all focal planes of confocal images were Z-stacked with the FLUOVIEW FV1000 software. Areas were measured in terms of pixels and analyzed with Fiji. Finally, the maximum area of the pituitaries in Fig. 1.12 were measured from the middle focal plane of confocal images. Areas were measured in terms of pixels and analyzed with Fiji software.

Finally, the expression of *pomca* in both the RPD and the PI cell populations was measured, and the values were expressed in terms of mean intensity which was calculated by dividing the sum of the intensity units in a selected area (RawIntDen) by the total number of pixels (area) with Fiji software.

1.2.8 Mutant rescue by cortisol

Exogenous cortisol (Hydrocortisone-powder, TCI H0533) was used to rescue the phenotypes in *cyp21a2* homozygous mutants. For this purpose, 60 embryos per replicate (*n = 2*)/treatments were collected from heterozygous females (XX) and homozygous males (XY) parents, expecting a genotype ratio of 1:1 with heterozygous mutants set as the control group (Fig. 1.10A, Table 1.3).

Embryos were first raised for 2 days in a methylene blue-containing water (MBW) and then moved into a 30 mL 1xERM medium-containing dish (1×ERM; 1 g/L NaCl, 30 mg/L KCl, 40 mg/L $CaCl_2$ • $2H_2O$ and 160 mg/L $MgSO_4$ • $7H_2O$). A cortisol stock solution (5nM) was prepared in 100% ethanol and applied to 2 dpf embryos for 5 days at a final concentration of 5µM. Ethanol at 1% final concentration (cortisol stock solution v/v) was administrated to the control treatment cortisol (-). The rearing medium as well as the survival and hatching rates, were daily exchanged and/or recorded.

Newly hatched larvae were sex and mutant genotyped, fixed in 4% PFA and the expression of *pomca* as well as *cyp17a2* in the pituitary and the interrenal gland, respectively, was analyzed by in situ hybridization (Fig. 1.10A, Table 1.4).

1.2.9 Steroid hormones measurement

Medaka larvae heterozygous (control) and homozygous mutants at 13 dph: days post-hatching (whole-body) were used for the analysis. Larvae were genotyped and grouped into pools of 5 and 3 individuals per biological replicate (*n = 3*), flash-frozen in liquid nitrogen, and left drying overnight in a freeze-drying unit (UT-1000 EYELA+GCD-051X ULVAC). Next, steroid hormones were extracted and quantitatively analyzed by a liquid chromatography-mass spectrometer (LC-MS/MS) as previously reported (Lee et al, 2020; Han et al., 2020).

Briefly, each sample was spiked with 20 μL of an internal standard mixture (cortisol-d_4, 17α-hydroxyprogesterone-d_8, and pregnenolone-d_4: 0.2 μg/mL; progesterone-d_9, 17α-hydroxypregnenolone-d_3, 3-methoxytyramine-d_4, and epinephrine-d_6: 0.1 μg/mL; testosterone-d_3: 0.02 μg/mL; DHEA-d_6: 0.5 μg/mL; testosterone sulfate-d_3: 1 μg/mL) and pulverized with 1 mL methanol using a TissueLyser (Qiagen, Hilden, Germany) at 25 Hz for 10 min with three zirconia beads (3.0 mm I.D., Toray Industries, Tokyo, Japan). The sample was centrifuged at 11 000 g for 10 min twice and the supernatant was evaporated under nitrogen stream at 40°C. The dried sample was then reconstituted with phosphate buffer (2.0 mL, pH 7.2), and loaded onto an Oasis cartridge (60 mg, 3 mL). After washing twice with 10% methanol (0.7 mL), steroids were eluted with methanol (1 mL, twice) and evaporated under nitrogen stream at 40°C. The dried sample was reconstituted with 50 μL of methanol and centrifuged on an ultrafree-MC centrifugal filter for 5 min at 15 000 g. Thereafter, 50 μL of 10% (*v/v*) dimethyl sulfoxide was added to the ultrafree-MC centrifugal filter and centrifuged for 5 min at 15 000 g. Finally, 5 μL of aliquot was injected into the LC-MS system.

1.2.10 Statistical analysis

The statistical software OriginPro 2022 (OriginLab, Northampton, USA) was used to analyze and plot all graphs in this study. The Student's *t*-test was applied for means comparison between two samples. In the case of means comparison of more than two samples, the one-way ANOVA followed by the Tukey *post-hoc* test was applied instead.

1.3 Results

1.3.1 Sequence homology, conservation, and expression of *cyp21a2*

The single active copy of the human *CYP21A2* gene on chromosome 6 (ENSP00000415043) was used as a reference to search for orthologs among vertebrates by the BLAST tool on Ensembl. As a result, the synteny confirmed the presence of a single copy in all of the organisms used in the analysis.

In the particular case of medaka, an ortholog to the human *CYP21A2* was identified on chromosome 16 (ENSORLG00000006896) (Fig. 1.1). Since teleost underwent a whole-genome duplication during evolution, the identified medaka *cyp21a2* gene was then BLASTED against medaka genome at the nucleotide and amino acid level, however, no other copy was retrieved after the search.

The synteny analysis also allowed to identify that the *cyp21a2* locus is flanked by the well-conserved genes *complement 4b (c4b)* and *tenascin xb (tnxb)* which have a high synteny degree. These genes were duplicated during evolution on chromosome 11 in medaka. However, despite having identified several genes on chromosome 16 that have a paralog on the 11, that was not the case for the *cyp21a2* gene. Thus, it is likely that a duplicated copy of the *cyp21a2* in teleost was likely lost during evolution, and the *cyp21a2* gene on chromosome 16 is the single active copy in the medaka fish.

The identified medaka *cyp21a2* gene encodes a protein of 451aa (amino acids). It has a single P450 domain which is about 99% of the entire protein (Fig. 1.4C), and shares high sequence homology with other teleosts CYP21A2 proteins, about 71-83% (Fig. 1.2, Table 1.2). Interestingly, it also shares high sequence homology with the human CYP21A2 protein about 38% (Table 1.2).

The medaka *cyp21a2* was found to be highly expressed in the interrenal gland (the adrenal counterpart in teleost) by either RT-PCR and in situ hybridization. In medaka, the liver and the ovary also express *cyp21a2* (Fig. 1.3).

1.3.2 Generation of *cyp21a2* mutant by CRISPR/Cas9

In order to understand the roles of CYP21A2 in medaka and considering its high conservation among vertebrates, a loss-of-function mutant allele was generated by the CRISPR/Cas9 system.

The resultant mutant allele isolated during F1 screening has a frameshift mutation with 9 base insertions in the first exon after the third methionine (Fig. 1.4A-B), which encodes a prematurely truncated protein that lacks 432 residues out of the 451 total residues and about 97% of the P450 domain (Fig. 1.4C).

Wild-type medaka requires about 6-7 days to hatch, however, *cyp21a2* homozygous mutants display a delay of about 2-3 days in the time to hatch (Fig. 1.5A) but eventually hatch at 11 dpf. The survivability was as high as observed in wild-type during embryonic stages. However, after hatching the survivability was low. In fact, the genotypes ratio analyzed at three-time points before the sexual maturation stage (around 3 mph: months post-hatching in medaka) showed that the survivability decreased over time, and only about 10% of the homozygous mutants obtained from the crossing of heterozygous females XX and homozygous males XY reached adulthood (Fig. 1.5B). For subsequent analyses, $cyp21a2^{+9}$ mutant medakas were obtained from the same crossing condition.

1.3.3 The *cyp21a2* homozygous mutant show an increase of cortisol metabolic precursors

The cortisol-deficiency condition in our *cyp21a2* homozygous mutant line was confirmed by extracting steroid hormones from whole-body 13 dph larvae (heterozygous mutant was the control group), and profiling them by LC-MS/MS (Fig. 1.6, Table A.1). The profile in fact confirmed a cortisol deficiency leading to decreased cortisone levels in the homozygous mutant larvae.

The levels of 11-deoxycortisol were also found to be significantly reduced in the homozygous mutant. However, very interestingly, the levels of metabolic precursors of cortisol such as the 17α-hydroxyprogesterone and the 21-deoxycortisol were found at significantly higher levels in the homozygous mutant. Regarding the other steroid hormones, no significant differences were observed (Fig. 1.6). Therefore, cortisol deficiency leads to a hormonal imbalance in medaka.

1.3.4 The *cyp21a2* homozygous mutant displays upregulation of *pomca* and interrenal gland hyperplasia

Expression of ACTH in the cortisol-deficient medaka was analyzed by WISH of its mRNA (*pomca*) in the pituitary of newly hatched larvae. The total area of *pomca*-expressing cells in the pituitary (WISH-positive area) was quantified, and as a result, a significant increase of the total area was observed in the pituitary of the homozygous mutant (Fig. 1.8A, Table A.2).

Later, to evaluate the possibility of interrenal hyperplasia, the expression of a P450 enzyme working upstream of CYP21A2 in the cortisol biosynthetic pathway was analyzed, for instance, the *cyp17a* gene. Medaka has two paralogs of this gene named *cyp17a1* and *cyp17a2*, however, only the later was found to be expressed in the interrenal

gland by WISH (Fig. 1.7), this is consistent with a previous report (Zhou et al., 2007). Then, the total area of WISH-positive signals was measured and a significant increase was observed in the homozygous mutant (Fig. 1.8B, Table A.3). Interrenal hyperplasia was clearly observed in both female and male homozygous mutants at 4.5 mph (Fig. 1.9).

No differences related to *pomca* expression and interrenal hyperplasia were observed between the wild-type and heterozygous mutant larvae (Fig. 1.8). Thus, regulation of *pomca* transcripts and normal interrenal gland development requires the activity of the CYP21A2 enzyme in medaka.

1.3.5 Cortisol administration ameliorates the phenotypes of *cyp21a2* homozygous mutants

A rescue experiment with exogenous cortisol (hydrocortisone) was conducted at the embryonic stage by administrating cortisol in the rearing medium for 5 days (Fig. 1.10A). Interestingly, 5 days of cortisol treatment shortened the time required to hatch in the homozygous mutant to that observed in the wild-type which is about 6-7 days (Fig. 1.10B). It should be pointed out that cortisol administration did not cause either lethality or defects during embryogenesis as judge by the external appearance of hatchlings (Fig. 1.10C).

The levels of expression of *pomca* was then analyzed by FISH and confocal microscopy, and the total area of the FISH signal was quantified. As a result, the values were as reduced as that observed in the hetero-untreated control group (Fig. 1.11A, Table A.4). Similarly, interrenal hyperplasia (analyzed by the expression of *cyp17a2*) was successfully rescued upon cortisol administration (Fig. 1.11B, Table A.5). As with *pomca*, no differences were observed between the treated and untreated heterozygous groups (Fig. 1.11B).

1.3.6 Two *pomca*-expressing cell populations with different responsiveness to cortisol levels in the pituitary of medaka

Despite the fact that the area of *pomca* increases in homozygous mutants, the size of the pituitary did not increase at least at the hatching stage (Fig. 1.12, Table A.6), although it is noteworthy to mention that the size of the pituitary increases with age (Fig. A.2). Then, the number of *pomca*-expressing cells was counted, and interestingly, a significant increase was observed in homozygous mutants (Fig. 1.14A).

The expression analysis of *pomca* by FISH combined with confocal microscopy imaging allowed to recognize two cell populations in the pituitary of medaka (Fig 1.13). One is located in the *rostral par distalis*: RPD (anterior domain) and the other is in the *pars intermedia*: PI (posterior domain) of the pituitary, as observed in a 3D reconstruction image from confocal images (Fig. 1.13A).

The number of *pomca*-expressing cells was then counted in the two populations identified and, a significant increase was observed in cells specifically from the RPD area in the homozygous mutant (Fig. 1.14B, 1.15A, Table A.7). The increase observed was about two-to-three times higher than the control group meaning that these cells contribute the most to the differences observed in the total number, this considering that the number of cells in the PI did not change in homozygous mutants (Fig. 1.14B, 1.15B, Table A.7). Accordingly, the expression of *pomca* (mean intensity) in cells from the RPD was significantly upregulated in homozygous mutants (Fig. 1.16A, Table A.8). Notably, both the number of cells and *pomca* expression were successfully restored to the values observed in the heterozygous control group upon cortisol administration (Fig. 1.14B, 1.15A).

Remarkably, no differences were observed in the number of cells between the heterozygous and homozygous mutants (Fig. 1.14B). Nevertheless, *pomca* was

significantly downregulated in the cells from the PI in homozygous mutants. Cortisol administration successfully restored the values of *pomca* in cells from the PI to those observed in the heterozygous-untreated control group (Fig. 1.16B, Table A.8). Thus, two populations of *pomca*-expressing cells in the pituitary of medaka have different responsiveness to the levels of cortisol.

1.4 Discussion

During evolution humans have retained two copies of the *CYP21A2* gene, although only one has been reported to be functional and the other a pseudogene (Riepe et al., 2005; Araújo et al., 2007; Auer et al., 2023). In teleost, several P450 (CYP) enzymes have been duplicated during the whole-genome duplication event that teleost underwent in the past. For instances, the widely studied aromatase gene *cyp19a1a* and *cyp19a2*, or the *cyp17a1* and *cyp17a2* that in this study were found to have a different expression pattern (Fig. 1.7). However, the synteny analysis for the *cyp21a2* gene in medaka revealed a single copy of this gene on chromosome 16 (Fig. 1.1), which shares about 38% of identity with the human CYP21A2 protein (Fig. 1.2). Thus, the duplicated copy of the *cyp21a2* gene originated during genome duplication in medaka, it is believed to have been lost during evolution. Therefore, the copy found on the chromosome 16 can be considered as the functional orthologs in medaka.

A comprehensive analysis of the systemic effects of the cortisol deficiency due to the lack of the CYP21A2 enzyme in medaka, revealed that the homozygous mutants have a delay in the time to hatch (Fig. 1.5A) and a low survival rate after hatching with nearly 10% of them reaching adulthood (Fig. 1.5B). The high lethality during the larval stage in medaka resembles the high lethality of infants diagnosed with the classic or salt-wasting

form of CAH in humans (Merke and Auchus, 2020). Moreover, cortisol-deficient medakas were unable to synthesize cortisol and cortisone (Fig. 1.6). Instead, cortisol metabolic precursors such as the 17α-hydroxyprogesterone and 21-deoxycortisol were significantly high in the mutant (Fig. 1.6). This data shows that the genetic disruption of *cyp21a2* can results in a systemic glucocorticoid deficiency in medaka.

Upregulation of ATCH (addressed by the expression of its mRNA *pomca* in this study) as well as interrenal hyperplasia, were also observed in the homozygous mutant (Fig. 1.8). This indicates that the CYP21A2 enzyme is crucial for interrenal gland development as well as for the transcriptional activity of *pomca*. These phenotypes are in accordance with those described for CYP21A2 deficiency in humans (Auer et al., 2023), *Cyp21a1*-deficiency reported in mice (Gotoh et al., 1994; Hornstein et al., 1999) and *cyp21a2*-deficiency in zebrafish (Eachus et al., 2017). Importantly, high expression of *pomca* and interrenal hyperplasia were successfully rescued upon administration of cortisol (hydrocortisone) at embryonic stage (Fig. 1.11). Thus, it is anticipated that the *cyp21a2* mutant medaka is of valuable resource to explore the mechanism behind the phenotypes here described (Fig. 1.17).

One of the intriguing mechanisms identified in this study was one related to the upregulation of *pomca* in the pituitary of medaka. Two populations of cells expressing *pomca* respond differently to changes in cortisol levels (Fig. 1.14B, 1.16). The two populations are described as RPD and PI in this study (Fig. 1.13), and are likely equivalent to the anterior and posterior domain described in zebrafish by Sun and colleagues (2010).

In zebrafish, the anterior domain has been reported as the sensitive center to decreasing levels of cortisol (To et al., 2007; Sun et al., 2010). In agreement with this, an increase in expression was observed in cells from the RPD in mutant medakas (Fig. 1.16A). This was rescued with cortisol administration, which suggest that these cells are

indeed sensitives to variations in cortisol. In this study interestingly, the number of cells was also found to significantly increase under low levels of cortisol and were restored upon cortisol administration. In contrast, the number of cells in the PI did not changed under cortisol deficiency and remained unchanged when exposed to exogenous cortisol. Besides, *pomca* was downregulated in the PI in homozygous mutant, however, interestingly, this could be rescued upon cortisol administration. The difference in the number of cells and responsiveness to the levels of cortisol by *pomca*-expressing cells in the pituitary of medaka remains to be addressed.

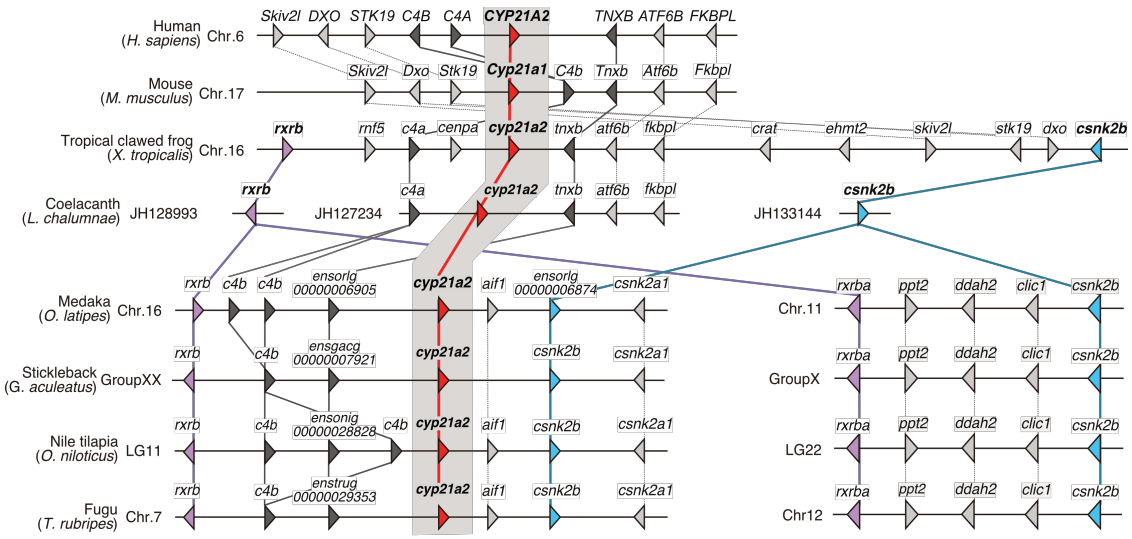

Figure 1.1 Synteny of the cyp21a2 gene

A single copy of the *cyp21a2* gene in chromosome 16 of medaka is highlighted in red. The well-conserved neighbor genes *c4* and *tnxb* are highlighted in dark grey. The genes *rxrb* (purple) and *csnk2b* (light-blue) flanking the *cyp21a2* locus on chromosome 16 have paralogs on chromosome 11.

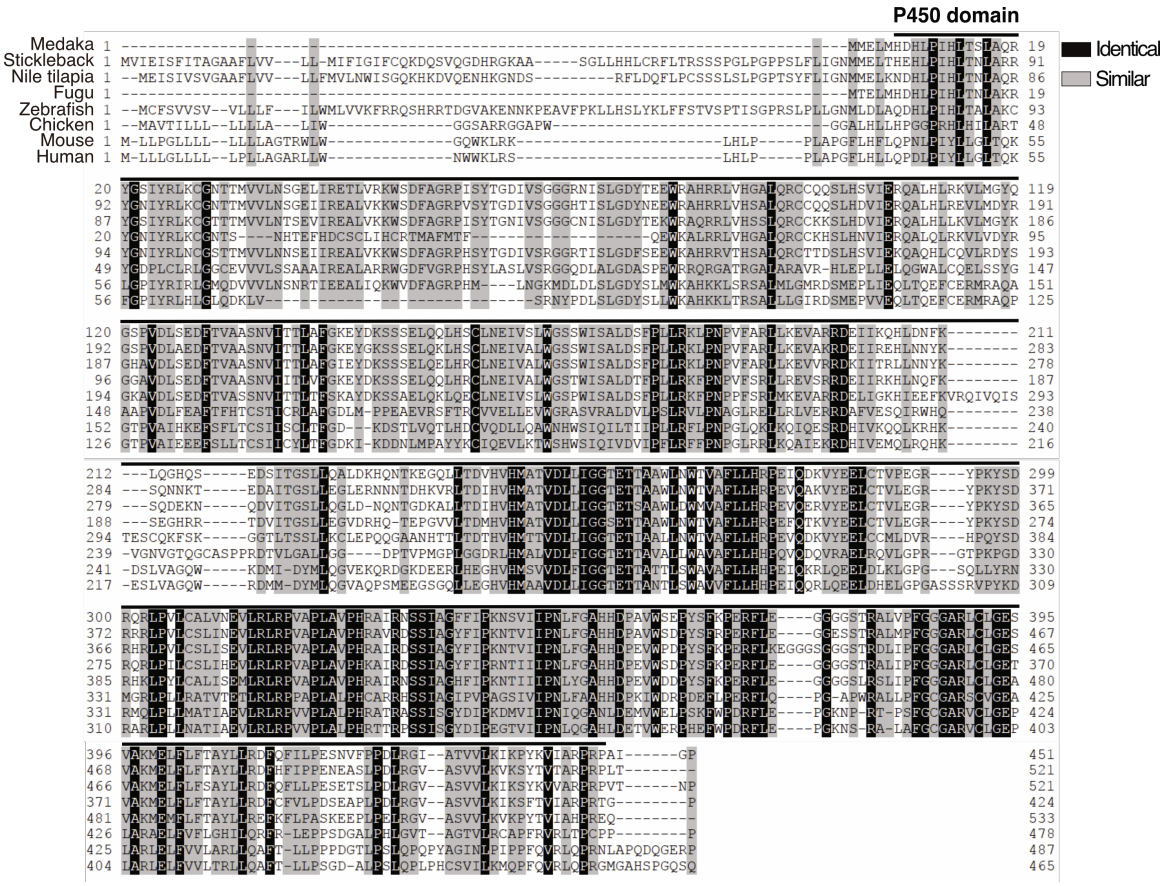

Figure 1.2 Sequence conservation of the CYP21A2 protein

Multiple CYP21A2 amino acid sequences alignment among vertebrates. The top black bar indicates the P450 domain.

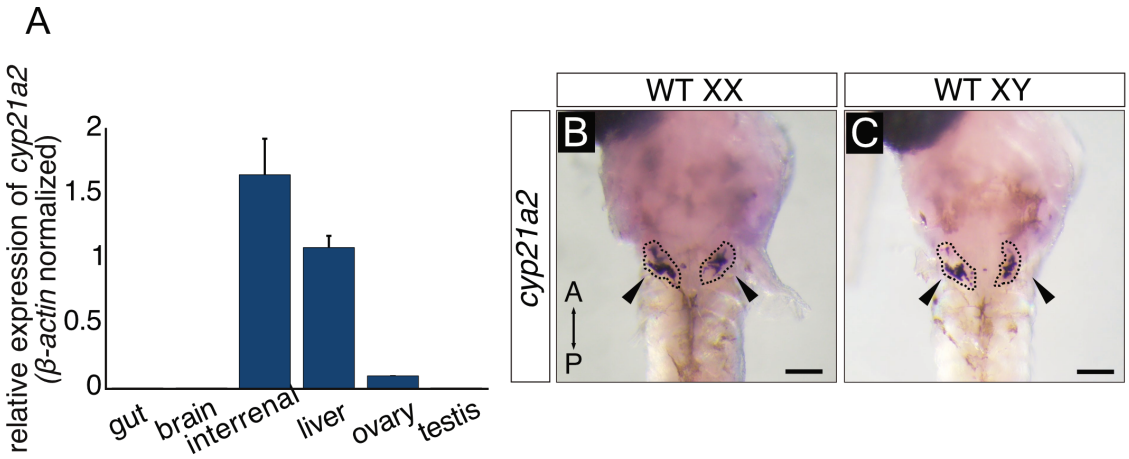

Figure 1.3 Relative expression of cyp21a2 and WISH of P450 enzymes

(A) Relative expression of *cyp21a2* in multiple tissues following the method 2^-ΔΔCt. Values were *β-actin* normalized and the first biological replicate of the liver was set as standard control. Graph is presented with error bar, S.E. **(B-C)** WISH of *cyp21a2* in the interrenal gland at hatching stage. The interrenal gland is highlighted with black-dashed lines. Black arrowheads indicate positive signals, respectively. Scale bars, 100 µm.

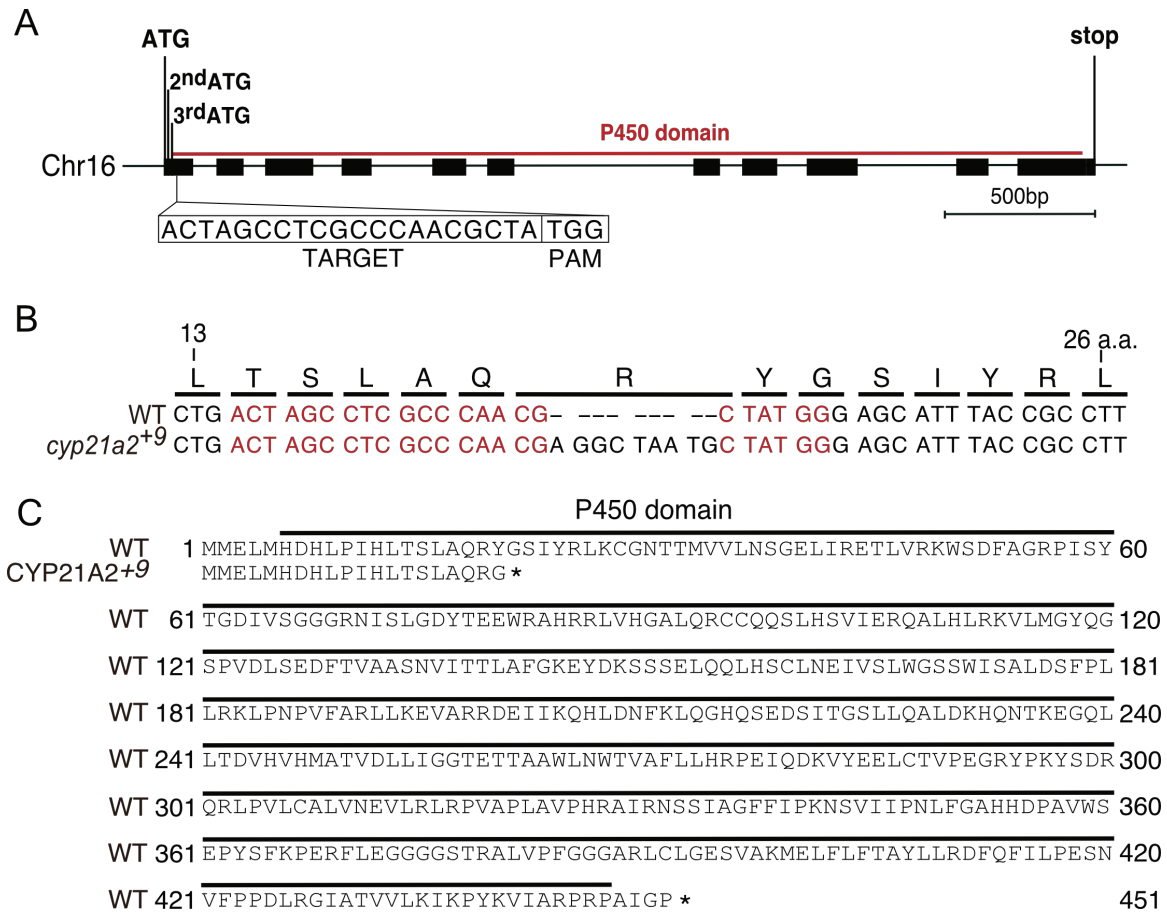

Figure 1.4 Generation of *cyp21a2* loss-of-function mutant by CRISPR/Cas9

(A) Genomic structure of the *cyp21a2* gene on chromosome 16 of medaka. Exons are presented in black boxes and the P450 domain is indicated with a red bar. The gRNA was designed on the first exon after the third methionine. **(B)** Nucleotide and amino acid sequences of wild-type (WT) and mutant (*cyp21a2*$^{+9}$, 9 bases insertion) alleles. The gRNA target site is highlighted in red. **(C)** Amino acid sequences of wild-type (WT) and *cyp21a2*$^{+9}$ mutant alleles. The top black bar indicates the P450 domain and asterisks indicate the stop codon.

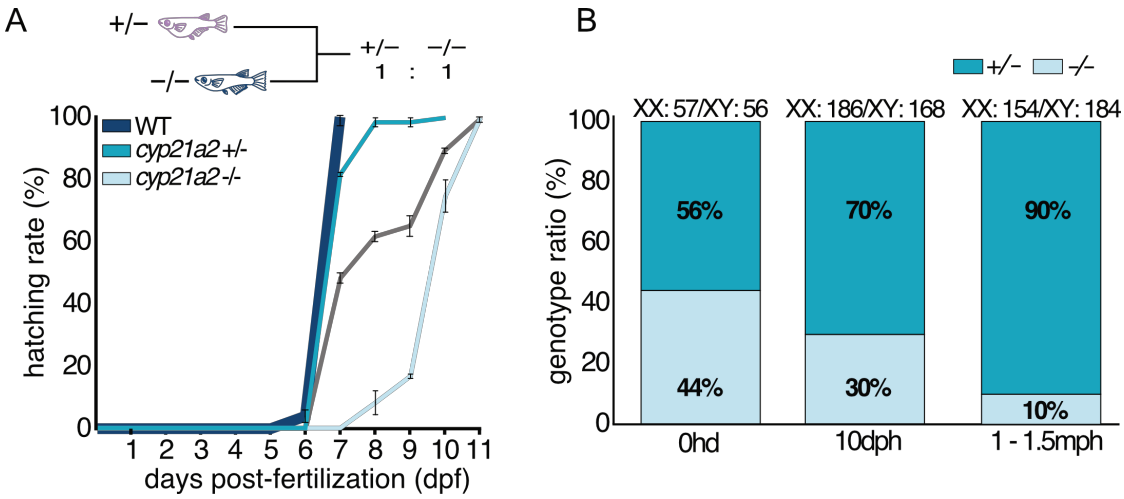

Figure 1.5 Hatching and genotype ratio of *cyp21a2* mutants

(A) Hatching rate and time of wild-type (WT), heterozygous and homozygous mutants. The grey line indicates the combined hatching rate of heterozygous (XX) and homozygous (XY) parents offsprings, before genotyping. **(B)** Genotype ratio of heterozygous and homozygous mutants at 0 hatching days (0 hd), 10 days post-hatching (10 dph), and 1-1.5 months post-hatching (1-1.5 mph) collected from heterozygous females (XX) and homozygous males (XY), parents. Numbers on the top of the bars indicate the number of fish per genetic sex.

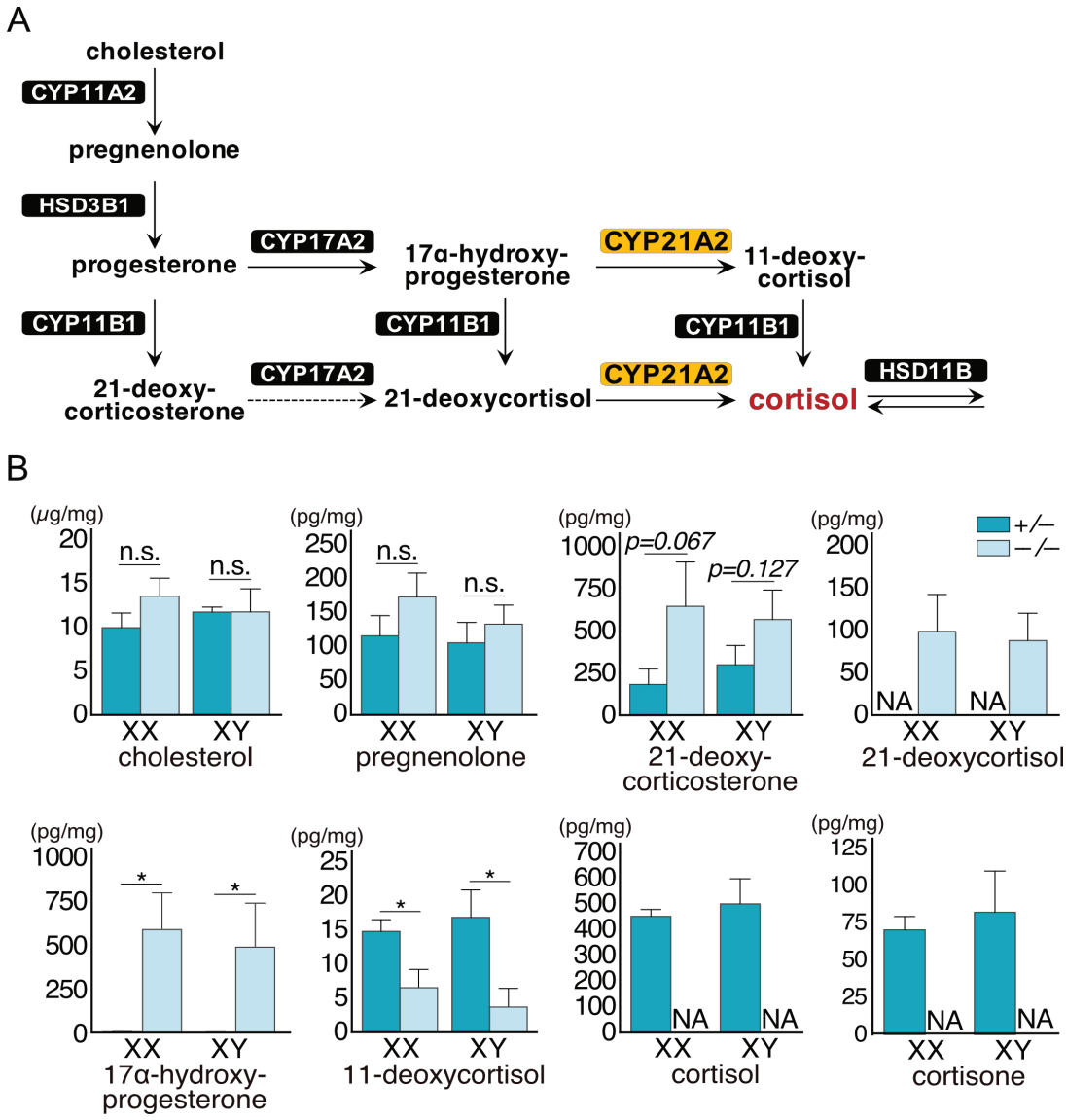

Figure 1.6 Steroid hormones profile in *cyp21a2* mutants

(A) Cortisol biosynthetic pathway. **(B)** Levels of steroid hormone extracted from heterozygous (control) and homozygous mutant larvae at 13 dph, and expressed as an amount of the steroid found in 1mg of dried larvae. All graphs are presented with bar, mean; error bar, S.E.; N.A., not applicable (due to a low amount), n.s., non-significant; *$P < 0.05$ by Student's *t*-test.

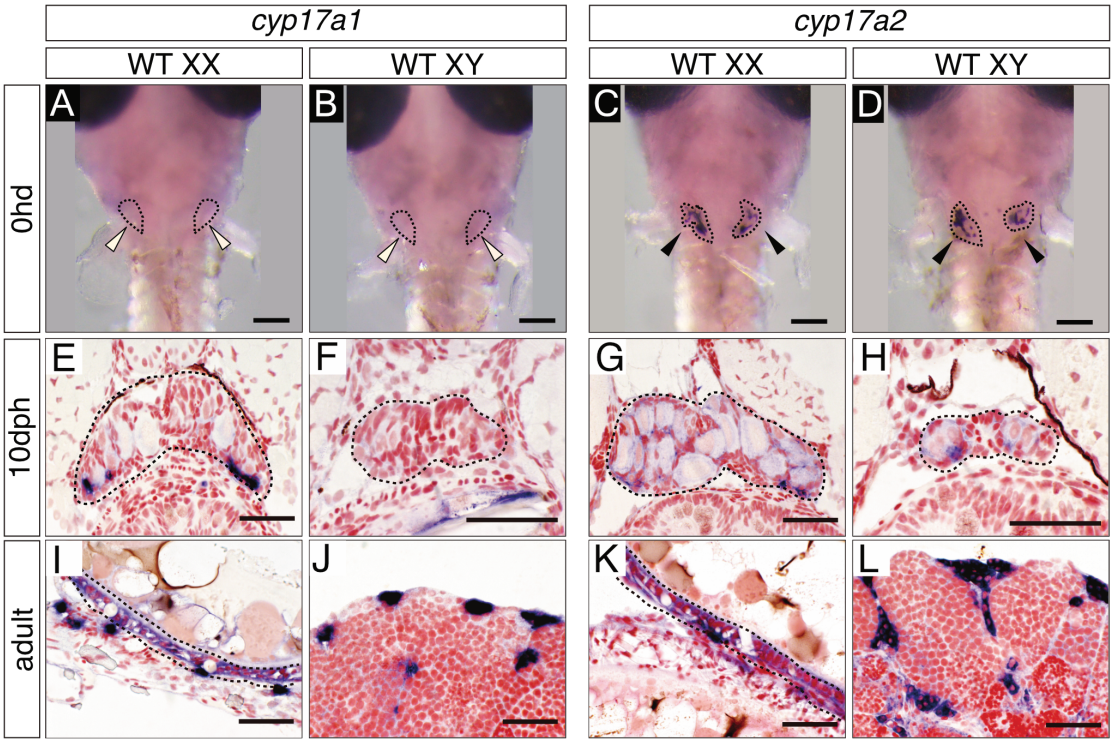

Figure 1.7 WISH of *cyp17a1* and *cyp17a2*

Expression of *cyp17a1* and *cyp17a2* in the **(A-D)** interrenal gland at hatching stage (0hd) which is highlighted with black-dashed lines (black and white arrowheads indicate positive and negative signals, respectively), **(E-H)** in gonads of 10 dph larvae (black dashed-lines, gonadal area), and **(I-L)** adult gonads, where signals were principally observed in steroidogenic cells i.e. theca cells **(E, G, I, and K)** and Leydig cells **(J and L)** from the ovary and testis, respectively. Scale bars, (A-D) 100µm, (E-L) 50 µm.

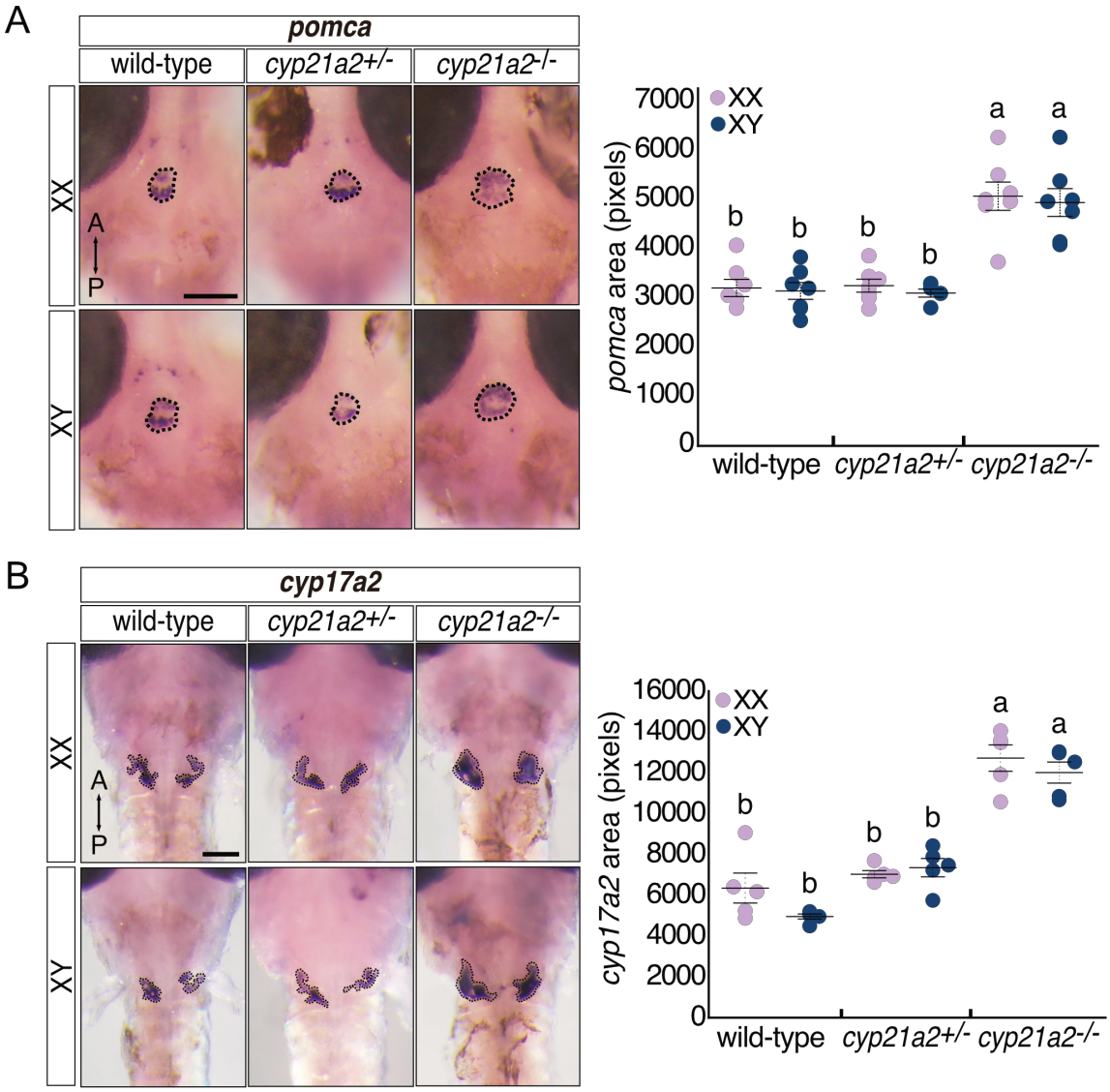

Figure 1.8 WISH of *pomca* and *cyp17a2*

WISH of **(A)** *pomca* and **(B)** *cyp17a2* in wild-type, heterozygous, and homozygous mutant medakas at the hatching stage. Black-dashed lines indicate the WISH-positive area used for quantification with Fiji software. Dot plots show the quantification results. Each dot represents one individual, $n = 7$ (*pomca*) and $n = 5$ (*cyp17a2*). Bar, mean; error bar, S.E. Different letters denote statistical differences, one-way ANOVA followed by Tukey *post-hoc* test. Scale bars, 100 µm.

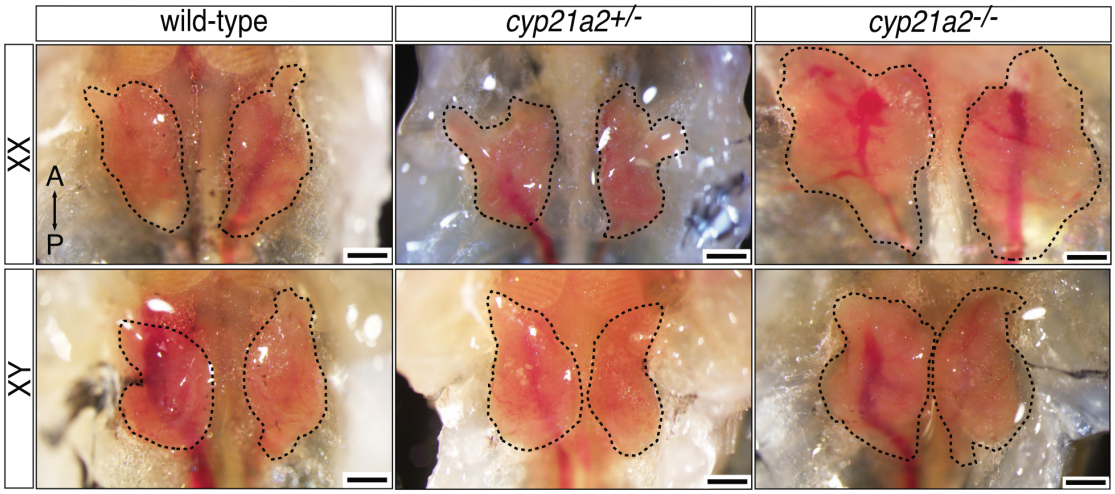

Figure 1.9 Interrenal hyperplasia in *cyp21a2* homozygous mutants

Interrenal glands of wild-type, heterozygous, and homozygous mutants at 4.5 months old are highlighted with black-dashed lines. Pictures show a ventral view. Scale bars, 500 µm.

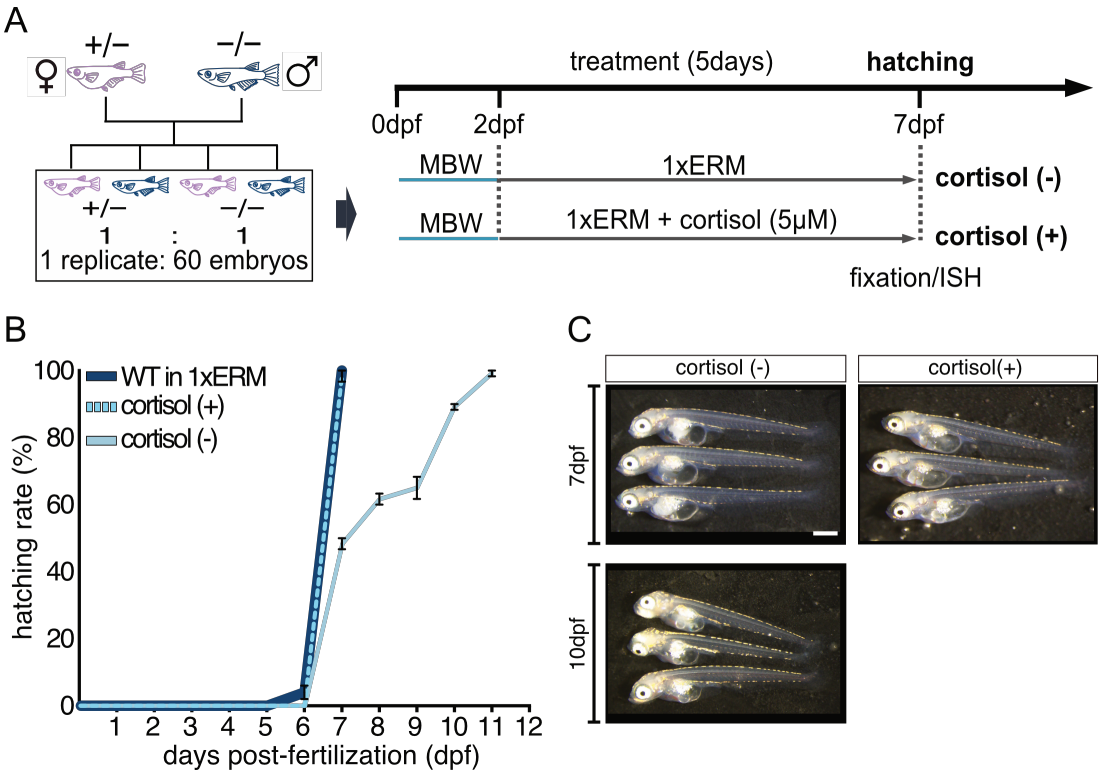

Figure 1.10 Cortisol rescue of *cyp21a2* mutants

(A) Schematic representation of the rescue experiment with cortisol during the embryonic stage. **(B)** Hatching rate of wild-type embryos raised in 1x ERM buffer (control), cortisol (-), and cortisol (+) treatments. **(C)** External appearance of hatchlings under cortisol (-) and cortisol (+) treatments.

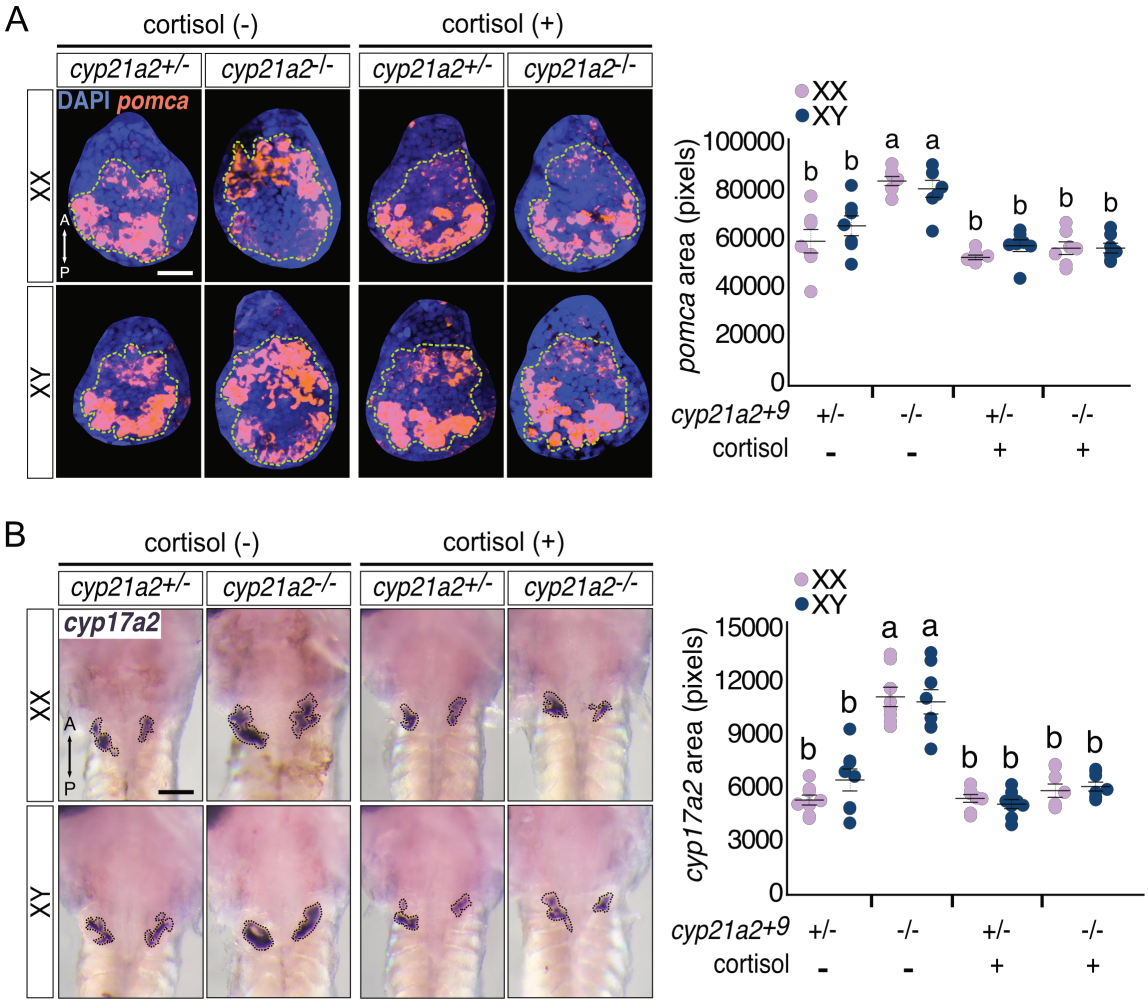

Figure 1.11 Cortisol rescue of *cyp21a2* homozygous mutant phenotypes

(A) FISH and confocal imaging of *pomca* in the pituitary of *cyp21a2* mutants under cortisol (-) and cortisol (+) conditions at the hatching stage. Light-green dashed lines indicate the area used for image quantification. **(B)** WISH of *cyp17a2* in *cyp21a2* mutants under cortisol (-) and cortisol (+) conditions at the hatching stage. Dot plots show the quantification results. Each dot represents one individual, n = 7 (*pomca*) and n = 8 (*cyp17a2*). Bar, mean; error bar, S.E. Different letters denote statistical differences, one-way ANOVA followed by Tukey *post-hoc* test. Scale bars, (A) 20 µm, (B) 100 µm.

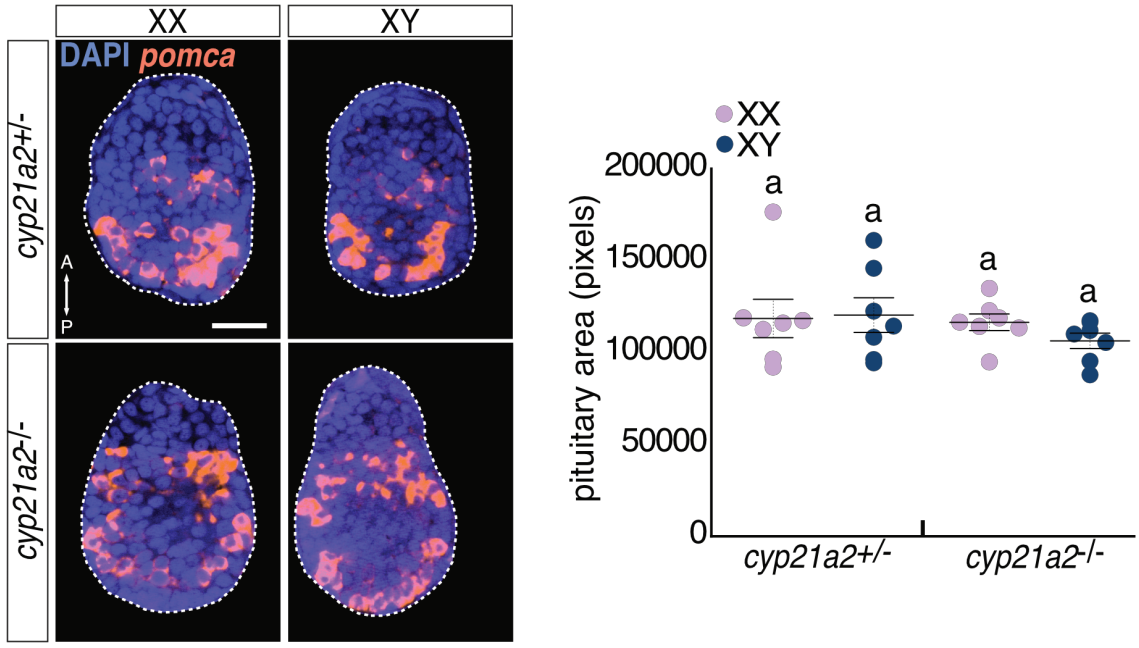

Figure 1.12 Maximum pituitary area of *cyp21a2* mutants

White-dashed lines indicate the maximum pituitary area of heterozygous (control) and homozygous mutants at the hatching stage. Dot plot shows the quantification results. Each dot represents one individual, n = 7. Bar, mean; error bar, S.E. Same letters denote no statistical differences, one-way ANOVA followed by Tukey *post-hoc* test. Scale bar, 20 μm.

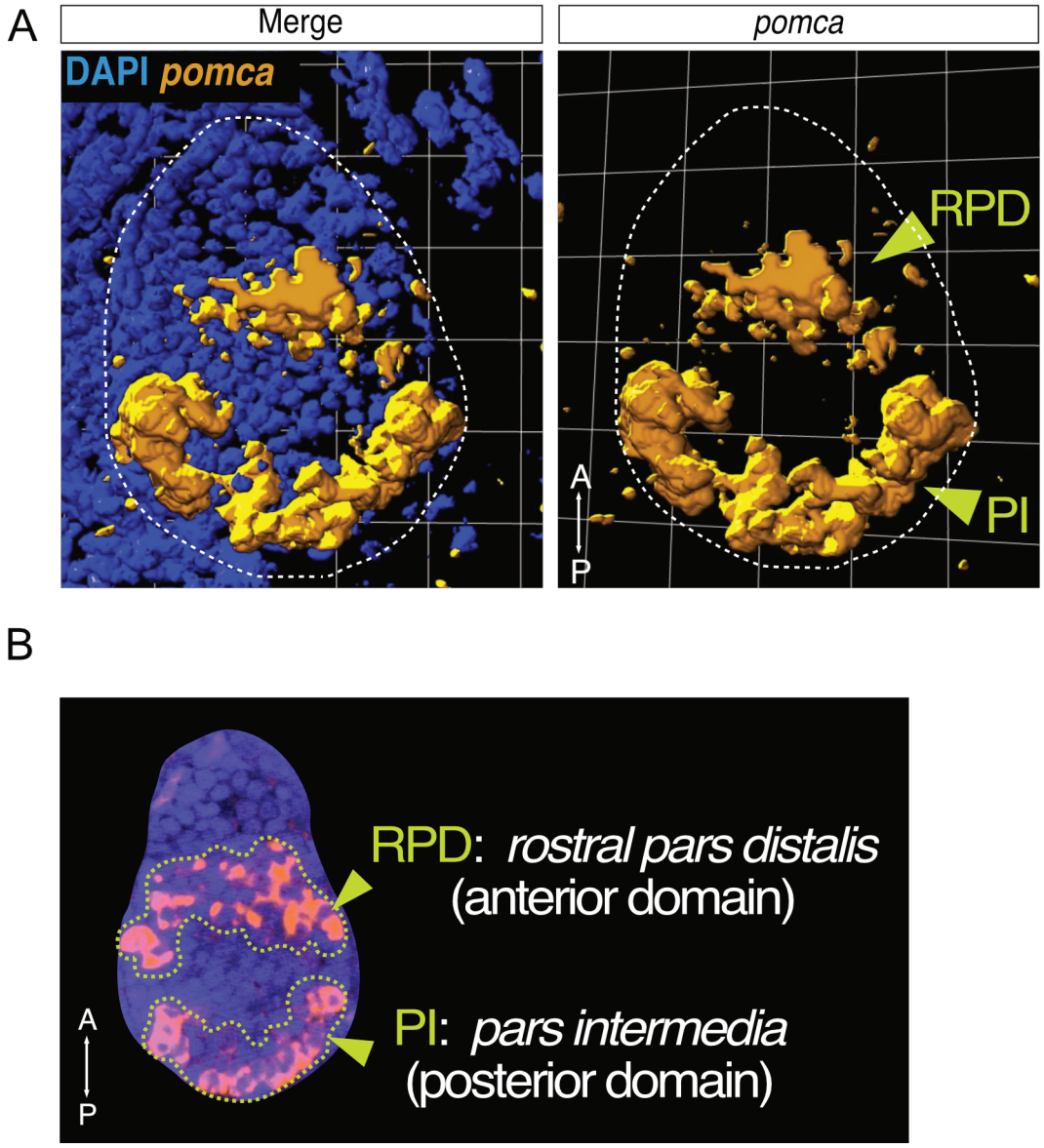

Figure 1.13 Two *pomca*-expressing cell populations in the pituitary of medaka

(A) 3D reconstruction of FISH/confocal microscope images for *pomca* at the hatching stage highlighting two cell populations. **(B)** Two *pomca*-expressing cell populations, one in the RPD and the other in the PI are highlighted with light-green arrowheads and dashed lines.

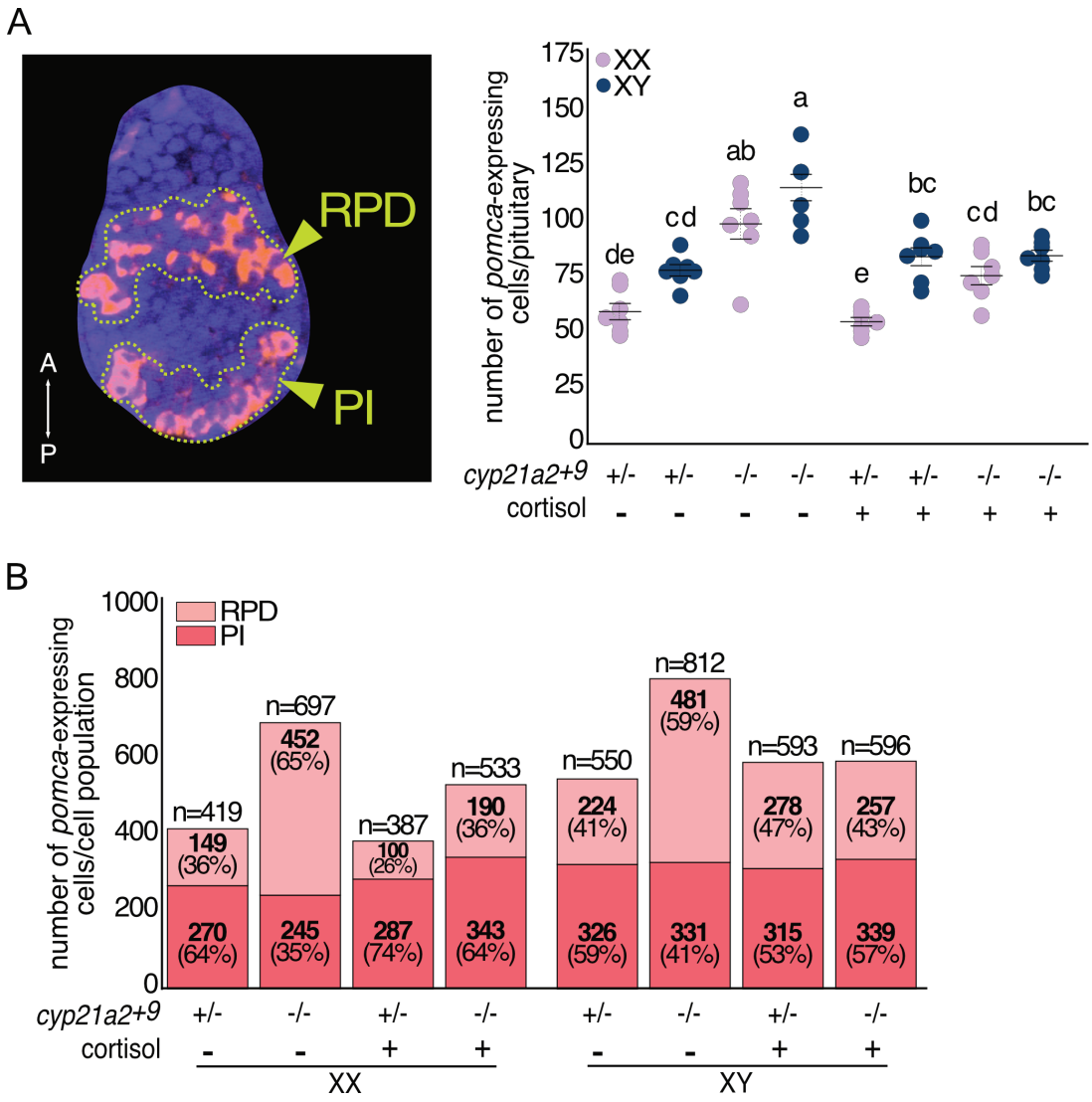

Figure 1.14 Variations in the number of *pomca*-expressing cells per population

(A) Number of *pomca*-expressing cells counted from 7 pituitaries per sex/genotype raised under cortisol (-) and cortisol (+) conditions. Dot plot shows the quantification results. Each dot represents one individual, n = 7. Bar, mean; error bar, S.E. Different letters denote statistical differences, one-way ANOVA followed by Tukey *post-hoc* test. **(B)** Number of *pomca*-expressing cells in the two populations (RPD and PI) of the medaka pituitary. The numbers on the top of the bars represent the total number of cells counted from 7 pituitaries per sex/genotype raised under cortisol (-) and cortisol (+) conditions.

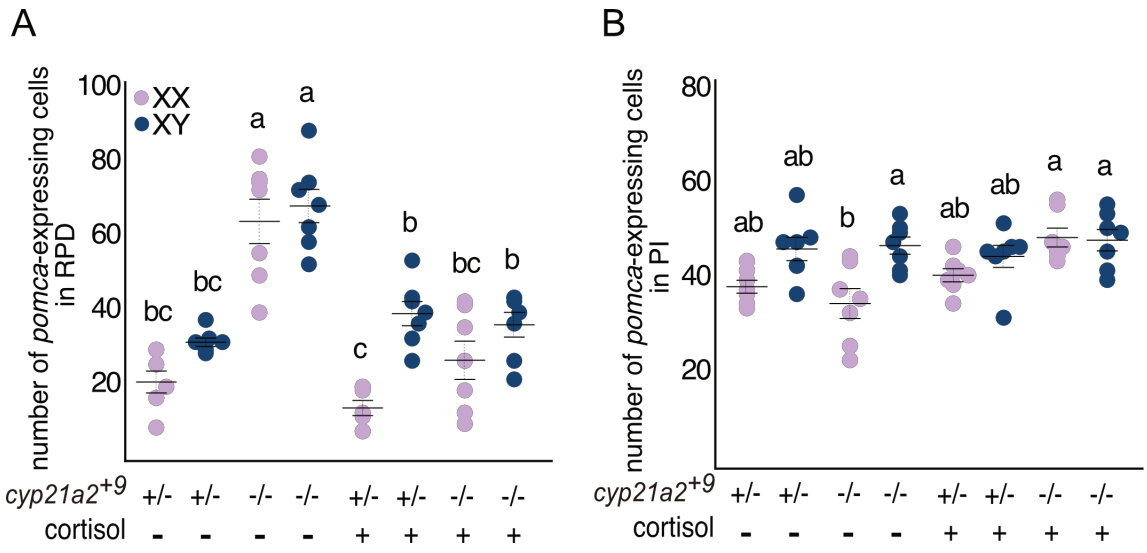

Figure 1.15 Number of *pomca*-expressing cells (statistical analysis)

Bar plots with the total number of *pomca*-expressing cells in the **(A)** RPD and the **(B)** PI populations. Each dot represents one individual, $n = 7$. Bar, mean; error bar, S.E. Different letters denote statistical differences, one-way ANOVA followed by Tukey *post-hoc* test.

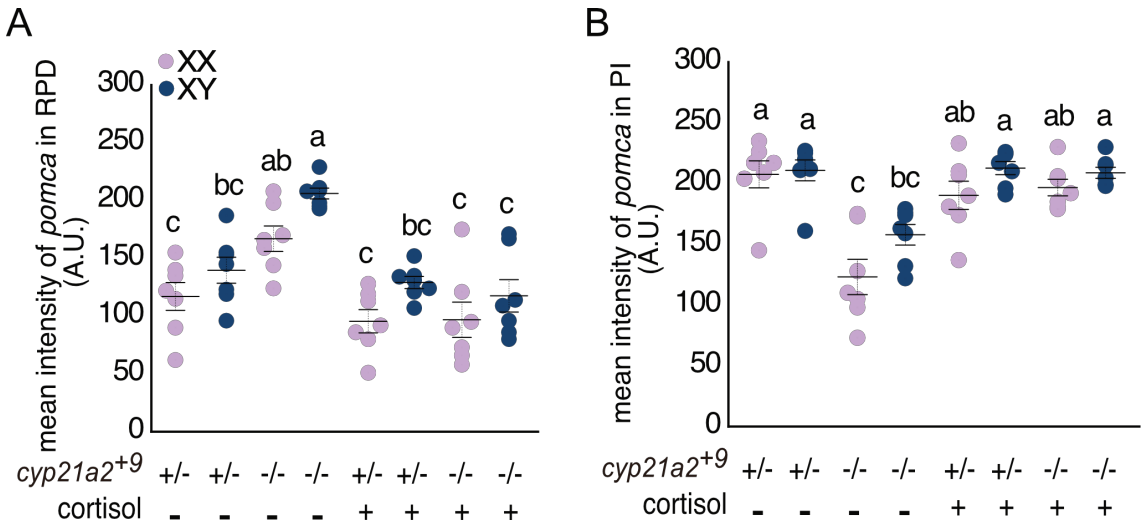

Figure 1.16 Mean intensity of *pomca* in the pituitary of medaka

Mean intensity of *pomca* in the **(A)** RPD and **(B)** PI cell populations, measured from 7 pituitaries per sex/genotype raised under cortisol (-) and cortisol (+) conditions. Dot plots show the quantification results. Each dot represents one individual, n = 7. Bar, mean; error bar, S.E. Different letters denote statistical differences, one-way ANOVA followed by Tukey *post-hoc* test.

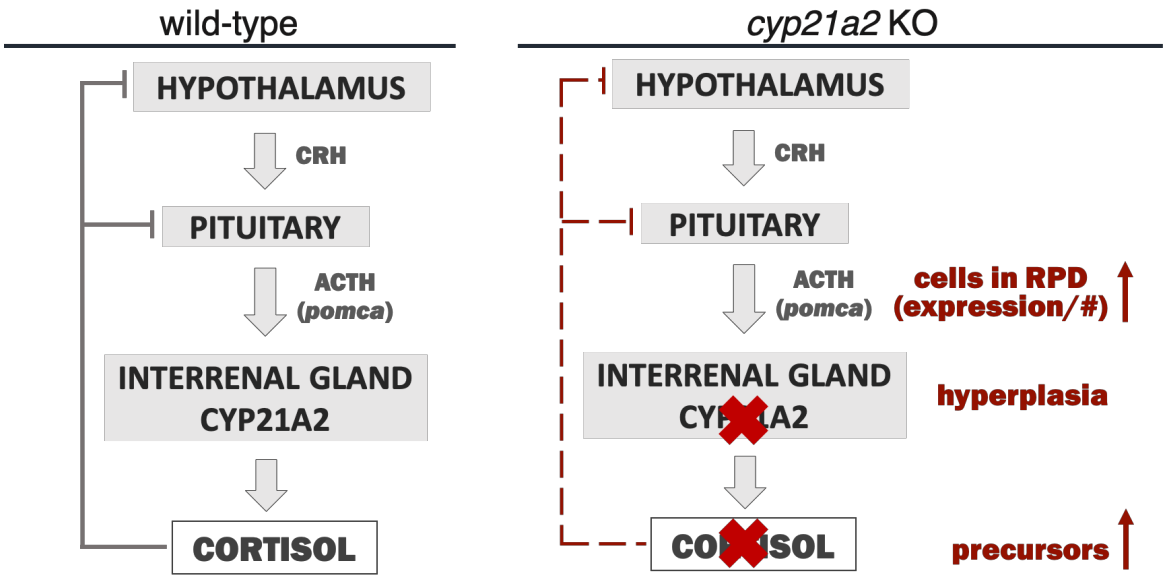

Figure 1.17 Systemic effects of the cortisol deficiency in the teleost fish medaka

The lack of CYP21A2 enzyme negatively impacts the post-hatching survivability in medaka. In addition, it creates a condition of systemic cortisol deficiency, which leads to an increase in the number of cells alongside an upregulation of *pomca* (ACTH) in *pomca*-expressing cells of the RPD area in the pituitary. Then, high levels of ACTH eventually result in interrenal hyperplasia. These are typical phenotypes of the human CAH condition.

Table 1.1 Ensembl IDs of CYP21A2 orthologs for sequence conservation analysis

#	Common name	Scientific name	Gene_ID	Transcript/Protein_ID	Location	Comments
1	Medaka	*Oryzias latipes*	ENSORLG00000006896	ENSORLP00000008663	Chr16	
2	Stickleback	*Gasterosteus aculeatus*	ENSGACG00000007916	ENSGACP00000010487	Group XX	
3	Nile tilapia	*Oreochromis niloticus*	ENSONIG00000002824	ENSONIP00000077417	LG11	
4	Fugu	*Takifugu rubripes*	ENSTRUG00000016091	ENSTRUT00000041286	Chr7	Protein was predicted with Genetyx v.14
5	Zebrafish	*Danio rerio*	ENSDARG00000037550	ENSDARP00000125284	Chr16	
6	Chicken	*Gallus gallus*	ENSGALG00010003186	ENSGALP00010004438	Chr16	
7	Mouse	*Mus musculus* (CL57BL6)	ENSMUSG00000024365	ENSMUSP00000025223	Chr17	
8	Human	*Homo sapiens*	ENSG00000231852	ENSP00000415043	Chr6	

Table 1.2 Percentage of sequence conservation of some vertebrate CYP21A2 orthologs at amino acid level

	Identity matrix (%)							
	Medaka	Stickleback	Nile tilapia	Fugu	Zebrafish	Chicken	Mouse	Human
Medaka	*							
Stickleback	83	*						
Nile tilapia	82	79	*					
Fugu	77	77	76	*				
Zebrafish	71	66	65	68	*			
Chicken	44	42	41	40	41	*		
Mouse	42	40	39	38	39	43	*	
Human	38	39	38	39	39	43	71	*

Table 1.3 Survival and hatching rate related to cortisol rescue experiment

1. Wild-type						
embryos/replicate: 50						
dpf	wt1		wt2		wt3	
	dead	hatched	dead	hatched	dead	hatched
1	0	0	0	0	0	0
2	0	0	0	0	0	0
3	0	0	0	0	0	0
4	0	0	0	0	0	0
5	0	0	0	0	0	0
6	0	1	0	1	0	4
7	0	49	0	49	0	46
Total	0	50 (100%)	0	50 (100%)	0	50 (100%)

2. Cortisol (-)				
embryos/replicate: 60				
dpf	C(-)1		C(-)2	
	dead	hatched	dead	hatched
1	0	0	0	0
2	0	0	0	0
3	0	0	0	0
4	0	0	0	0
5	0	0	0	0
6	0	0	0	0
7	0	28	0	30
8	0	8	0	8
9	1	1	0	3
10	0	17	0	12
11	0	5	0	7
Total	1 (1.7%)	59 (98.3%)	0	60 (100%)

3. Cortisol (+)				
embryos/replicate: 60				
dpf	C(+)1		C(+)2	
	dead	hatched	dead	hatched
1	0	0	0	0
2	0	0	0	0
3	0	0	0	0
4	0	0	0	0
5	0	0	0	0
6	0	0	0	0
7	2	58	0	60
Total	2 (3.3%)	58 (96.7%)	0	60 (100%)

1xERM (5 days)
dpf: day post-fertilization

Table 1.4 Genetic sex and genotype related to cortisol rescue experiment

	Cortisol (-)			Cortisol (+)		
	XX	**XY**	**Total**	**XX**	**XY**	**Total**
+/-	41	30	71	41	30	71
-/-	24	24	48	32	15	47
Total	65	54	119	73	45	118

Table 1.5 Primers and probes used in this chapter

Experiment	Primer name	Sequence (5' - 3')
sex-typing	dmy-FAM (TaqMan MGB probe)	tggcttcaccgttgga
	cyp19a-VIC (TaqMan MGB probe)	acaacaaatatggagacatt
	tq-dmy-F	cggtaaattgacgcacagcat
	tq-dmy-R	tccagtaagttgcagagtttcgtt
	tq-cyp19a-F	tggcacagccagcaactatta
	tq-cyp19a-R	tccgttgatccacactcgaa
CRISPR/Cas9	80bp cr/tracr-F	gttttagagctagaaatagcaagttaaaataaggctagtc cgttatcaacttgaaaaagtggcaccgagtcggtgctttt
	80bp cr/tracr-R	aaaagcaccgactcggtgccacttttcaagttgataacg gactagccttattttaacttgctatttctagctctaaaac
	T7-F	taatacgactcactatag
	tracr-R	aaaagcaccgactcggtg
	cyp21a2-gRNA-F2	taatacgactcactataggtagcctcgcccaacgcta
	cyp21a2-gRNA-R2	ttctagctctaaaactagcgttgggcgaggcta
	cyp21a2-qPCR-F	cttgtaggagcagcatctgga
	cyp21a2-qPCR-R	ggtgattacttgtgtttccacattt
mutant genotyping	cyp21a2-WT_check-F	tagcctcgcccaacgctatg
	cyp21a2-+9_check-F	ctcgcccaacgaggctaatg
	cyp21a2-+9_check-R	agcaccaccatggcttaaaa
WISH/FISH	ISH_cyp21a2_F	gatgcacgatcacctaccaa
	ISH_cyp21a2_T7R	ggccagtgaattgtaatacgactcactatagggtgagaa cgacagtggcaatc
	ISH_cyp17a1_F	ctgctctggagggtgagaac
	ISH_cyp17a1_T7R	ggccagtgaattgtaatacgactcactatagggtctcatc gtggtgcagagac
	ISH_cyp17a2_F	agtttgtgctccgagctgat
	ISH_cyp17a2_T7R	ggccagtgaattgtaatacgactcactatagggttggaat gaccacaacctca
	ISH_pomca_F (Rahmad Royan et al., 2021)	atgtataccgtttggttgct
	ISH_pomca_T7R (Rahmad Royan et al., 2021)	ggccagtgaattgtaatacgactcactatagggaaatgct tcatcttgtaggag
RT-qPCR	qPCR_b-actin_F	tggcgcttgactcaggattt
	qPCR_b-actin_R	gcagatgcctggggtgttta
	qPCR_cyp21a2_F	ccttcccactgctgagaaaa
	qPCR_cyp21a2_R	ctttgatgcccttgcaactt

CHAPTER 2. The *cyp21a2* mutant medaka reveals a new role of cortisol in reproduction

Collaborative work statement

This chapter describes a collaborative effort of José Carranza, Kazuki Yamada, Jongsung Noh, and Man Ho Choi, under the supervision of Dr. Minoru Tanaka. Kazuki Yamada performed the immunohistochemistry in germ cells and gene expression of *cyp21a2* in follicles. Jongsung Noh and Man Ho Choi performed the mass spectrometry analyses. All other experiments were conducted by José Carranza.

2.1 Introduction

Cortisol is mainly referred to as the stress-response steroid hormone. A chronic stress condition, for example, has been correlated with an increase in cortisol levels which interestingly could lead to a suppression of reproductive activity (Russell and Lightman, 2019). On the other hand, cortisol deficiency due to 21OHD leads to infertility in humans (Reichman et al., 2014).

This infertility is believed to be of multifactorial cause. One of them is the virilization of the external genitalia in 46,XX patients which is also considered as a hallmark in the classic form of CAH. Importantly, 46,XY patients with CAH has not defects related to the sexual differentiation except for hypogonadism (Engels et al, 2018; Auer et al, 2023). The impairment of the hypothalamus-pituitary-gonad (HPG) axis where the synthesis and the dynamic of the secretion of gonadotropins are severely affected, and the polycystic ovary syndrome (PCOS) which has been proposed as a result of high adrenal-derived androgen levels (Papadakis et al., 2019; Merke and Auchus, 2020; Auer et al., 2023), are among the

other factors. In fact, not only the excess of androgens but also the hypersecretion of progesterone could negatively act on gonadal development and physiology (Reichman et al., 2014).

In a mouse, mutation in the *Cyp21a2* gene recapitulates some of the phenotypes observed in CAH such as increase ACTH and adrenal hyperplasia. However, the data on reproductive aspects is very limited because of the problems of embryos viability. However, model for human 21OHD (Hornstein et al., 1999; Riepe et al., 2005). Nonetheless, a *Cyp11b1* null mouse where the mineralocorticoid synthesis was preserved allowing mice to survive showed several defects related to reproductive functions, such as female infertility and defects in ovarian development (Mullins et al., 2009).

In teleosts, a loss-of-function mutation of the *cyp17a2* in zebrafish results in a compromised fertility in females with defects in the differentiation of sexual characteristics and oogenesis (Shi et al., 2022). In the case of tilapia, genetic disruption of the *cyp11c1* gene led to female infertility due to an arrest in oogenesis (Xiao et al., 2022).

In this chapter, the impact of cortisol-deficiency on medaka reproductive aspects is presented. For instance, defects on gonadotropins fluctuations, ovulatory issues, significant increase of sex steroids and PCOS-like phenotype are here described. Importantly, these defects have been reported as reproductive key features of human 21OHD (Reichman et al., 2014; Yogi and Kashimada, 2023). Moreover, phenotypes differing from those reported in humans such as compromised fertility in females only, and failure in oocyte meiotic arrest found in the *cyp21a2* mutant medaka are also described in this chapter.

2.2 Materials and methods

2.2.1 Fish strain and maintenance

The medaka (*Oryzias latipes*) Cab strain was used in all experiments. Medakas were raised at 29ºC during the embryonic stage. After hatching, larvae were raised in freshwater at 25 ± 0.5ºC under a 14 h light and 10 h dark photoperiod.

2.2.2 Gonadosomatic index

The body and ovary weight were measured using a weighing balance (Shimadzu ATX84, Sartorius). Then, the gonadosomatic index (GSI) was calculated with the following formula (Awaji and Hanyu, 1987):

$$GSI = \frac{\text{weight of gonad}}{\text{weight of fish body}} \times 100$$

2.2.3 Fertility

Five months old medakas were used to check their fertility. Three individuals of each genotype were crossed with female or male wild-type adult fish (4 - 5 month old) in separate tanks as pairs (3 biological replicates per genotype). The fertility of wild-type fish was assessed beforehand. Since eggs were collected daily for 5 days, then the fertilization rate of an individual is equivalent to the average number of eggs fertilized over 5 days.

2.2.4 Steroid hormones measurement

All steroid hormones profiles in this Chapter were conducted by following the protocol described in section 1.2.9 (Chapter 1). Nevertheless, details on sample preparation are described below.

Total blood was extracted from 4.5month old adult fish by a puncture of the caudal vasculature with a glass needle (Narishige, G-100), coated with heparin sodium salt at a concentration of 206U/mL (Nacalai, 17513-4). Extracted blood was then spotted on a filter paper (Whatman grade 3, 1003-185) and dry out at room temperature. Blood-spotted paper was used for steroid hormones measurement by mass spectrometry.

Follicles were isolated and pooled into 3 groups: small (S), medium (M), and large (L) size (Fig. 2.8B). These correspond to stages I-IV (S), V-VII (M), and VIII-X (L) based on a medaka oocyte development scale (Iwamatsu et al., 1988). Then, follicles were flash-frozen in liquid nitrogen and left to dry overnight in a freeze-drying unit (UT-1000 EYELA+GCD-051X ULVAC). Dried follicles were used for steroid hormone measurement by mass spectrometry.

Gonads were dissected at 8 h before ovulation (00:00 h) which correlates with the time for MIH synthesis. Gonads were flash-frozen in liquid nitrogen and left to dry overnight in a freeze-drying unit (UT-1000 EYELA+GCD-051X ULVAC). Dried gonads were used for steroid hormone measurement by mass spectrometry. Moreover, Gonads were weighed before and after freeze-drying.

2.2.5 Histology and PAS staining

Histology sections were prepared as previously described (Nishimura et al., 2018). In brief, whole-gonads were fixed in BOUIN solution. After several washes in 1xPTW, samples were dehydrated by a serial dehydration step with ethanol. The Technovit kit 8100 (Heraus Kulzer, 64709012) was then used for making resin-based sectioning blocks from gonadal samples, which were sectioned to a 4 µm or 7 µm thickness, for testis and ovaries,

respectively. Sections were colored by the PAS Schiff-metanil yellow method (Quintero et al., 1991).

2.2.6 Paraffin sections

Ovaries were fixed in 4% PFA overnight, then replaced with 100% MeOH and stored at -30ºC until use. Fixed samples were treated with 100%EtOH, for 15 min at RT twice, treated with xylene (Wako, 244-00081) three times of 5 min each, and embedded in paraffin (Paraplast Plus, Sigma – P3683) for about three times of 15 min each. Paraffin blocks were then sectioned at 7~9 μm and used for immunohistochemistry.

2.2.7 Immunohistochemistry (IHC)

Paraffin: tissue sections were deparaffinized and rehydrated. Then, sections were subjected to a heat-induced epitope retrieval (HIER) in a microwave (National Microwave) for about 20 min in a 10mM citrate buffer, 0.05% Tween, and pH 6.0. After retrieval, slides were cool down for 20 min, and rinse with MilliQ water twice and 1xPBS once. An anti-medaka OLVAS (rabbit, 1:200, Lab stock) and anti-medaka LH receptor (rat, 1:200, gifted by Dr. Ogiwara from Hokkaido University) were used as primary antibodies. An anti-rabbit-Alexa fluor 488 (1:200, Invitrogen), and anti-rat-Alexa fluor 568 (1:200, Invitrogen) were used as secondary antibodies. Nuclei were stained with DAPI (5μg/ml, Thermo Fischer Scientific-D1306).

Germ cells at 0 and 5dph: larvae were dissected (removal of air bladder) and fixed in 4% PFA overnight, then replaced with 100% MeOH and stored at -30ºC until use. Fixed larvae were then rinse three times in 1xPTW and blocked with Blocking One Solution (Nacalai, 03953-95). An anti-medaka OLVAS (rat, 1:200, Lab stock) and anti-medaka

SYCP1 (rabbit, 1:400, Lab stock) were used as primary antibodies. An anti-rat-Alexa fluor 488 (1:200, Invitrogen), and anti-rabbit-Alexa fluor 647 (1:200, Invitrogen) were used as secondary antibodies. Nuclei were stained with DAPI (1:200, Thermo Fischer Scientific-D1306).

GnRH1 and LH: pituitaries were dissected and fixed in 4% PFA overnight, then replaced with 100% MeOH and stored at -30ºC until use. Fixed pituitaries were then rinse three times in 1xPTW and blocked with Blocking One Solution (Nacalai, 03953-95). An anti-medaka LH (mouse, 1:150, gifted by Dr. Ogiwara from Hokkaido University) and anti-medaka GnRH1 (rabbit, 1:150, gifted by Dr. Okubo from The University of Tokyo) were used as primary antibodies. An anti-mouse-Alexa fluor 568 (1:200, Invitrogen), and anti-rabbit-Alexa fluor 488 (1:200, Invitrogen) were used as secondary antibodies. Nuclei were stained with DAPI (1:200, Thermo Fischer Scientific-D1306).

2.2.8 LH immunofluorescence and images quantification

As described in section 2.2.7, pituitaries dissected at 23 h, 16 h and 3 h before ovulation and fixed in 4% PFA overnight, then replaced with 100% MeOH and stored at -30ºC until use. Fixed pituitaries were then rinse three times in 1xPTW and blocked with Blocking One Solution (Nacalai, 03953-95). An anti-medaka LH (mouse, 1:150, gifted by Dr. Ogiwara from Hokkaido University) and an anti-mouse-Alexa fluor 488 (1:200, Invitrogen) were used as primary and secondary antibodies, respectively. Nuclei were stained with DAPI (1:200, Thermo Fischer Scientific-D1306).

Samples were scanned with a confocal microscope (Olympus, FLUOVIEW FV1000) at 1 μm step size. The expression of LH was measured in terms of gray scale (fluorescence intensity) with Fiji software. However, considering the uneven size of the samples, a total

of 9 ROIs of the same size covering the area of the LH expressing cells were created. Next, the gray scale was quantified in each ROI and the average was plotted in Fig. 2.14.

2.2.9 RT-qPCR

Cyp21a2 in follicles: total RNA was purified with TriPure Isolation Reagent (ROCHE, 11667165001) from small, medium and large follicles isolated from wild-type medaka. Complementary DNA (cDNA) was synthesized from total RNA with ReverTra Ace (TOYOBO, FSQ-301) and used as a template for RT-qPCR with KOD SYBR qPCR Mix (TOYOBO, QKD-201). Primer sets are described in Table 2.1.

Maturation and ovulation-related genes: total RNA was purified with TriPure Isolation Reagent (ROCHE, 11667165001) from fully-grown oocytes at 10 different time points covering the entire process of oocyte maturation in medaka (Fig. 2.15). Complementary DNA (cDNA) was then synthesized from total RNA with ReverTra Ace (TOYOBO, FSQ-301) and used as a template for RT-qPCR with KOD SYBR qPCR Mix (TOYOBO, QKD-201). Primer sets used to amplify *hsd17b12, ep4b, pai1,* and *mmp15* are described in Table 2.1.

2.2.10 Cell transplantation

Fertilized eggs (*cyp21a2+/-_olvasp*:EGFP cross) were raised in an 1xERM medium until the 8~16-cell stage, stage at which embryos were dechorionated. At the morula stage, EGFP+ cells were transplanted from mutant donors to wild-type recipients. Donors and recipients were raised as pairs in an agarose plate at RT. The next day, donors were sex and genotyped, and recipients were pooled accordingly until hatching (Fig. 2.9).

Chimera medakas at 3mph were crossed with wild-type medakas to check their fertility. After eggs collection, fish were fixed for histology analysis.

2.2.11 In vitro ovulation (IVO)

Mature follicles (with completed germinal vesicle break down: GVBD) were isolated at 3 h before ovulation which correlates with the light onset in the medaka room (8:00 am). Follicles were then culture in L-15 medium at 26ºC for 11 h. The ovulation, judge by the release of the mature oocyte from their follicle cells, was recorded hourly (Fig. 2.18A).

At the end of the in vitro culture, follicles were flash-frozen in liquid nitrogen and subjected to gene expression analysis for *mmp15, pai1 and ep4b* (ovulation-related genes) by RT-qPCR. Details on RT-qPCR are described in section 2.2.9.

2.3 Results

2.3.1 The *cyp21a2* mutant medaka shows typical secondary sex characteristics

A steroid hormone profile was performed on 1-3µL of total blood from the 10% of the homozygous mutants that reached adulthood by LC-MS/MS (Fig. 2.1). This analysis was conducted with the aim of ruling out any other hormonal imbalance different to that observed in the analysis using medaka larvae, described in Chapter I (Fig. 1.6).

As a result, a reduction in the levels of 11-deoxycortisol and more importantly significantly high levels of 17α-hydroxyprogesterone and 21-deoxycortisol (cortisol metabolic precursors) was observed in adult homozygous mutants. This was consistent with the results on mutant larvae at 13dph (Fig. 2.1). Nonetheless, this time unexpectedly, cortisol could be detected although at low levels in adult homozygous mutants, which suggests a CYP21A2-independent cortisol biosynthesis pathway in medaka.

Besides the hormonal imbalance, an obvious interrenal and pituitary hyperplasia in adult homozygous mutants were observed (Fig. 1.9). Therefore, hereafter all experiments related to the analysis of the impact of cortisol on medaka reproductive aspects were conducted in these adult fish.

In humans, the sex reversal phenotype of external genitalia is often reported in 46, XX patients with deficiency in the CYP21A2 enzyme. However, *cyp21a2* homozygous mutant medakas showed typical secondary sex characteristics similar to those observed in wild-type, such as short round-shape fins and urogenital papilla in females. In males, a long and sharpened dorsal and anal fins were observed (Fig. 2.2). Over several generations, only 2 out of more than 100 homozygous mutants were recorded to have undergone a female-to-male sex reversal event. Therefore, sex reversal events were low in our *cyp21a2* mutant line.

2.3.2 Gonadal morphology and fertility in *cyp21a2* homozygous mutants

Homozygous mutant males were fertile (Fig. 2.3A-B) and no defects were observed at either the tissue or cellular level in the testis (Fig. 2.3C-F). In contrast, homozygous mutant females showed ovarian enlargement which resulted in a significantly high gonadosomatic index (GSI), over 50% (Fig. 2.4).

Mutant females were infertile and never spawned eggs (Fig. 2.5A, B.1). Accumulation of many fully-grown oocytes was observed in mutant ovaries and histological sections revealed a certain degree of tissue disorganization (Fig. 2.5B-E). No statistically significant differences were observed in terms of fertility between heterozygous mutant females and the wild-type (Fig. 2.5A, B.1). These results, therefore, show a clear sexual difference in terms of reproduction in the *cyp21a2* homozygous mutant medaka.

2.3.3 Compromised fertility in *cyp21a2* homozygous mutant is due to systemic cortisol deficiency

Two hypotheses were thought to possibly explain to some extent the ovarian enlargement observed in homozygous mutant females (Fig. 2.4). First, cortisol is involved in germ cell proliferation (higher in the mutant), or second, cortisol is involved in oogenesis.

To address the first, the number of germ cells were counted on confocal images from 0-dph to 5-dph larvae. However, no significant increase in either the number of germ cells or the percentage of germ cells in meiosis was observed (Fig. 2.6), suggesting a possible role for cortisol in oogenesis. In this regarding, the expression analysis of *cyp21a2* in medaka ovary by WISH, revealed that small oocytes (primary and previtellogenic oocytes) express *cyp21a2* (Fig. 2.7A-B). This data was later corroborated by a significantly high expression of *cyp21a2* in small oocytes by RT-qPCR (Fig. 2.7C).

WISH and RT-qPCR data suggested a possible role of *cyp21a2* in the medaka germline. Since *cyp21a2* mRNA was mainly detected in small oocytes, it was hypothesized that cortisol may be synthesized by the CYP21A2 enzyme in medium (vitellogenic) or large (late vitellogenic and post-vitellogenic) oocytes in the medaka ovary, and thus play a cell-autonomous role. This possibility was preliminary confirmed by detecting cortisol in a steroid hormones profile from whole ovaries by mass spectrometry analysis. Cortisol was not detected in homozygous mutant ovaries (Fig. 2.8A). Subsequently, steroid hormones were extracted and analyzed from isolated follicles classified as small, medium, and large oocytes (Fig. 2.8B). Interestingly, cortisol was detected in large follicles in the heterozygous control group. High levels of 17α-hydroxyprogesterone were detected in homozygous mutant follicles instead (Fig. 2.8B).

Next, to probe the hypothesis that medaka germline (likely oocytes) are capable of synthesizing cortisol by the CYP21A2 and that this is essential for oogenesis, chimera medakas where generated by transplanting mutant germ cells expressing EGFP under the control of *olvas* promoter (a germ cell marker) into a wild-type host or recipient (Fig. 2.9). Sexually mature adult chimeras (~3mph) were then crossed with wild-type males to assess their fertility. However, unexpectedly, EGFP+ and EGF-(EGFP) eggs from chimera females could be collected. After genotyping, all EGFP+ and EGFP- were heterozygous and wild-type embryos, respectively (Fig. 2.10).

Chimera medakas transplanted with either XX or XY (germ cells) did not show any defects in oogenesis (Fig. 2.11, B.2). Likewise, no defects were observed in the F1 at the hatching stage (Fig. 2.12) or in the ovary of chimera medakas (Fig. 2.13). Thus, the cortisol detected in the ovary of medaka by mass spectrometry analysis, is mainly of systemic origins rather than from the germline, and most likely supplied by the interrenal gland. Moreover, although the presence of the CYP21A2 protein in the medaka germline was not analyzed in this study, cell transplantation results revealed that, if present, CYP21A2 protein is indispensable for oogenesis and embryogenesis in a germ cell-autonomous mechanism.

2.3.4 HPG-axis related genes are expressed in *cyp21a2* homozygous mutants

The mass spectrometry data from follicles at different stages showed that systemic cortisol is mainly supplied to late-vitellogenic and post-vitellogenic follicles (described as L: large follicles in Fig. 2.8B). These follicles are in the maturation phase, which is known to be tightly controlled by the activity of gonadotropins, particularly the luteinizing hormone or LH. Therefore, the expression of the hypothalamus-pituitary-gonad (HPG)

axis-related genes was analyzed by immunofluorescence and confocal microscopy. As a result, the proteins GnRH1, LH, and LHr (receptor) were found expressed in homozygous mutant females (Fig. 2.13).

Considering that medaka is a daily spawning fish, it was then asked whether the LH fluctuation, rather than the expression, is impaired under the deficiency of cortisol. To analyze this possibility, pituitaries were isolated at three different time points: 23 h, 16 h, and 5 h before light onset in our fish room which correlates with the ovulation time in medaka (Fig. 2.14). LH fluctuation was studied by quantifying the fluorescence intensity of confocal images of pituitaries. As a result, an increase in the intensity of the fluorescence was observed in both the heterozygous (control) and homozygous mutant pituitaries at 16 hours before ovulation, which correlates with the time reported for LH surge in medaka (Fig. 2.14) (Ogiwara et al., 2013). However, interestingly, the signal in the control group decreases as the time for ovulation gets closer (5 h), and the intensity of the fluorescence of LH in the mutant was still high and over the values observed in the control group (Fig. 2.14G). Thus, cortisol deficiency negatively influences LH fluctuation in medaka.

2.3.5 PCOS-like phenotype in *cyp21a2* homozygous mutants

The disruption of the LH fluctuation in homozygous mutant females prompted us to analyze the oocyte maturation process in medaka. Large follicles were isolated at ten different time points expecting to cover the entire maturation process considering the daily spawning nature of the medaka fish (Fig. 2.15).

In the wild-type, only one batch of large follicles were observed at each time point. In the homozygous mutant, multiple batches of follicles undergoing maturation and oocyte growth simultaneously were observed instead. This reminded of the PCOS phenotype

described in humans (Fig. 2.15). The expression of the *hsd17b12* gene which encodes the enzyme responsible for the synthesis of the maturation inducing hormone or MIH was then analyzed. As a consequence, while in the wild-type this enzyme was found strictly and timely expressed at 8 h before ovulation, an aberrant expression was observed in the homozygous mutant (Fig. 2.16A). In fact, the *hsd17b12* gene was found expressed in follicles from 16 h to 8 h before ovulation. It is noteworthy to say that homozygous mutant oocytes also undergo GVBD.

Curiously, at the time of ovulation in the wild-type, ovulated and mature oocytes were found in the ovarian cavity. However, in the homozygous mutant, non-ovulated oocytes in the ovary were noticed (Fig. 2.15). A gene expression analysis of some ovulation-related genes including *pai1, ep4b,* and *mmp15* was conducted, and as a result, all of them were specifically expressed in follicles at the maturation phase. The genes were found expressed not only at a time different to that from the wild-type, but also highly upregulated in mutant follicles (Fig. 2.16B-D).

Disruption of the LH fluctuation, aberrant expression of *hsd17b12* (whose expression depends on the activity of the LH), and the PCOS-like phenotype observed in homozygous mutants, prompted to analyze the levels of 17α-hydroxyprogesterone, MIH, and androgens in the mutant ovary. Indeed, significantly high levels of 17α-hydroxyprogesterone and MIH were found in mutant ovaries. Although not statistically significant, high levels of androgens were also detected in mutant ovaries (Fig. 2.17). These factors may contribute to the development of the PCOS-like phenotype observed in mutant female medakas.

2.3.6 Ovulation defects in *cyp21a2* homozygous mutants

Since non-ovulated follicles were observed in mutant ovaries, an in vitro ovulation system was established (Fig. 2.18A). Follicles were isolated at 3 h before ovulation, and after 11 h of in vitro culture over 90% of the oocytes were successfully ovulated in the heterozygous control group. In contrast, homozygous mutant follicles failed to do so, remaining retained in their follicle cells even after 11 h of in vitro culture (Fig. 2.18B, B.3). Relative expression of three ovulation-related genes *mmp15, pai1* and *ep4b*, showed an aberrant expression pattern in mutant follicles (Fig. 2.18C).

Subsequent analysis of the morphological changes in granulose cells during maturation was conducted by histology. Importantly, granulose cells acquired a cubic shape in the following stages after expression of the *hsd17b12* gene at 8 h before ovulation in wild-type follicles (Fig. 2.19A-C, B.4). In the mutant, however, granulose cells showed signs of nuclei fragmentation. Besides, granulose cells were found isolated within the follicle cells layer suggesting defects in cell junctions (Fig. 2.19D-F, B.5).

2.3.7 Parthenogenetic activation in *cyp21a2* homozygous mutants

A very interesting phenomenon was observed in mutant follicles during the time course of the in vitro ovulation experiment, that is parthenogenetic activation (Fig. 2.21A-B).

One hour after in vitro culture, around 30% of the homozygous mutant oocytes showed signs of parthenogenetic activation. Mutant oocytes proceeded to 1-cell stage without fertilization, and eventually stopped before zygotic activation (Fig. 2.21C-D). The activated zygote remains within the follicle cells. This phenomenon was not only restricted

to our in vitro ovulation system, since this phenomenon was also observed in mutant ovaries (Fig. 2.21F).

2.4 Discussion

Although homozygous mutant medakas at 13dph were unable to synthesized cortisol, mass spectrometry analysis of steroid hormones on total blood from sexually mature mutants revealed low levels of cortisol. This data suggests an activation of a CYP21A2-independent pathway for the synthesis of cortisol. Although alternative or backdoor pathways for androgen synthesis in which the *cyp17a1* is the key factor, has been described (Fukami et al., 2013; Storbeck et al., 2019), no alternative pathways have been described for cortisol. One possible explanation could be that unlike mammals where a single CYP17A1 enzyme has a dual activity 17,20 lyase and hydroxylase, teleost fish has retained two copies of the *cyp17a* gene, the *cyp17a1* (hydroxylase and lyase) and the *cyp17a2* (hydroxylase) (Pallan et al., 2015). Interestingly, CYP17A2 is the only one expressed in the interrenal gland (Fig. 1.7). Thus, considering the several alternative pathways already described for this enzyme, it is possible that the CYP17A2 may be involved in the low synthesis of cortisol in the CYP21A2-deficient medaka. The low levels of cortisol detected in the CYP21A2-deficient medakas could then explain why 10% of the homozygous mutants survive till adulthood, nonetheless, it also put in evidence that although synthesized, the levels of systemic cortisol in mutant medakas are insufficient to prevent the appearance of the typical phenotypes of the cortisol-deficiency condition.

In humans, it has been reported that 46, XX patients diagnosed with 21OHD experience either sex reversal or virilization of the external genitalia (Merke and Auchus, 2020; Auer et al., 2023). In contrast, high adrenal-derived androgens do not affect the

sexual differentiation of 46, XY patients (Merke and Auchus, 2020). Accordingly, in *cyp21a2* mutant medakas, males did not show defects in the development of sexual (secondary) sex characteristic and fertility. However, unlike in humans, mutant females did not undergo masculinization of the secondary sex characteristics (Fig. 2.2). In fact, only 2 out of more than 100 homozygous mutant females were recorded as a sex reversal.

Accumulation of precursor steroids such as 17α-hydroxyprogesterone leads to androgen excess through the androgen backdoor pathway in humans (Reisch et al, 2019; Storbeck et al., 2019). Although no statistically significant, high levels of androgens were detected in mutant females (Fig. 2.17). This could potentially cause female-to-male sex reversal of medaka secondary sex characteristics, however, that was not the case. This discrepancy may be explained by 1) differences of the amount in the most potent androgen for the differentiation of the secondary sex characteristics between medaka (11keto-testosteone) and human (5α-dihydroxy testosterone) or 2) high estrogen levels (derived from 17OHP4) may counteract the virilizing effect of the androgens in medaka.

In addition to the masculinization of the external genitalia, a polycystic ovary syndrome or PCOS, ovulatory defects, menstrual irregularities, and infertility issues have been reported in 46,XX patients with 21OHD (Ghayee and Auchus, 2007; Merke and Auchus, 2020). This is mainly attributed to high levels of androgens as a consequence of the significant increase in levels of the 17-hydroxypregnenolone and 17-hydroxyprogesterone (17OHP4) which are destined to the androgen synthesis pathway by the *cyp17a1* enzyme through the androgen backdoor pathway (Pignatelli et al., 2019; Storbeck et al., 2019; Reisch et al, 2019). In agreement with this, ovulatory and granulose cells defects, and accumulation of fully-grown oocytes were observed in mutant females.

These phenotypes may explain the infertility issues found in females, and the androgen excess could in part explain the defects in the ovary.

Remarkably, considering that testosterone can be readily aromatized in E2 in the ovary by the activity of the CYP19A1, and a recent study in mice has proposed a direct and indirect (estrogen-ER) androgenic action could drives defects in the ovary (PCOS phenotype) (Hillier et al., 1994; Aflatounian et al., 2020), thus, further studies will help to clarify whether androgens or estrogens are the main cause of the phenotypes observed in *cyp21a2* mutant medakas.

Interestingly, mature oocytes in the homozygous mutant undergo spontaneous parthenogenetic activation (Fig. 2.22). This suggests a new role for cortisol in reproduction. The new mechanism for cortisol controlling meiotic arrest is an interesting direction for future studies. In Chapter 3, preliminary observations of this phenomenon are described.

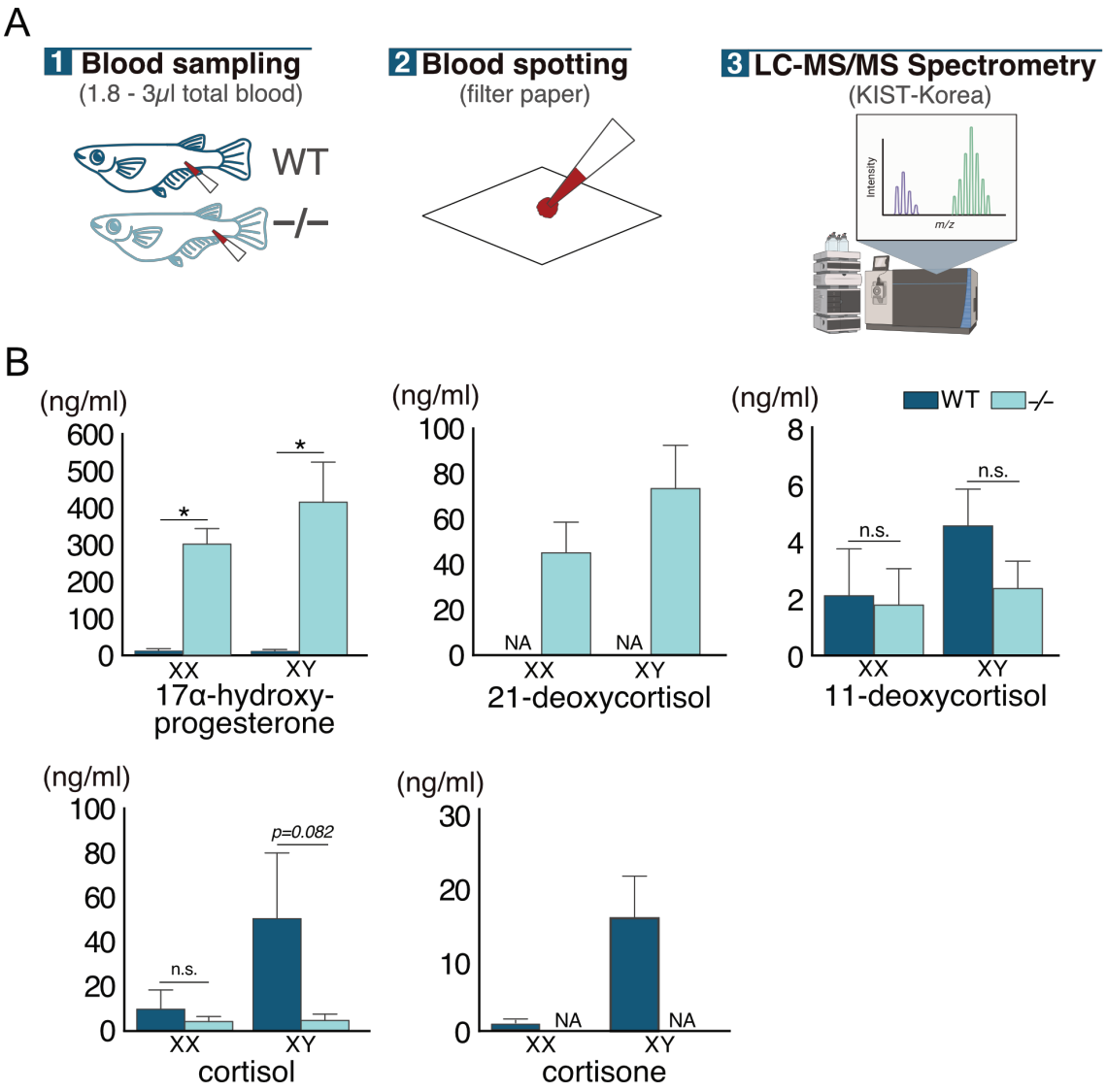

Figure 2.1 Steroid hormones profile in total blood

(A) Schematic representation of total blood sample collection and preparation for LC-MS/MS measurement. **(B)** Steroid hormones profile from total blood extracted from adult and sexually mature medakas. All graphs are presented with bar, mean; error bar, S.E.; N.A., not applicable (due to a low amount), n.s., non-significant; *$P < 0.05$ by Student's *t*-test.

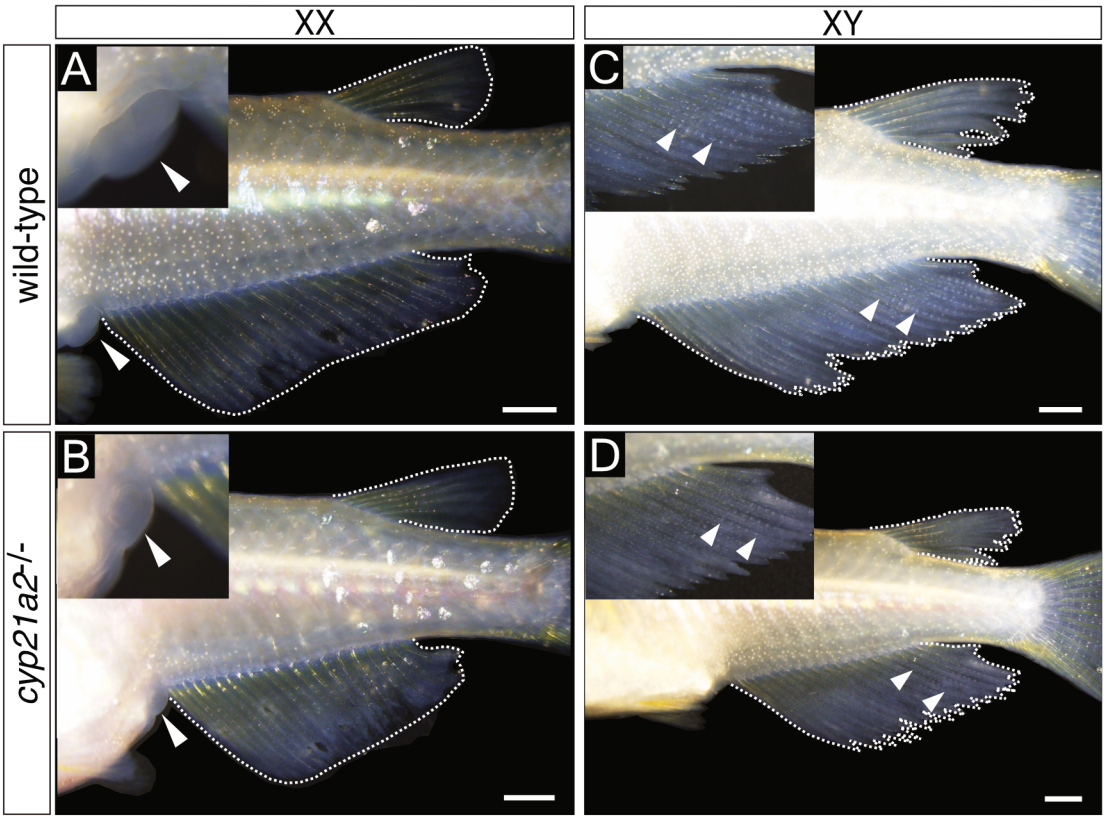

Figure 2.2 Secondary sex characteristics in *cyp21a2* homozygous mutants

Secondary sex characteristics in wild-type and homozygous mutant **(A-B)** females (white arrowheads indicate urogenital papilla) and **(C-D)** males (white arrowheads indicate spines). Scale bar, 1 mm.

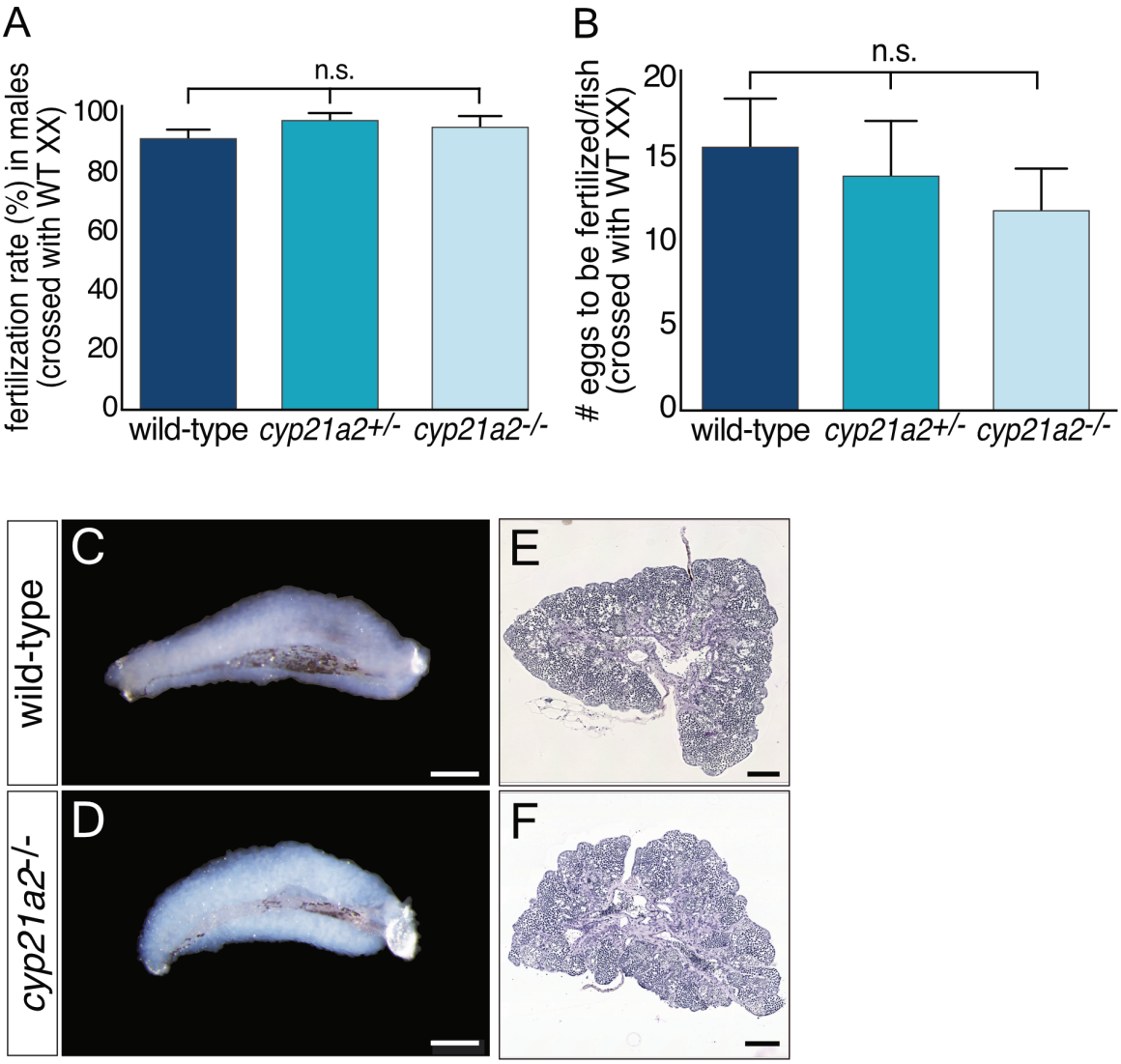

Figure 2.3 Fertility and morphology of the testis in homozygous mutant males

(A) Fertilization rate in males crossed with WT XX medaka. **(B)** Number of eggs spawned per female, and to be fertilized by XY medakas. n=3 males per genotype, data collected during 5 days. Graphs are presented with bar, mean; error bar, S.E; n.s, non-significant; by Student's *t*-test. **(C-D)** External morphology of the testes. **(E-F)** Cross section of the testes in C-D stained by the PAS Schiff-metanil yellow staining method. Scale bar, (A-B) 500 µm, (C-D) 100 µm.

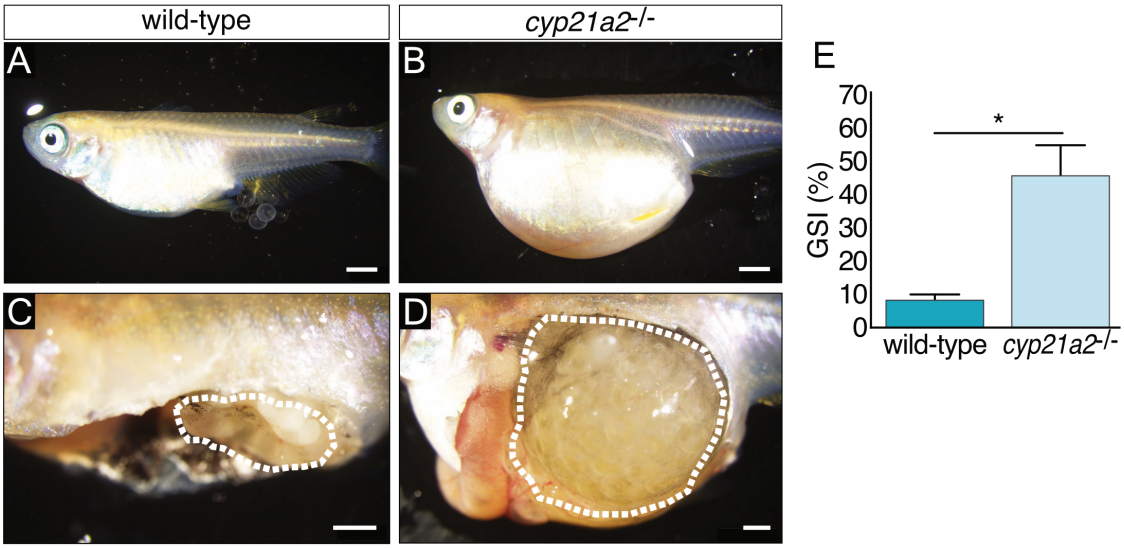

Figure 2.4 Appearance and GSI of *cyp21a2* homozygous mutant females

External appearance of **(A)** wild-type and **(B)** homozygous mutant females. **(C-D)** Appearance of the ovary related to the body cavity. The graph is presented with bar, mean; error bar, S.E; **P* < 0.01 by Student's *t*-test. Scale bar, (A-B) 2 mm, (C-D) 1 mm.

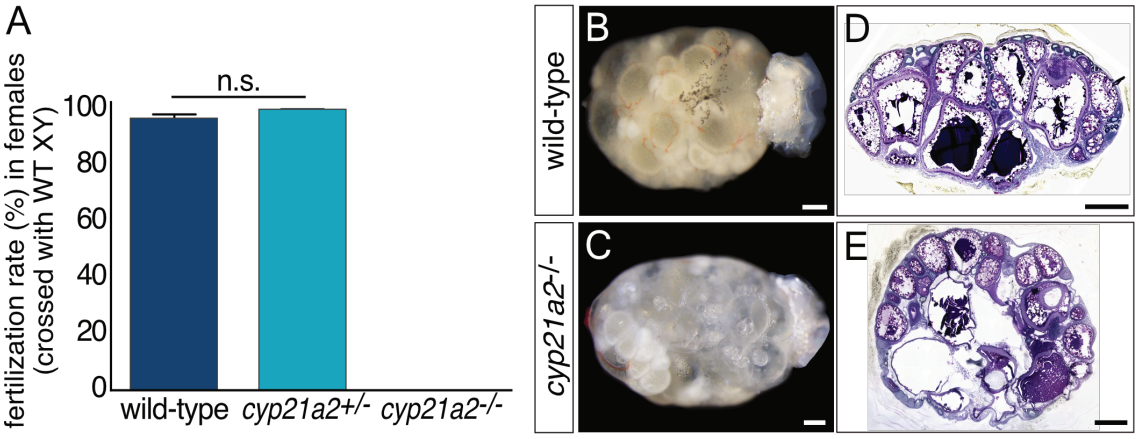

Figure 2.5 Fertility and morphology of the ovary in homozygous mutant females

(A) Fertilization rate in females crossed with WT XY medaka. n=3 females per genotype, data collected during 5 days. The graph is presented with bar, mean; error bar, S.E; n.s, non-significant; by Student's *t*-test. **(B-C)** External morphology of the ovaries. **(D-E)** Cross section of the ovaries in B-C stained by the PAS Schiff-metanil yellow staining method. Scale bar, 500 µm.

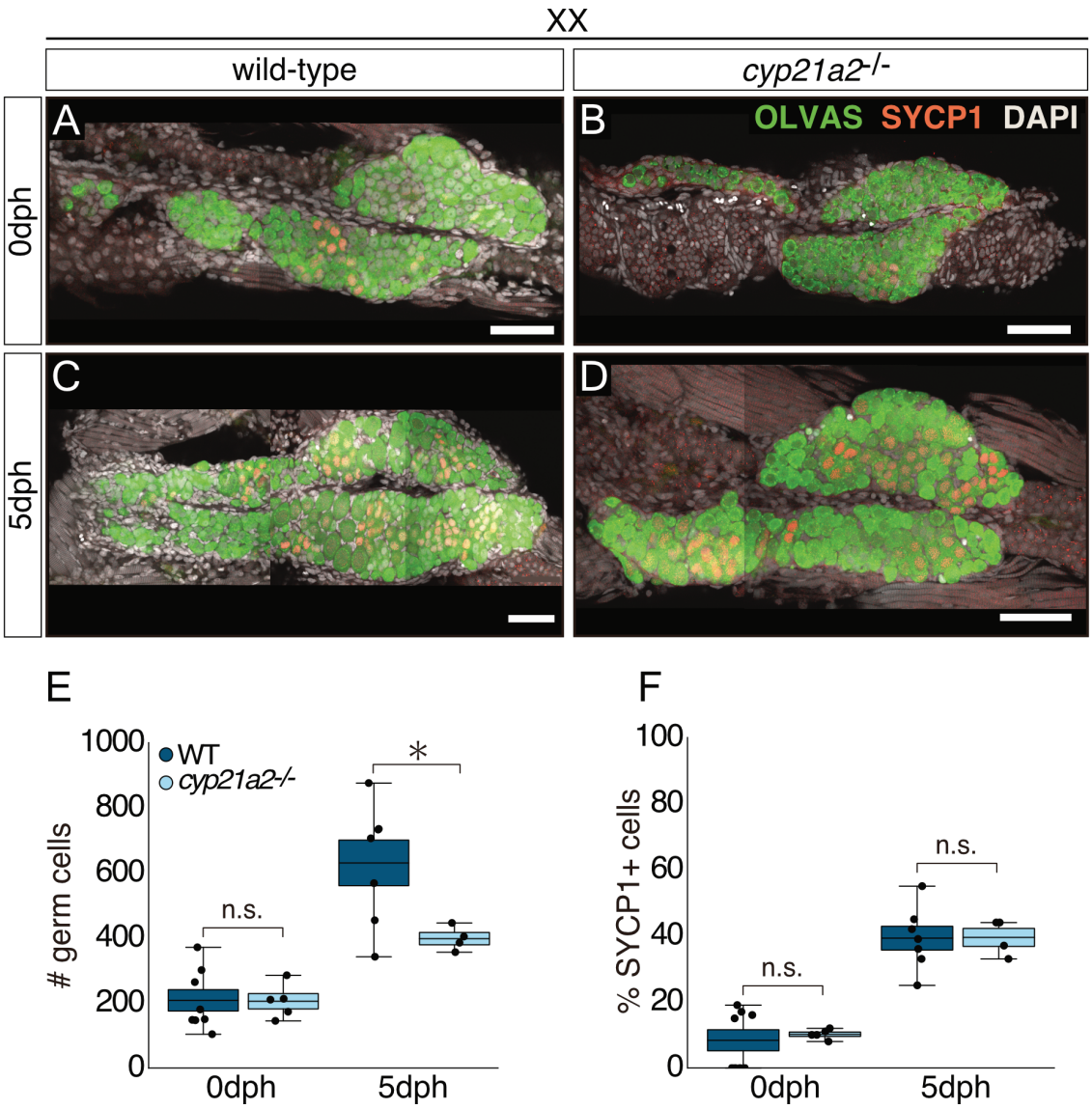

Figure 2.6 Germ cell proliferation at larval stage

Confocal images of 0dph and 5pdh larvae gonad from **(A, C)** wild-type and **(B-D)** heterozygous mutants. Germ cells were labelled with an anti-OLVAS (green) and meiocytes with an anti-SYCP1 (orange). Box plots are presented with bar, mean; error bar, S.E.; whiskers, 25 and 75 quartiles; n.s., non-significant; *$P < 0.05$ by Student's *t*-test. Scale bar, 50 µm.

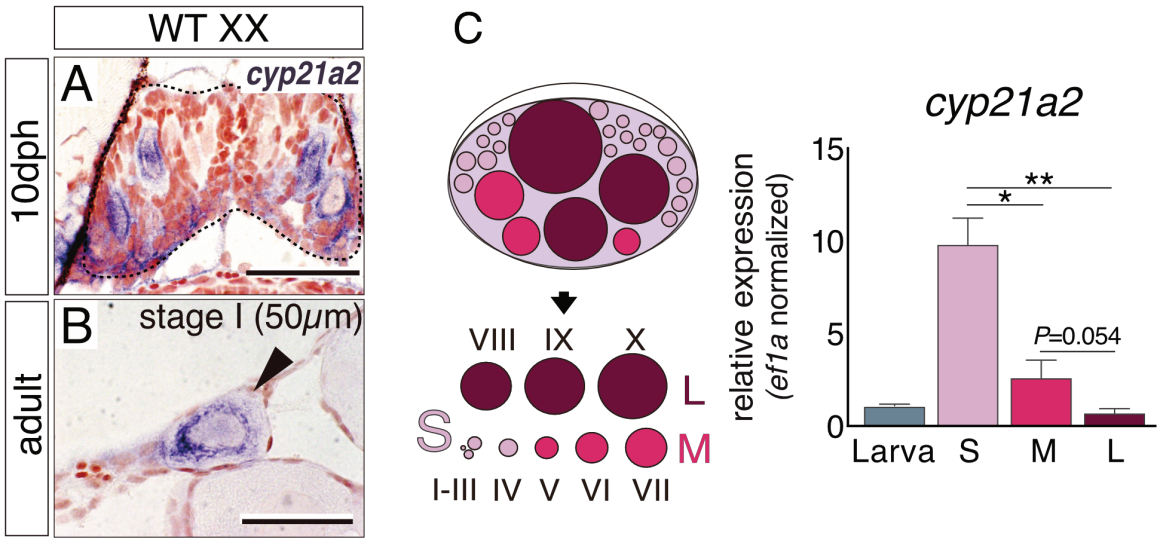

Figure 2.7 Expression of *cyp21a2* in the ovary

(A-B) WISH of *cyp21a2* in medaka ovaries. **(C)** Relative expression of *cyp21a2* in wild-type follicles. Values were *ef1a* normalized and larva was set as 1. The graph is presented with bar, mean; error bar, S.E.; **P* < 0.01, ***P* < 0.001 by Student's *t*-test. Scale bar, 50 μm.

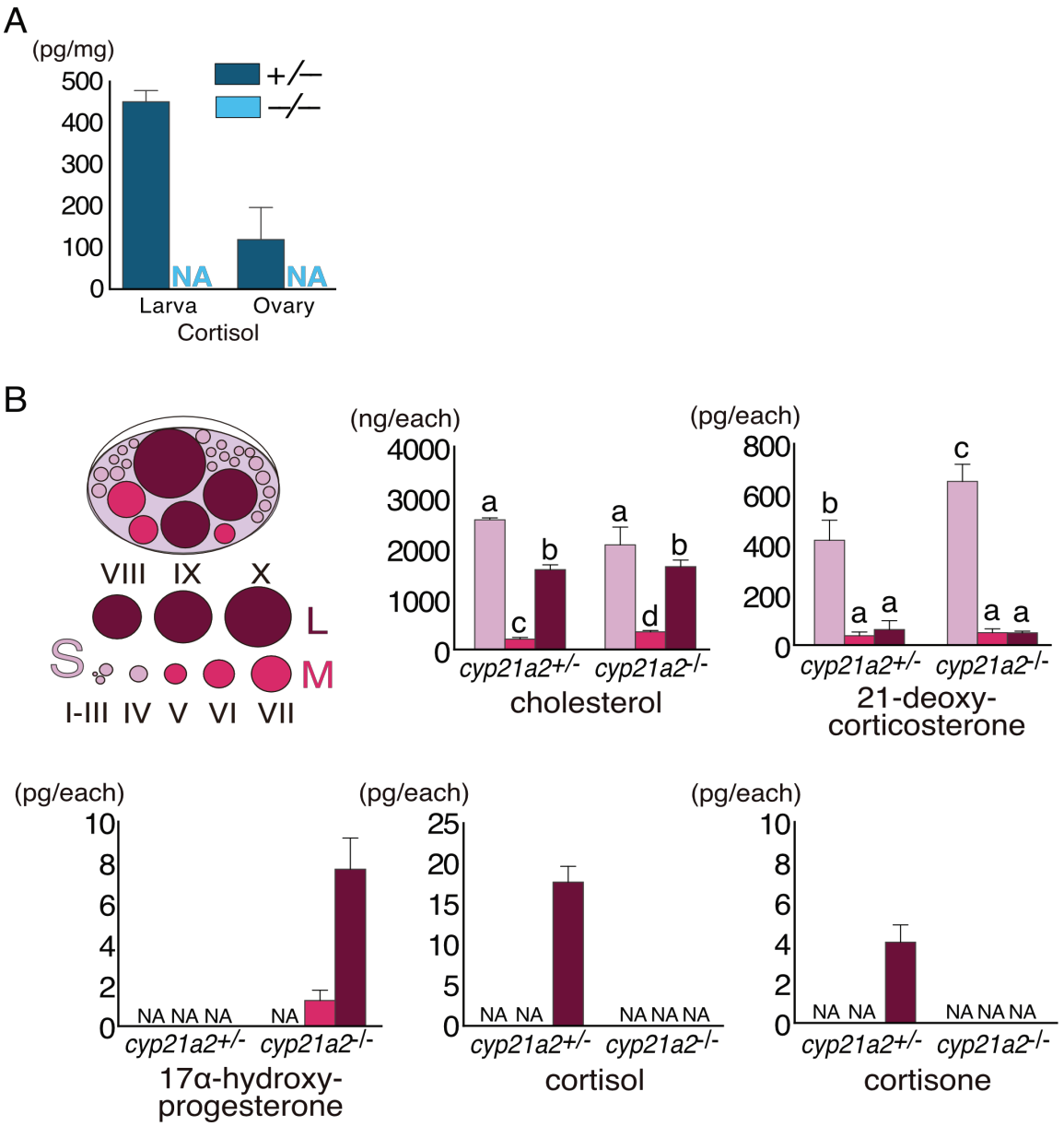

Figure 2.8 Steroid hormones profile from ovary and follicles

(A) Cortisol from whole ovaries. Values are expressed as pg of the steroid in 1 mg of dried sample. **(B)** Steroid hormones profile from three different sizes of follicles, expressed in terms of pg (ng in the case of cholesterol) per follicle. Graph are presented with bar, mean; error bar, S.E.; N.A., not applicable (due to a low amount). Different letters denote statistical differences, one-way ANOVA followed by Tukey *post-hoc* test.

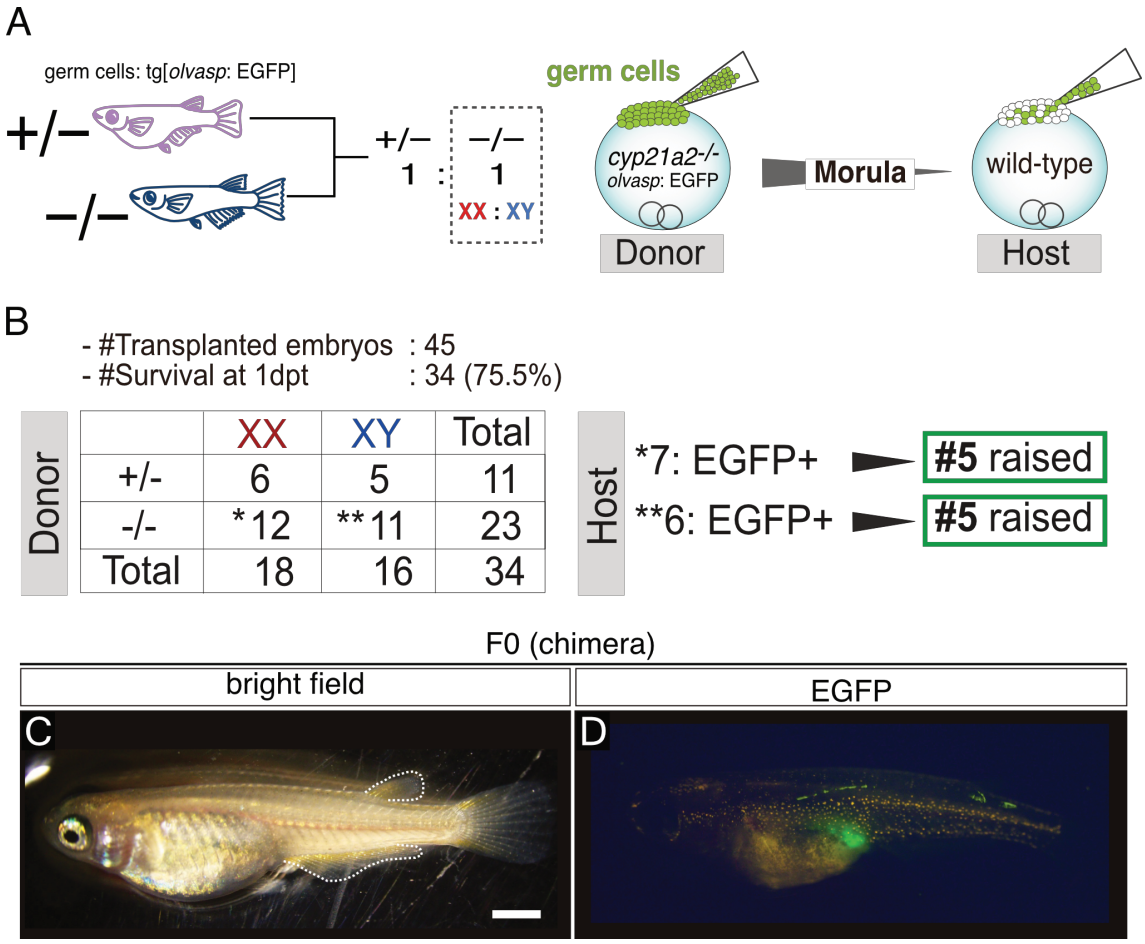

Figure 2.9 Generation of chimera medaka by cell transplantation

(A) General schema of the cell transplantation experiment. Details are described in the materials and method section "cell transplantation". **(B)** Number of transplanted embryos and successfully generated chimera medakas; dpt: days post-transplantation. **(C-D)** External appearance of a chimera female medaka showing EGFP signal in the gonadal area. Scale bar, 1 mm.

A

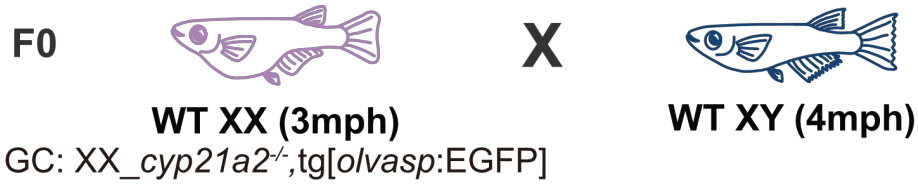

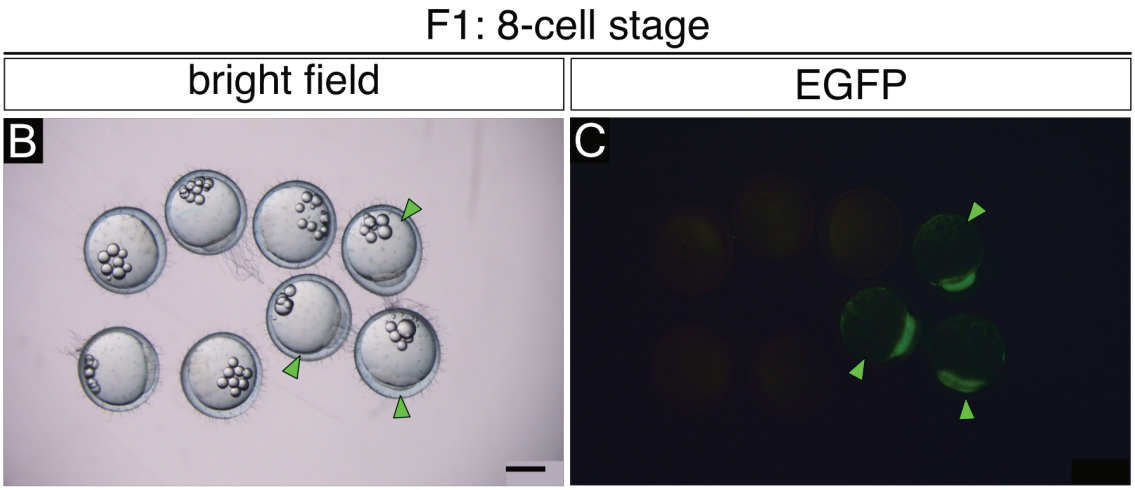

D

F1	EGFP+		EGFP-	
	XX	XY	XX	XY
WT	0	0	7	7
cyp21a2+/-	5	3	0	0

Figure 2.10 Genotyping of the F1 from chimera medaka

(A) Mating strategy of chimera medaka (XX germ cells) with XY wild-type medaka. **(B-C)** Embryos collected from A (green arrowhead; EGFP+ embryos). **(D)** Genotype and EGFP screening of the embryos from B. Scale bar, 500 µm.

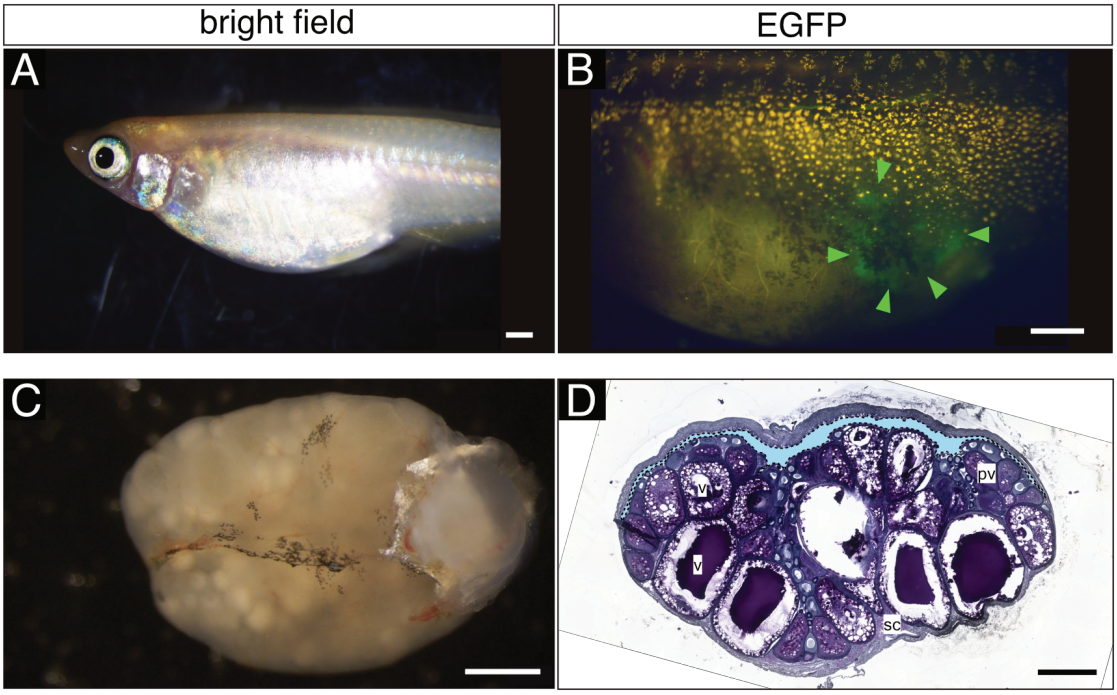

Figure 2.11 Ovarian morphology from chimera medaka

(A) External appearance of a chimera XX female medaka. **(B)** EGFP positive signal in the gonadal area. **(C)** morphology of the chimeric ovary. **(D)** Cross section of the ovary on C. Ovarian cavity is highlighted with a light-blue background. SC, stromal compartment; pv, previtellogenic oocyte; v, vitellogenic oocyte. Scale bar, (A-B) 1 mm, (C-D) 500 µm.

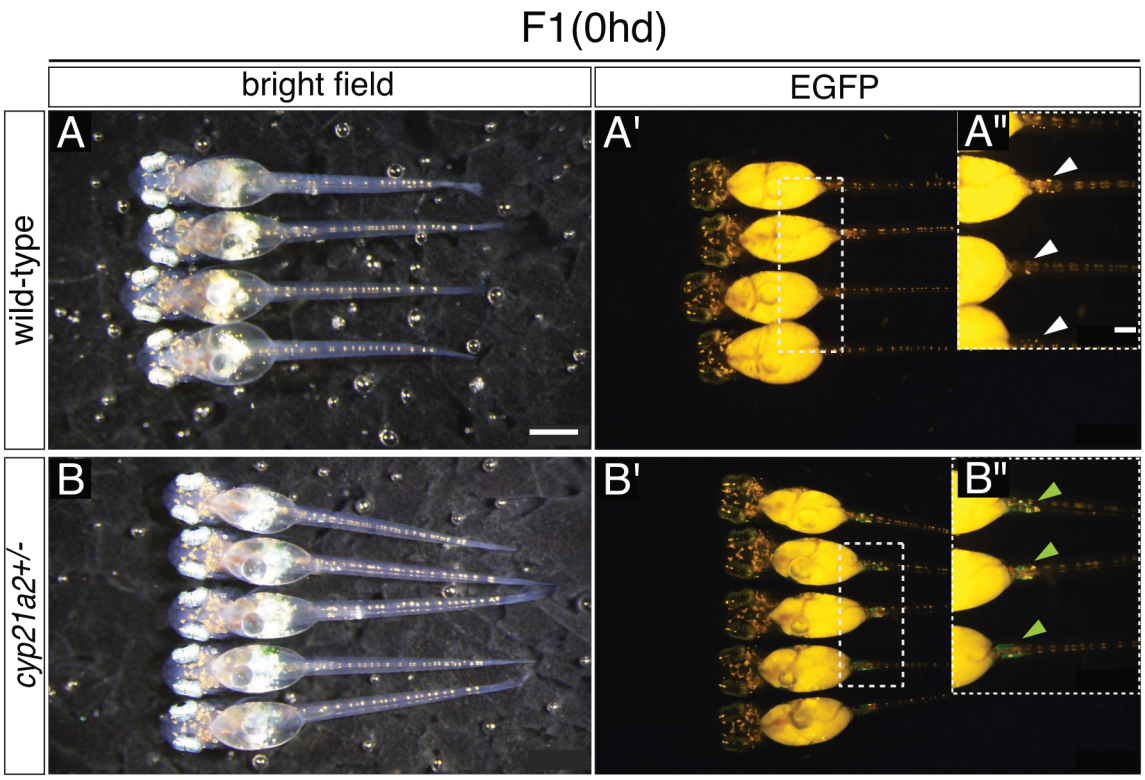

Figure 2.12 Appearance of the F1 from chimera medaka

External appearance of the **(A)** wild-type and **(B)** homozygous mutant hatchlings. White and green arrowheads indicate EGFP negative and positive, respectively. Scale bar, 500 μm.

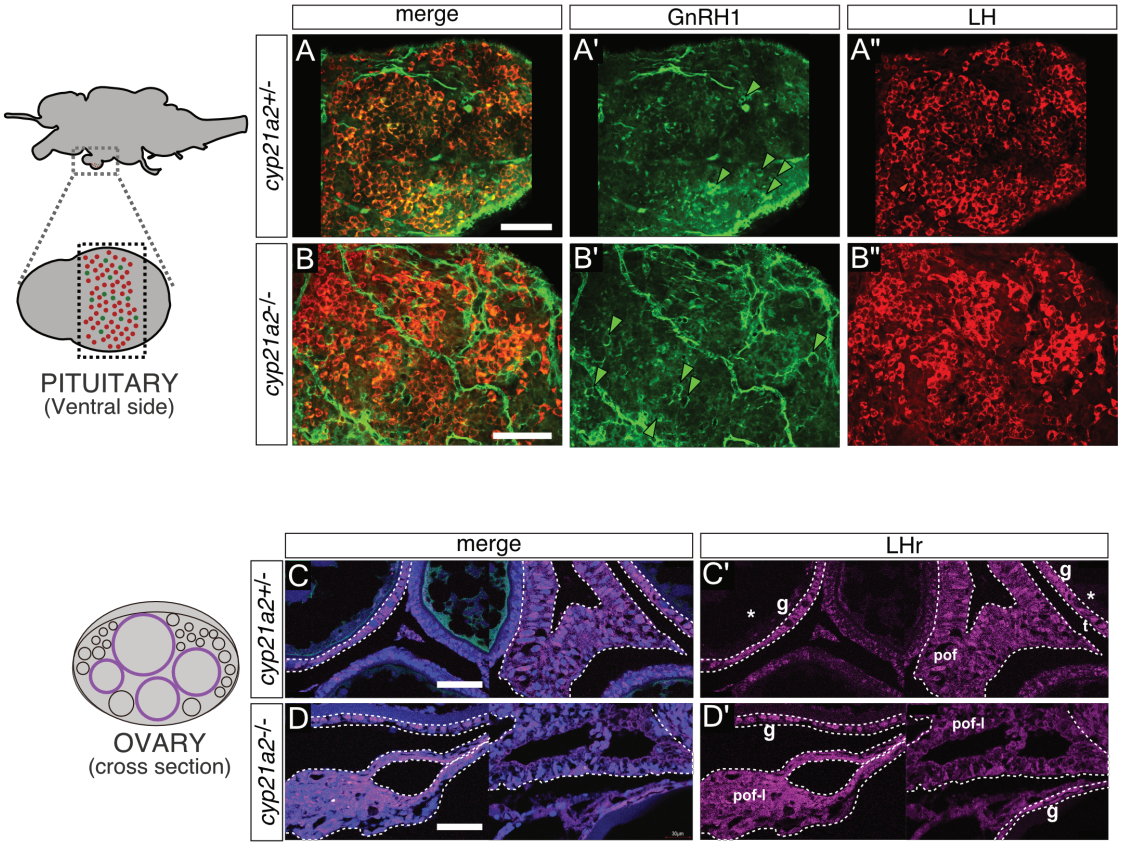

Figure 2.13 Expression of HPG-related markers in *cyp21a2* homozygous mutants

(A) Heterozygous adult female (XX) pituitary expressing (A') GnRH1 highlighted with green arrowheads and (A") LH. **(B)** Homozygous adult female (XX) pituitary expressing (B') GnRH1 highlighted with green arrowheads and (B") LH. Cross section of the ovary positive for LH receptor in **(C)** heterozygous and **(D)** homozygous mutant. g: granulose cell; t: theca cell; pof: post-ovulatory follicle; pof-l: post-ovulatory follicle-like; *oocyte. Scale bar, 50 µm.

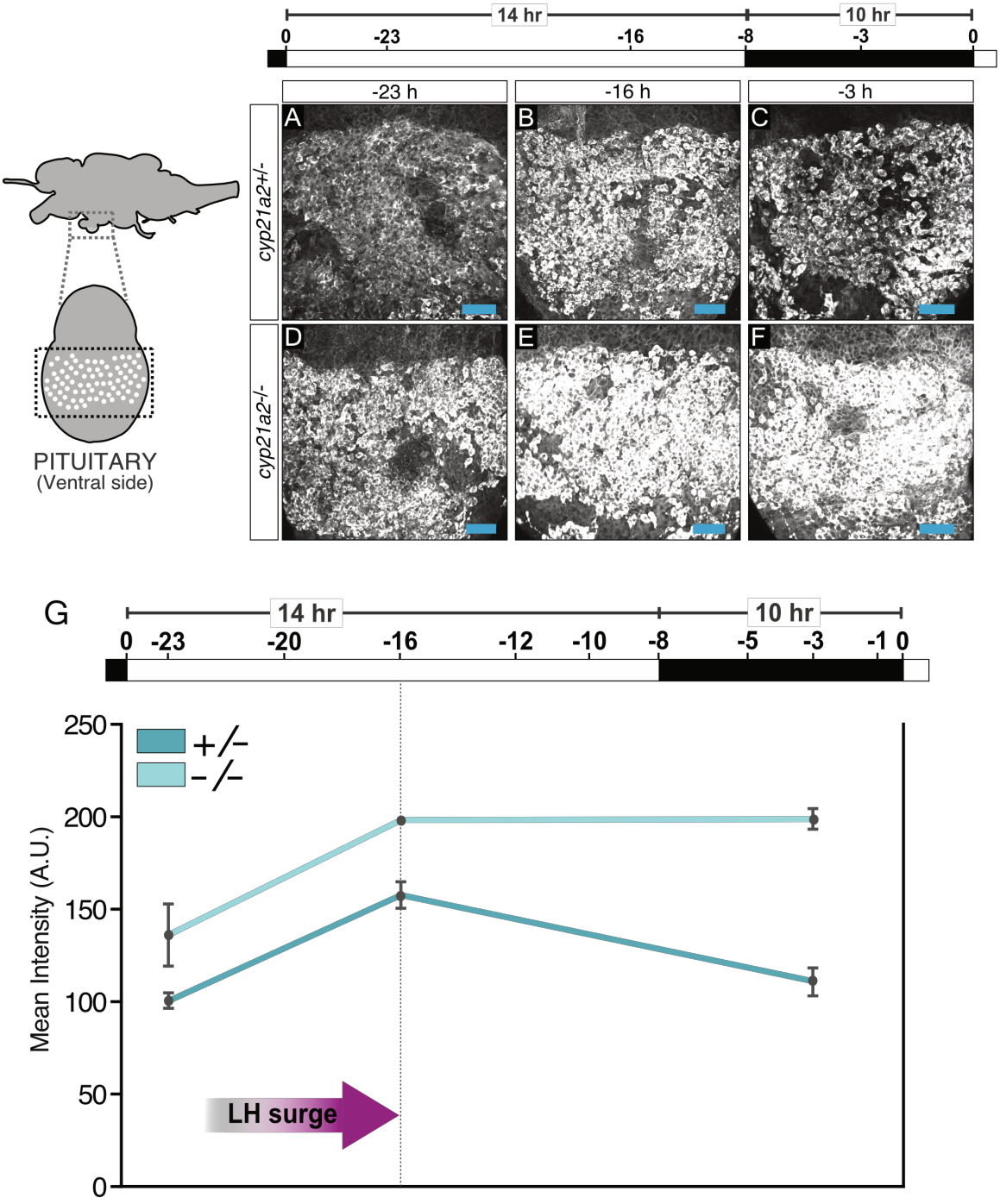

Figure 2.14 Expression and quantification of LH in *cyp21a2* homozygous mutants

LH in **(A-C)** heterozygous and **(D-F)** homozygous mutant pituitaries from XX females. Pituitaries were collected at 23 h, 16 h, and 3 h. **(G)** Mean Intensity of the LH fluorescence from confocal images on A-F. Scale bar, 40 µm.

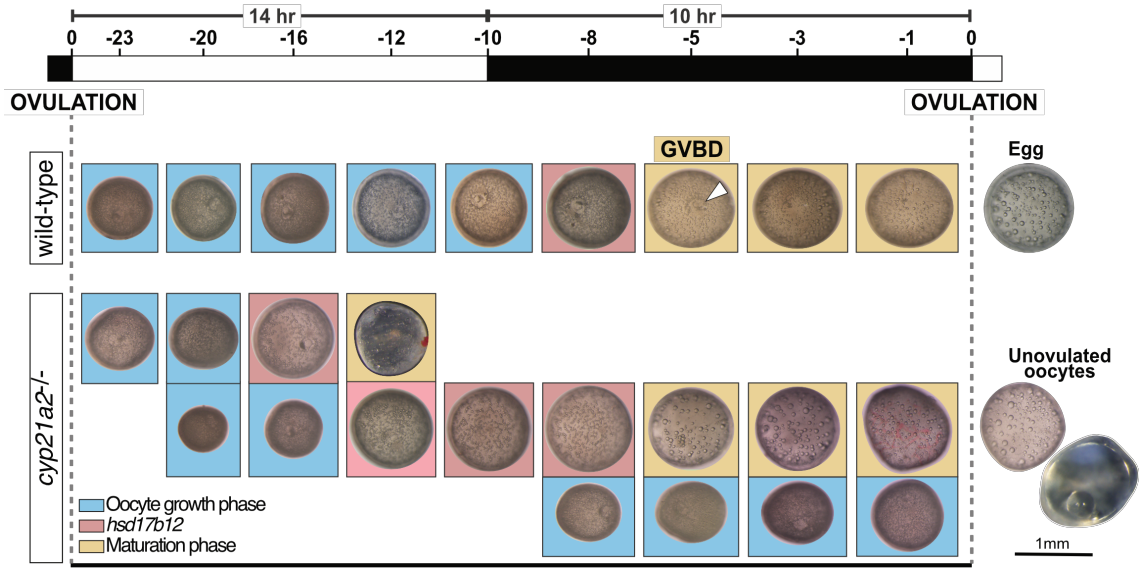

Figure 2.15 Oocyte maturation in *cyp21a2* homozygous mutants

Oocyte maturation process in medaka. Follicles were isolated at the specific time point. Background color is based on gene expression analysis of the *hsd17b12* enzyme. See Fig. 2.16.

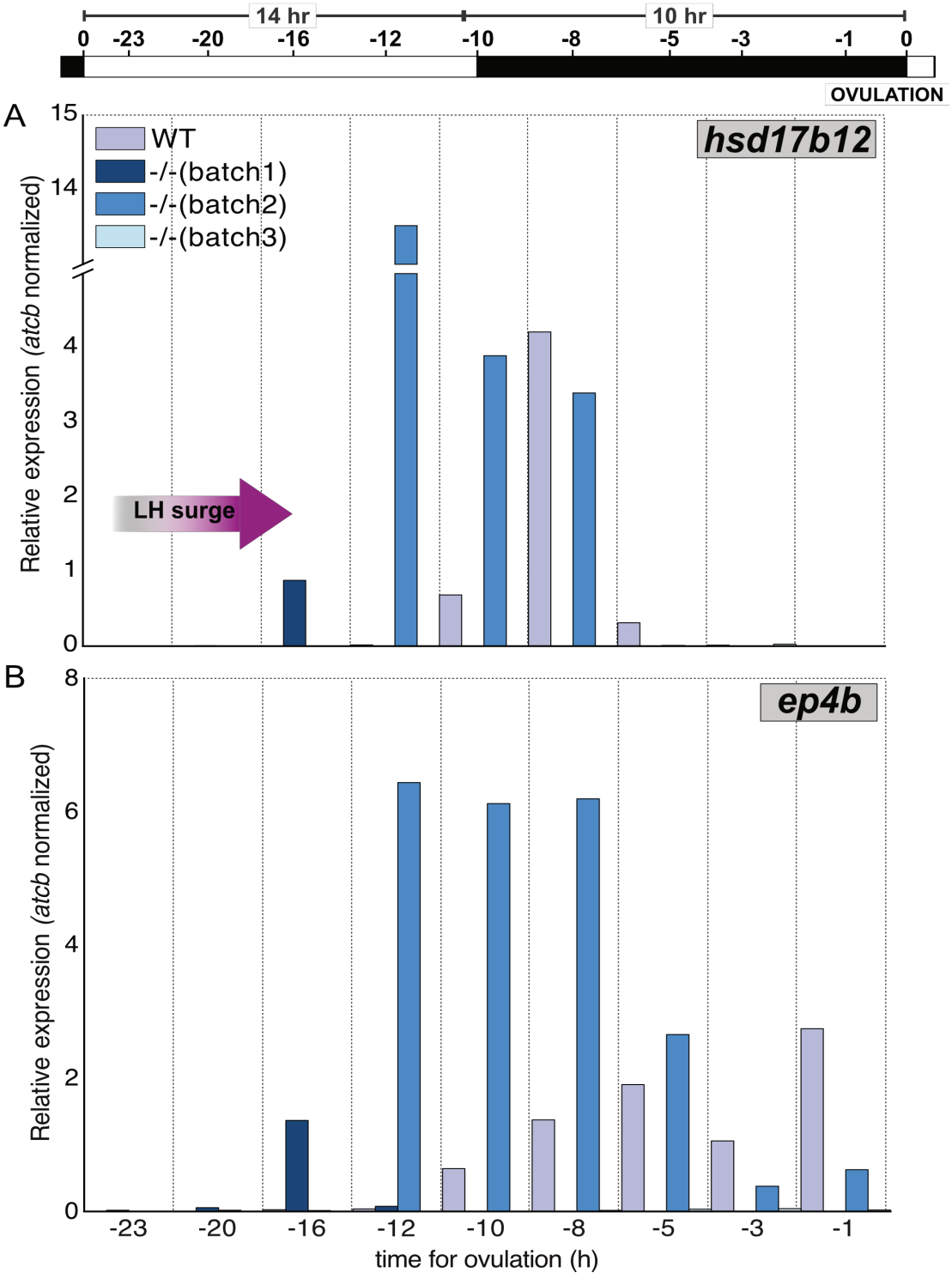

Figure 2.16 continued on next page

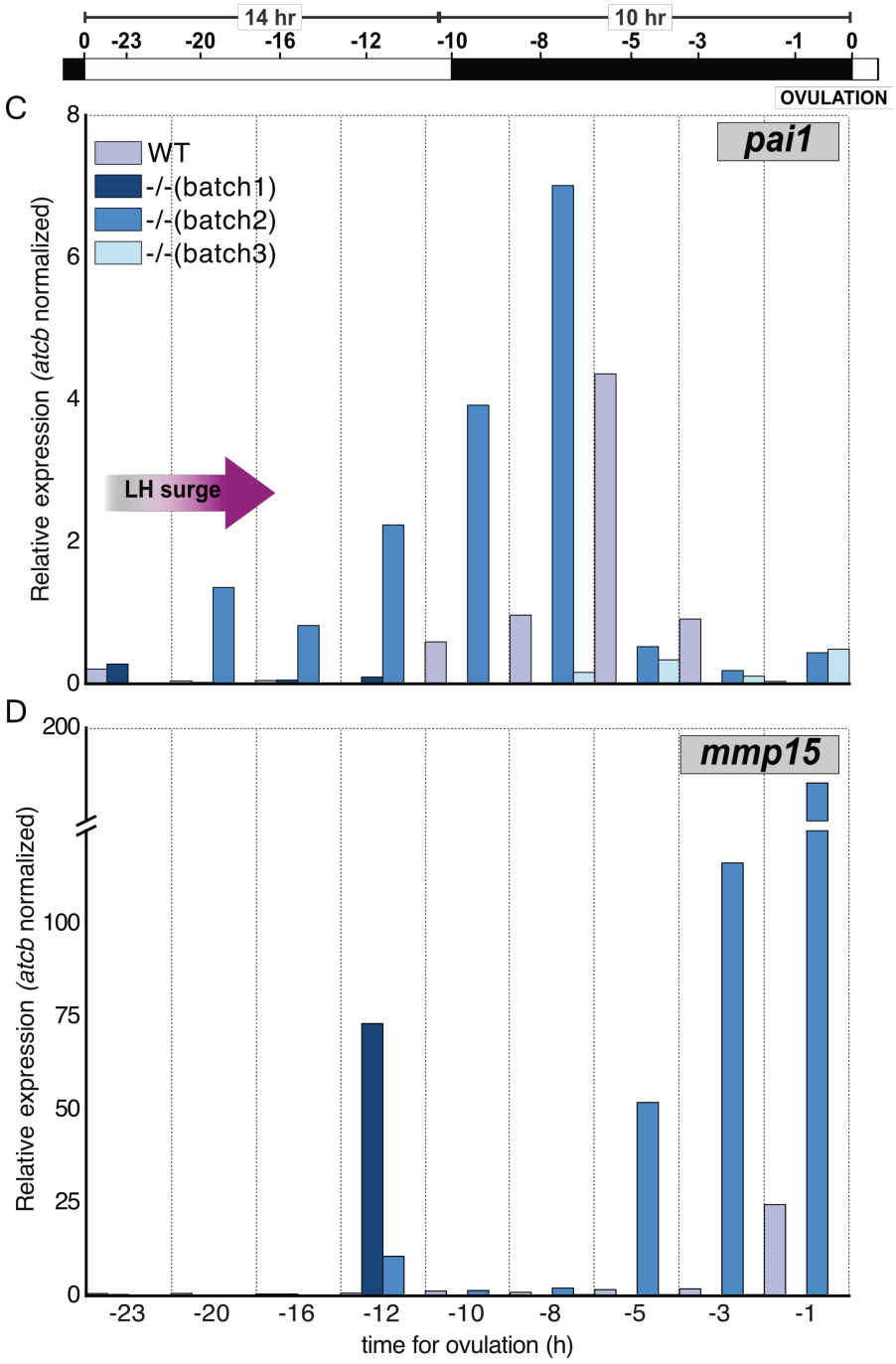

Figure 2.16 Expression of follicle maturation and ovulation-related genes

Relative expression of **(A)** *hsd17b12,* **(B)** *ep4b,* **(C)** *pai1*, and **(D)** *mmp15* in follicles from Fig. 2.15. Values were *β*-actin normalized, and the wild-type follicle at 10 h was set as 1 (standard). Bars show the expression of single follicle isolated and showed in Fig. 2.15.

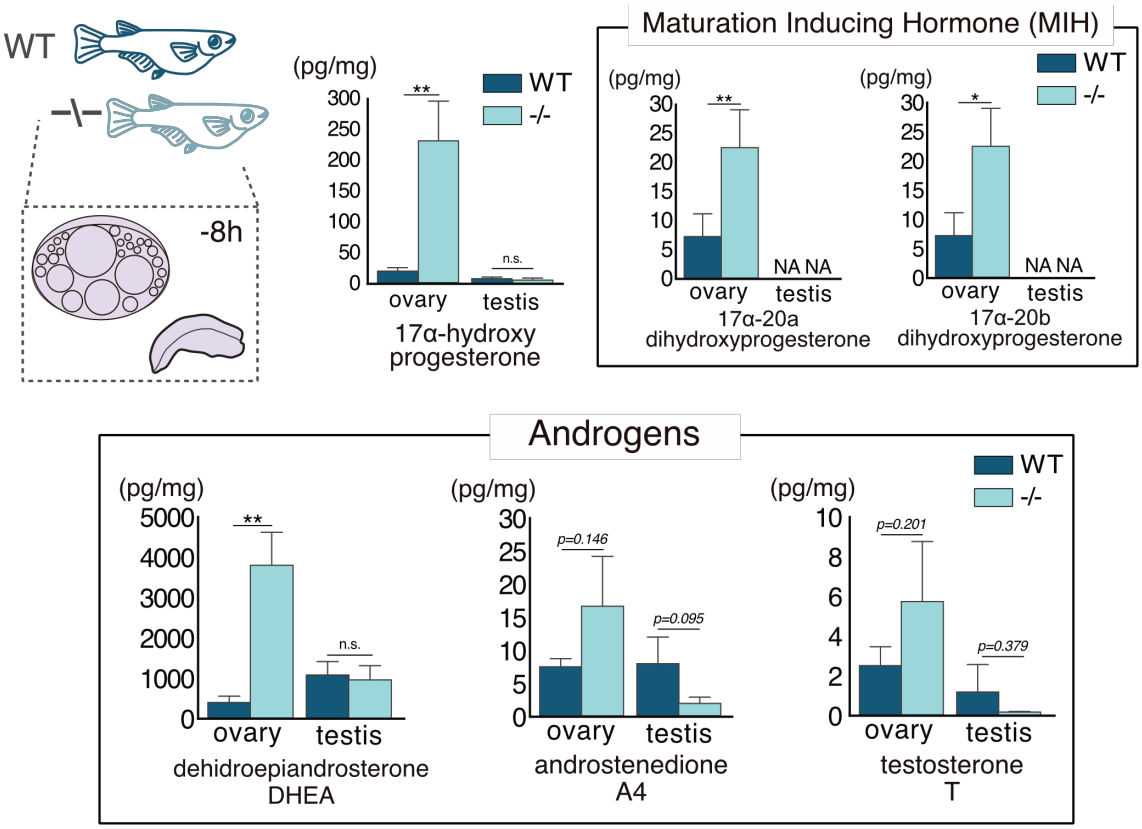

Figure 2.17 MIH and androgens profile in *cyp21a2* homozygous mutants

Steroid hormones profile from whole ovaries and testes. Values are expressed in terms of pg in 1 mg of wet gonad (weight before freeze-dried). Graph are presented with bar, mean; error bar, S.E.; N.A., not applicable (due to a low amount). *$P < 0.05$, **$P < 0.01$ by Student's *t*-test.

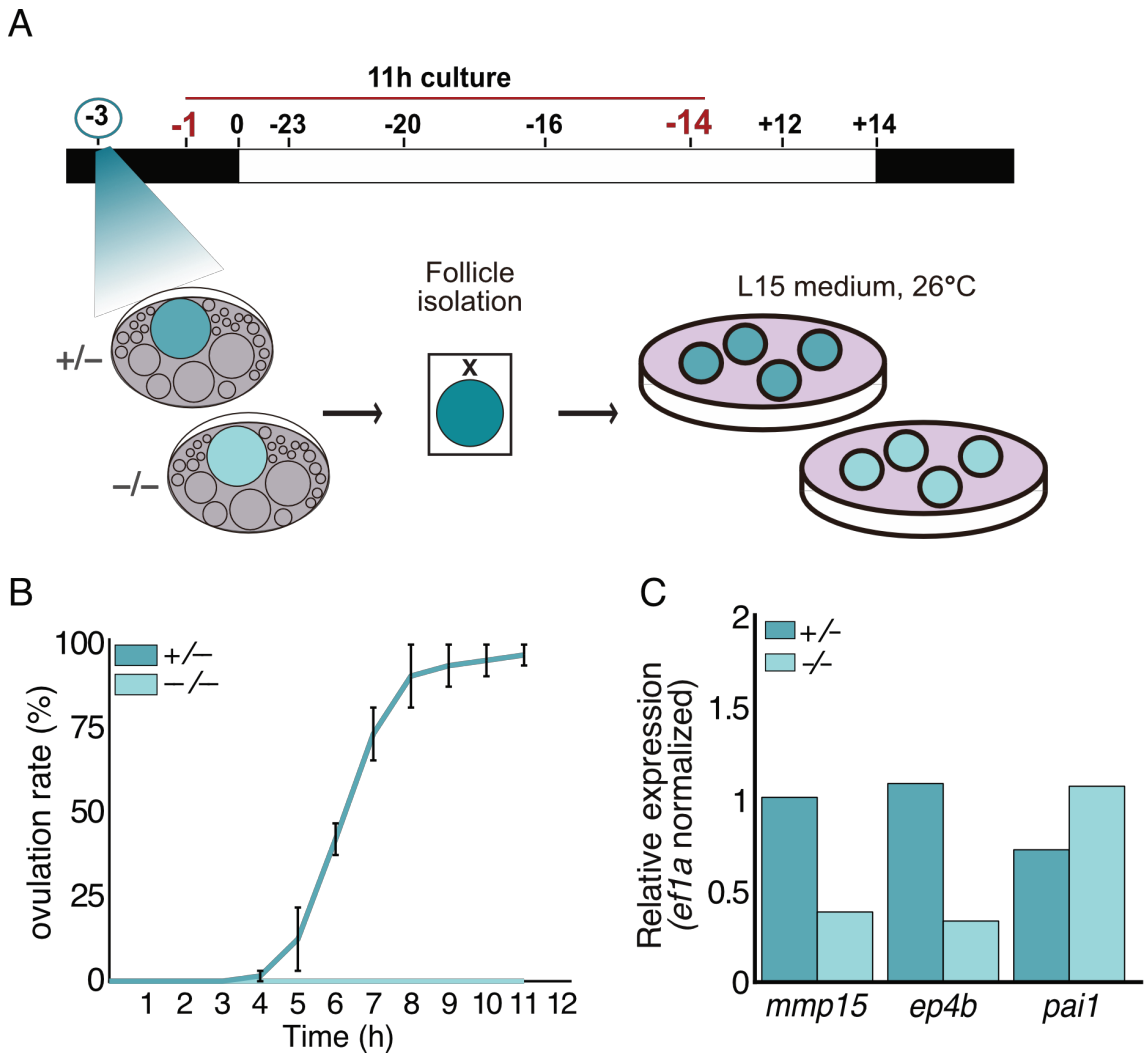

Figure 2.18 Ovulation defects in *cyp21a2* homozygous mutants

(A) Schematic representation of the in vitro ovulation system. **(B)** Ovulation rate. **(C)** Relative expression of the ovulation-related marker genes *mmp15, ep4b,* and *pai1*. Values were *ef1a* normalized and the heterozygous control group was set as 1.

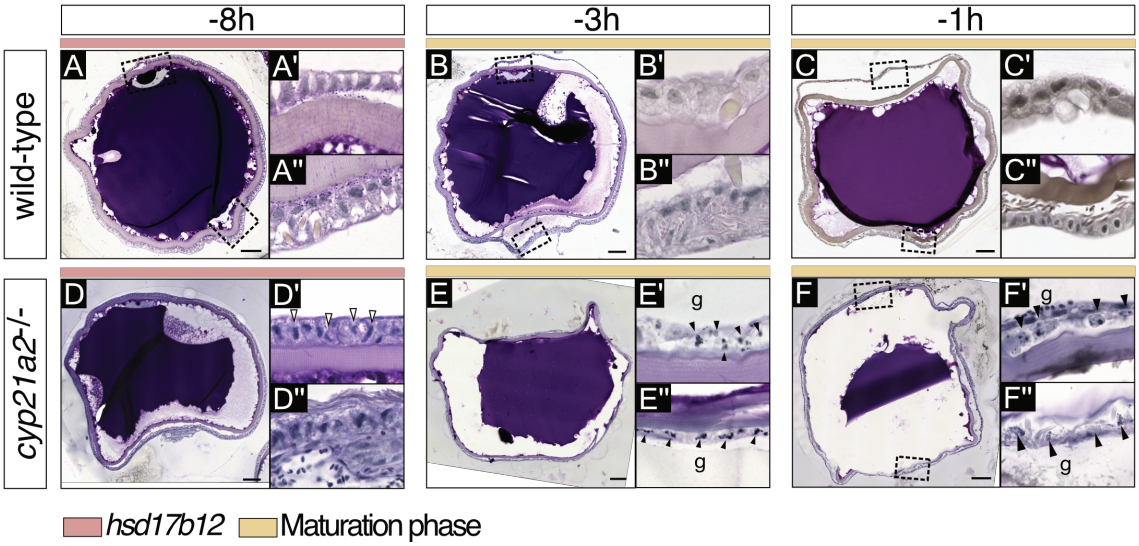

Figure 2.19 Morphological changes in granulose cells

Histological sections of **(A-C)** wild-type and **(D-F)** homozygous mutant follicles. Insets show a minified view of the black dashed lines box in follicles cross sections. g, granulose cells; white and black arrowhead indicates fusiform and fragmented granulose cells, respectively. Follicles were isolated 8 h, 3 h, and 1h before ovulation. Scale bar, 100 μm.

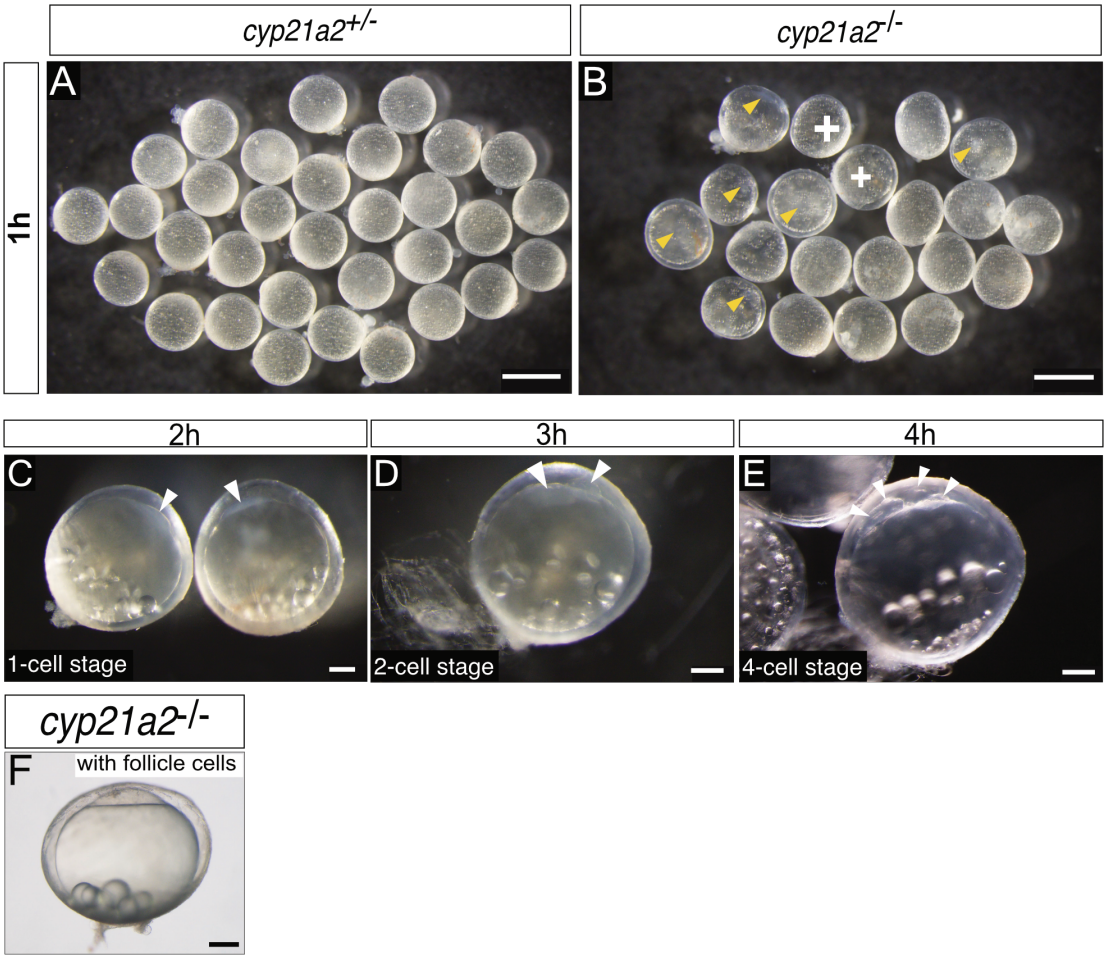

Figure 2.20 Parthenogenetic activation in *cyp21a2* homozygous mutants

(A-B) Follicles at 1 h of in vitro ovulation. In **(B)** yellow arrowhead indicates oocytes at 1-cell stage (parthenogenesis); white-cross, follicles where the space between the oocyte and the follicle cells became apparent. **(C-D)** parthenogenetic follicles from another independent in vitro ovulation experiment. **(F)** in vivo observed parthenogenetic follicle. Scale bar, (A-B) 1 mm, (C-E) 20 µm, (F) 200µm.

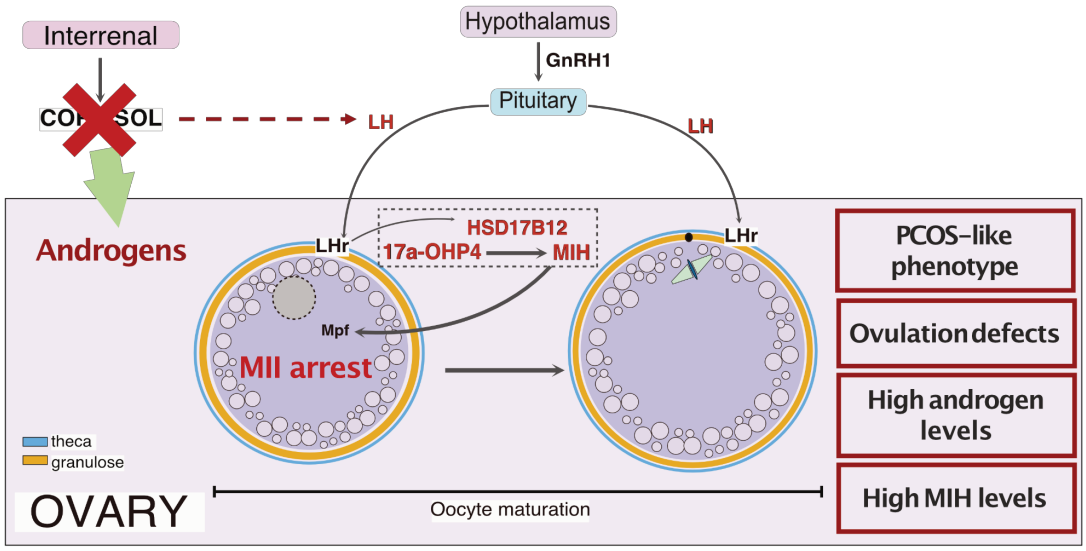

Figure 2.21 Working model for the role of cortisol in oogenesis.

The deficiency of cortisol due to a genetic disruption of the *cyp21a2* in the medaka fish, reveals possible roles of cortisol in the final steps of oogenesis. *cyp21a2* mutant females develop PCOS-like phenotype, has defects in ovulation, and mutant oocytes undergoes spontaneous parthenogenetic activation. Factors such as high androgen and MIH levels, in addition to a failure in LH fluctuation are presented in this study as some possible causes of the defects observed in mutant ovaries.

Table 2.1 Primers and probes used in this chapter

Experiment	Primer name	Sequence (5' - 3')
RT-qPCR	ef1a-qF1	caccggtcacctgatctaca
	ef1a-qR1	gctcagccttgagtttgtcc
	pai1-qF1	cccttcaaccccaaactgaca
	pai1-qR1	tcacatcgtagtccaccccatc
	ep4b-qF1	cagatggtgatcctgctcat
	ep4b-qR1	gccaggaggtcttcattgat
	mmp15-qF2	cgaggatggcagccctttta
	mmp15-qR2	ctgagaggatcgcatggtcg
	hsd17b12-like_qPCR_F	tcgtgaggctttgaacaccg
	hsd17b12-like_qPCR_R	tgttcttggaaggttccgca

CHAPTER III: Additional observations and future perspectives

Collaborative work statement

This chapter describes a collaborative effort of José Carranza and Kazuki Yamada, under the supervision of Dr. Minoru Tanaka. Kazuki Yamada performed WISH of glucocorticoid and mineralocorticoid receptors in ovaries. All other experiments were conducted by José Carranza.

3.1 Introduction

Studies on cortisol deficiency due to genetic disruption of key steroidogenic enzymes have shed light on the role of cortisol in female fertility. Its deficiency results in an impaired dynamic of gonadotropin secretion, increased sex steroids in the ovary, and importantly, defects in oogenesis (Mullins et al., 2009; Reichman et al., 2014; Shi et al., 2022; Xiao et al., 2022). Therefore, understanding of the cortisol dynamics and the and the stage(s) to which it exerts actions may provide critical insights into ovarian development and physiology.

Oogenesis is a process in which the follicles undergo a series of changes both at the cellular and molecular level. It can be categorized into 3 main stages: previtellogenic (primary growth and cortical alveoli), vitellogenic (vitello intake), and post-vitellogenic (maturation, meiosis resumption and ovulation) (Fig. 3.1) (Iwamatsu et al., 1988; Nagahama and Yamashita, 2008). Several studies suggest a role for cortisol acting on post-vitellogenic stage oocytes. Based on vitro studies, cortisol may promote oocyte maturation in medaka (Hirose, 1973) and oocyte hydration in rainbow trout (Milla et al., 2006). Cortisol injection in Nile tilapia could stimulate hydration and ovulation (Gennotte et al., 2012).

Interestingly, it has also been reported that cortisol may passively diffuse into and out of the oocyte in Mozambique tilapia (Tagawa et al., 2000), as well as to be incorporated into the oocyte during vitellogenesis (Faught and Vijayan, 2018). This suggest a possible action of cortisol in early stage oocytes. Moreover, in zebrafish cortisol could itself be maternally deposited into the oocytes during early stages (Nesan and Vijayan, 2013). This maternal cortisol is then critical for embryogenesis (Nesan and Vijayan, 2016).

Thus, in this chapter, preliminary results allowed to speculate a possible action of cortisol in previtellogenic oocytes (cortical alveoli and early-vitellogenic stages). In vitro culture, gene expression and RNAseq data is presented in support of this hypothesis. Hence, this represents an interesting pathway for future studies.

3.2 Materials and methods

3.2.1 WISH and FISH

WISH was performed as described in section 1.2.6. For WISH probes, cDNAs of *nr3c1a* (glucocorticoid receptor 1)*, nr3c1b* (glucocorticoid receptor 2), and *nr3c2* (mineralocorticoid receptor) genes were PCR-amplified from wild-type ovary. Primers are listed in Table 3.1.

3.2.2 IVO and cortisol rescue

Follicles at 21 ~ 20 h before ovulation (before LH prime for maturation) were isolated and maturation was induced in vitro by adding 17α,20β-dihydroxy-4-pregnen-3-one (MIH, Sigma P6285) or a combination of MIH + cortisol (hydroxycortisone, TCI H0533). Both MIH and cortisol were administrated at a final concentration of 1µg/ml. Ethanol at 0.1% final concentration was administrated in the control group. Follicles were culture in L-15

medium (phenol red -) at 26ºC. GVBD was used as a reference for a successful maturation (Fig. 3.2).

3.2.3 RNAseq

Mature (completed GVBD) and immature (before LH prime or also considered as the second largest follicles after ovulated oocytes) were isolated at 3h and 23h before ovulation, respectively. Five follicles per fish (XX) females, were isolated for a total of 3 biological replicates at the indicated time point (Fig. 3.3). Follicles were flash-frozen in liquid nitrogen and the RNA was purified by the RNAqueous Micro Kit (Invitrogen, AM1931). Next, libraries were prepared as previously described (Sasagawa et al., 2013). RNAseq libraries were amplified with a KAPA Hyper Prep Kit (Illumina, 07962347001). Finally, libraries were sequenced with a NextSeq 500/550 High Output kit v2 (75 cycles) at the gene center of Nagoya University.

RNAseq reads were then mapped to a CabToHdrR medaka genome (Lab genomic data). The mapping average was between 92~93% (Table C.1). An annotation file derived from NCBI, medaka NBRP, Ensembl, and Lab-RNAseq data was used for DEG analysis. The software iDEP 0.96 (Ge et al., 2018) was used for in silico analysis of the RNAseq data.

3.3 Results and discussion

3.3.1 A role for cortisol in regulating the final steps of oogenesis in medaka

As described in Chapter 2, systemic cortisol deficiency results in several defects in oogenesis. One of them is that mutant follicles fail to ovulate remaining in their follicle cells and within the stromal compartment (Fig. 2.5, 2.18 in Chapter 2). Therefore, to test

the possibility that cortisol may act on the largest oocytes and promote the completion of the final step of oogenesis, i.e. oocyte hydration and ovulation (Fig. 3.1), an in vitro oocyte maturation (IVOM) experiment was conducted in which maturation (GVBD completion) was induced by the administration of MIH in the culture medium (Fig. 3.2). GVBD was observed between 11 ~ 18 h of in vitro culture in both MIH and MIH+cortisol treatments. No GVBD was observed in the MIH (-) control group. However, intriguingly, ovulation was not observed in all of the treatments, even after 30 h of in vitro culture. No differences in terms of the time to reach the GVBD stage was observed in follicles treated with cortisol.

Curiously, preovulatory oocytes (preGVBD) of rainbow trout (*Oncorhynchus mykiss*) treated with 12ng/mL of cortisol could induce oocyte hydration as compared with those treated with MIH (also known as MIS: maturation inducing substance) (Milla et al., 2006). Accordingly, injection of 0.5mg/kg body weight of cortisol in Nile tilapia (*Oreochromis niloticus*) led to a twofold reduction of the time before ovulation. Thus, cortisol induced oocyte hydration and shortened the time required for ovulation (Gennotte et al., 2012). It is thus possible that in medaka not only cortisol but another factor is required to complete oogenesis. LH could be one of them. In fact, maturation (GBVD) and ovulation was reported in preGBVD medaka oocytes treated only with recombinant LH in vitro (Ogiwara et al., 2013). Therefore, future studies are needed to test the hypothesis of an LH and cortisol cooperative role in regulating oogenesis in medaka.

3.3.2 Cortisol may act on early oocytes to promote a successful maturation

Cortisol exerts its function on target tissues by binding to and activating specific corticoid receptors (Aedo et al., 2022). In fish, two types of corticoid receptors have been reported: mineralocorticoid (MR) and glucocorticoid (GR) receptors (Greenwood et al.,

2003). Then, the cortisol-receptor complex translocates to the nucleus and binds to glucocorticoid-response elements (GRE) in the promoter of target genes to activate or repress their transcription (Aluru and Vijayan, 2009). Interestingly, aldosterone synthase, the major mineralocorticoid in mammals, has not yet been documented in fish, and ligand-receptor affinity assays has demonstrated that cortisol could potentially activate both MR and GR in fish (Arterbery et al., 2011).

Most fish have preserved one MR and two GR during evolution (Greenwood et al., 2003). In agreement with this, medaka has also one MR and two GR. WISH analysis showed that the three receptors are expressed in the ovary of medaka. Specifically, previtellogenic or stage I oocytes express the three corticoid receptors (Fig. 3.3). This raises the possibility that cortisol may act on early-stage oocytes. Further studies on protein localization will help to clarify the target stage of cortisol.

Curiously, mass spectrometry analysis conducted in isolated follicles (Fig. 2.8B, chapter 2) showed that late and post-vitellogenic oocytes (before LH priming for maturation) had the highest cortisol concentration. Although immunodetection of the CYP21A2 protein (cortisol synthesis) was a limitation in this study, it is possible that the interrenal-derived cortisol supplied through the bloodstream to the oocytes is incorporated into the oocyte during vitellogenesis, perhaps by passive diffusion as in Mozambique tilapia (Tagawa et al., 2000), form the hormone-receptor complex and finally activate the well documented genomic-pathway (Aedo et al., 2022). Then, the accumulated cortisol may regulate for instance the competence for maturation in medaka oocytes. RNAseq analysis of follicles isolated at 23 h before ovulation time and importantly before LH priming for maturation (i.e. immature follicles) (Fig. 3.4) already showed a difference in expression pattern compared to wild-type. This difference became more obvious in mature

follicles (completed GVBD) at 3h before ovulation (Fig. 3.5). Thus, future studies exploring the role of the differentially expressed genes in the homozygous mutant follicles will help to clarify our understanding of the role of cortisol in oogenesis. Here, the *cyp21a2* mutant medaka is of great value in achieving this objective.

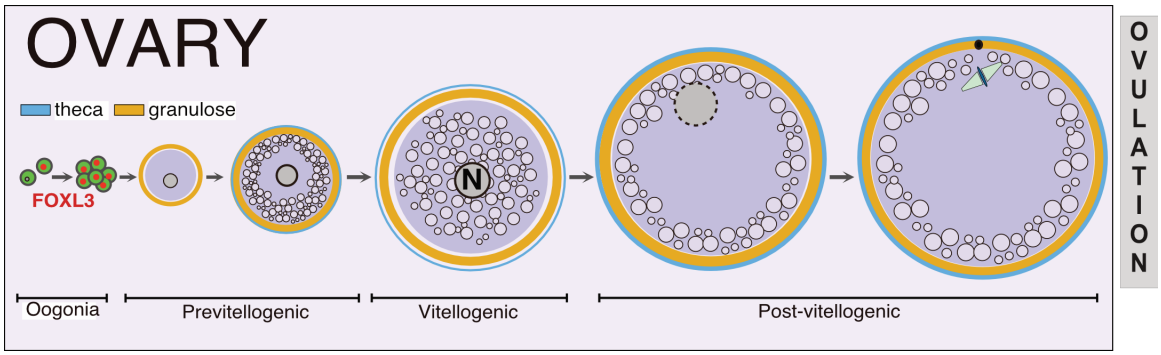

Figure 3.1 Stages of oocytes development

The expression in oogonia of the transcription factor FOXL3 is required for commitment to oogenesis. (Nishimura et al., 2015; Kikuchi et al., 2020). After several rounds of cystic division, oocyte undergoes the first meiotic arrest at diplotene of Meiosis I. At this stage, future oocyte is surrounded by gonadal somatic cells (future granulose and theca cells), to eventually form the follicle. Follicle will then undergo a series of morphological changes which have been extensively studied and characterized. Based on the medaka oocyte staging (Iwamatsu et al., 1988), oocytes are classified in previtellogenic, vitellogenic and post-vitellogenic stages.

A

Treatment		# Follicles used	GVBD	Ovulation	Dead
Control - 1	0.1% ethanol	16	0%	0%	1 (6.25%)
Control - 2	0.1% ethanol	16	0%	0%	2 (12.5%)
MIH - 1	1μg/mL	15	9 (60%)	0%	5 (33.3%)
MIH - 2	1μg/mL	15	9 (60%)	0%	6 (40%)
MIH+Cortisol - 1	1μg/mL (each)	15	8 (53.3%)	0%	8 (53.3%)
MIH+Cortisol - 2	1μg/mL (each)	15	5 (33.3%)	0%	11 (73.3%)

B

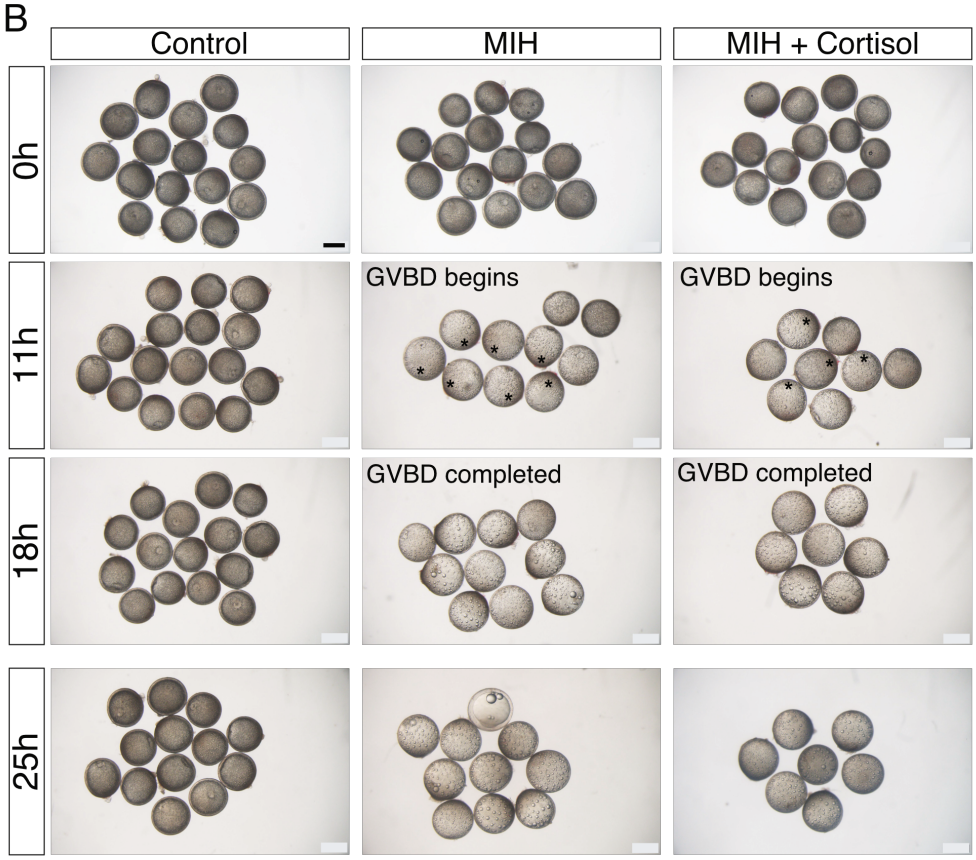

Figure 3.2 In vitro maturation of medaka oocytes

(A) Percentage of oocytes that completed maturation (GVBD) and ovulation in the IVOM system. **(B)** In vitro maturation of medaka oocytes. GVBD was first observed after 11 h of culture in either MIH and MIH+cortisol treatments. At 18 h of culture all oocytes have completed GVBD. *Oocytes in GVBD stage. Scale bar, 500µm.

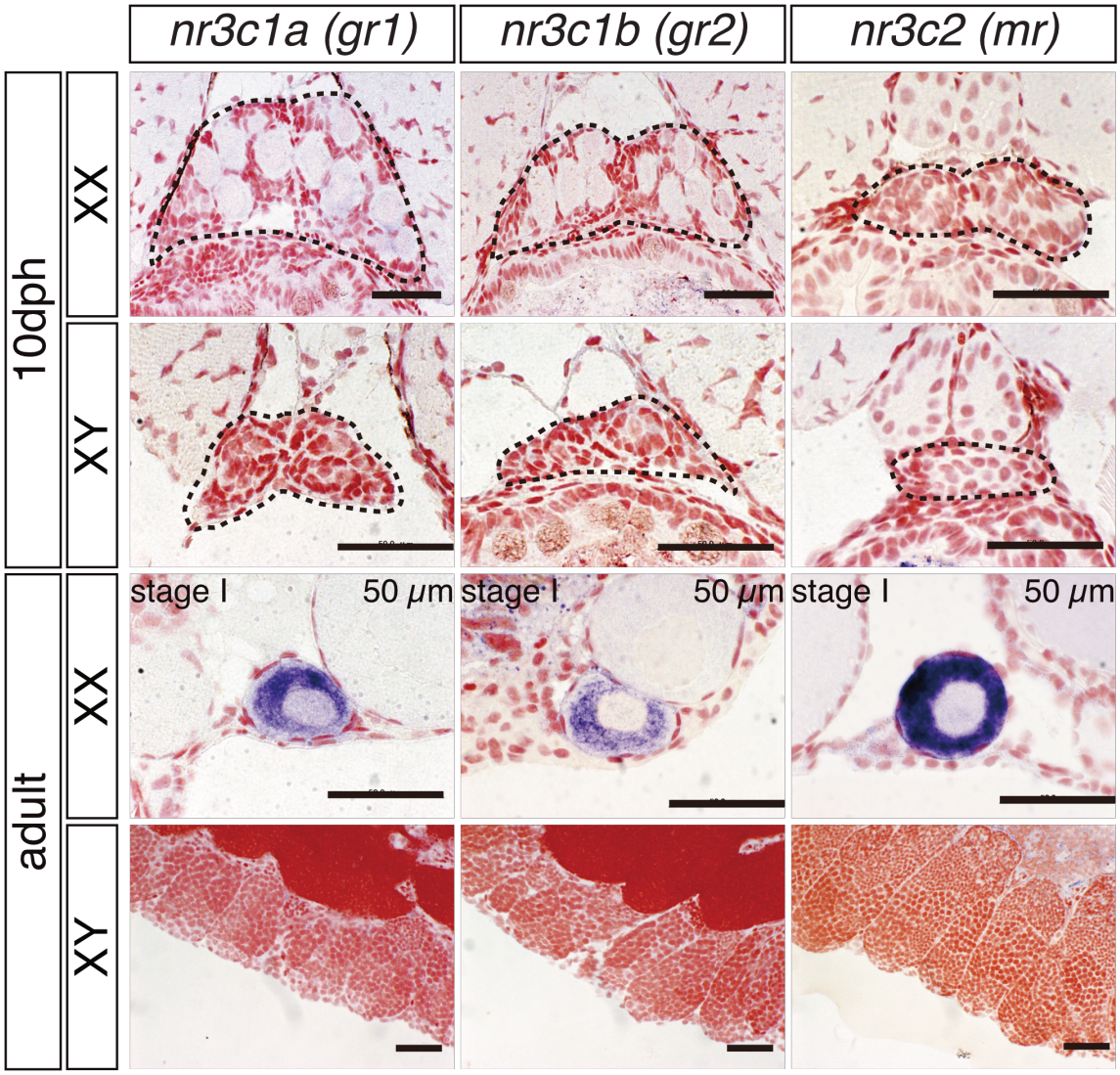

Figure 3.3 Expression of mineralocorticoid and glucocorticoids receptors in the ovary

WISH of medaka *mr* and *gr* in gonads at 10dph and adult. Gonads in 10dph larvae are highlighted with black-dashed lines. Positive signal was only detected in stage I oocytes (~50μm) of adult sexually mature ovaries. Scale bars, 50μm.

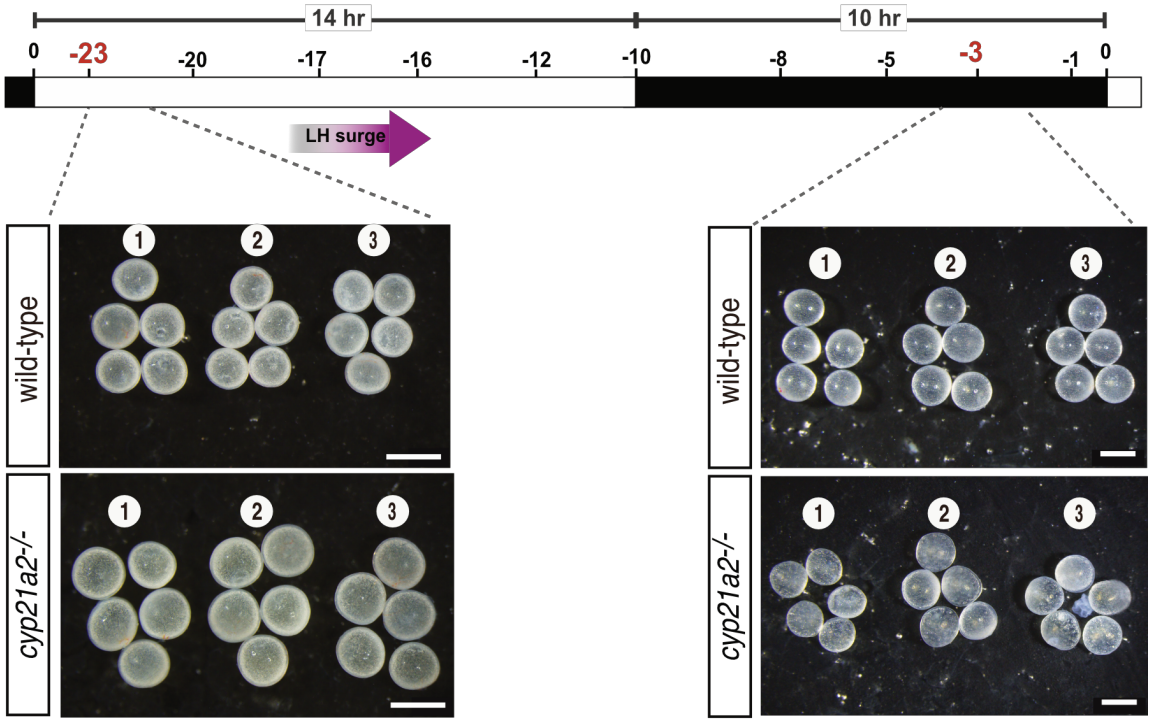

Figure 3.4 Sample preparation for RNAseq of mutant follicles

Follicles were isolated at 23 h (before LH priming for maturation, pre-GVBD) and 3 h (after LH priming, post-GVBD) before ovulation or light onset in the fish room. Follicles (*n=5*) were isolated from one ovary, thus each technical replicate is also a biological replicate.

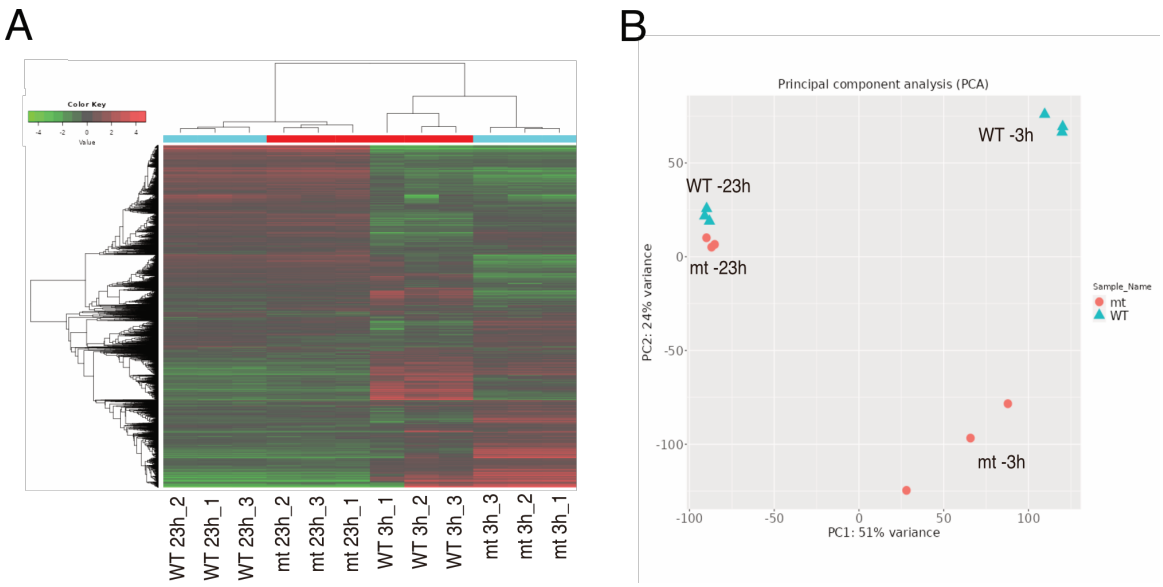

Figure 3.5 Differentially expressed genes (DEG) analysis from RNAseq

(A) Heat map of the top 5 000 most variable genes. **(B)** PCA component analysis. The PCA was plotted considering the reads count data (TMP normalized reads) as input. Both graphs were plotted with the software iDEP 0.96.

Table 3.1 Primers and probes used in this chapter

Experiment	Primer name	Sequence (5' - 3')
RT-qPCR	nr3c2-F	aggtggggaagtgttcagtg
	nr3c2-R-T7	ggccagtgaattgtaatacgactcactatagggtcagctgcaatcgaacaaac
	nr3c1a-F	gctcgaaataccgcagagac
	nr3c1a-R-T7	ggccagtgaattgtaatacgactcactataggggttgaagctgctgatggtga
	nr3c1b-F	ccagaaaaaccgaagctcag
	nr3c1b-R-T7	ggccagtgaattgtaatacgactcactatagggctctggtggaagagcaaagg
RNAseq libraries (Sasagawa et al., 2013)	RT primer	tatagaattcgcggccgctcgcgataatacgactcactatagggcgttttttttttttttttttttt
	Tagging primer	atagaattcgcggccgctcgcgatttttttttttttttttttttt
	Suppression primer	(NH 2)-gtatagaattcgcggccgctcgcgat

CONCLUSIONS

In the present study, the *cyp21a2* gene located on chromosome 16 of medaka, was genetically disrupted by the CRISPR/Cas9 system. A functional characterization of the phenotypes of homozygous mutants revealed that:

1. Deficiency of cortisol compromised the survivability of mutant medaka particularly after hatching.
2. Complex hormonal imbalances represented by accumulation of cortisol metabolic precursors (17α-hydroxyprogesterone and 21-deoxycortisol) were a hallmark in mutant medaka.
3. Notably, cortisol deficiency promotes upregulation of ACTH and interrenal gland hyperplasia in mutant medaka.
4. Confocal analysis of mutant pituitaries, revealed two populations of *pomca*-expressing cells that respond differently to the levels of systemic cortisol in medaka.
5. Cortisol deficiency leads to compromised fertility specifically in females. Changes in the dynamic of the activity of gonadotropins, PCOS-like phenotype, aberrant expression of maturation and ovulation-related genes, defects and granulose cells, and ovulation, are proposed as the causal matters for the observed infertility.
6. Increased levels of androgens and maturation-inducing hormone were observed in mutant ovaries.
7. Significantly, cortisol deficiency can result in parthenogenetic activation in mutant oocytes.
8. Cortisol may act on early oocytes to regulate aspects related to maturation.

APPENDIX A. Chapter 1 Supplementary Materials

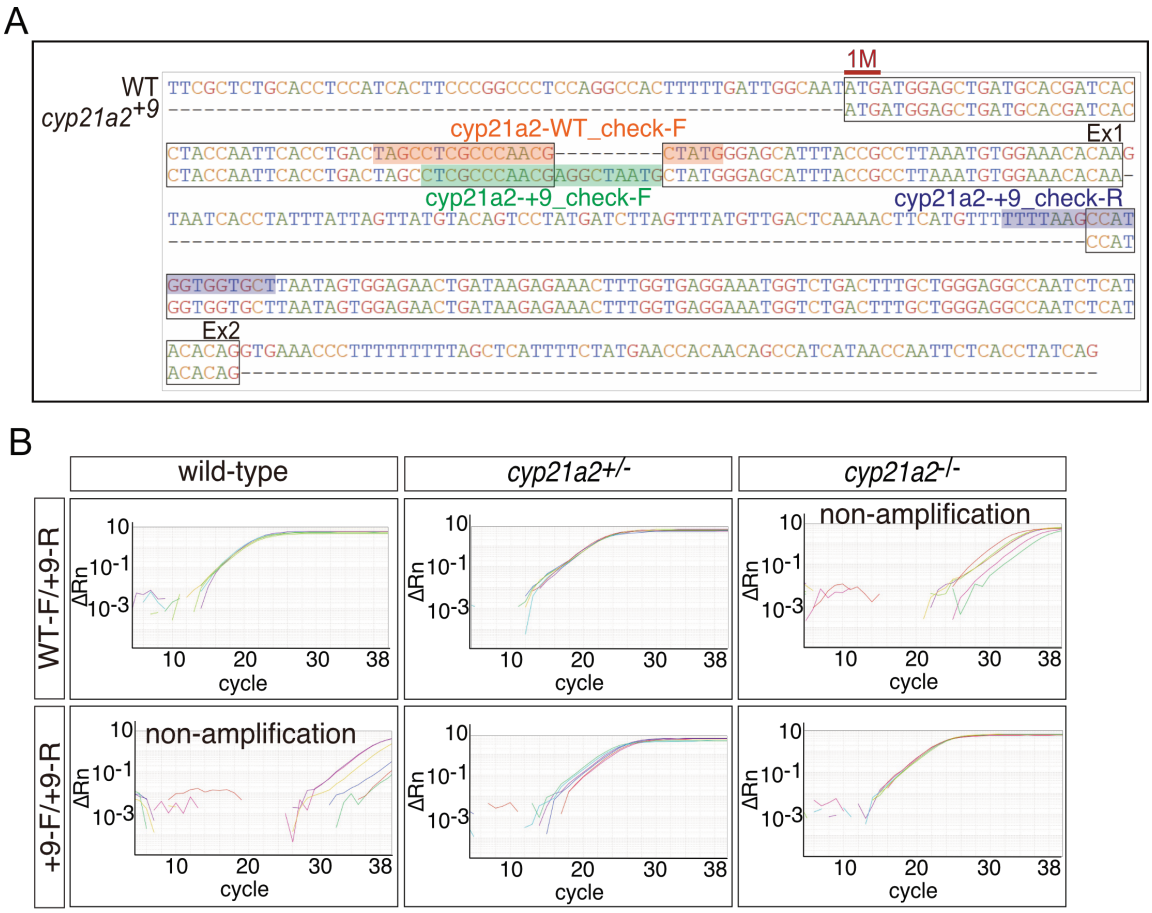

Figure A.1 Genotyping of the *cyp21a2* mutant allele

(A) Location of the primers for genotyping of the mutant allele. **(B)** Examples of qPCR amplification plots (genotyping).

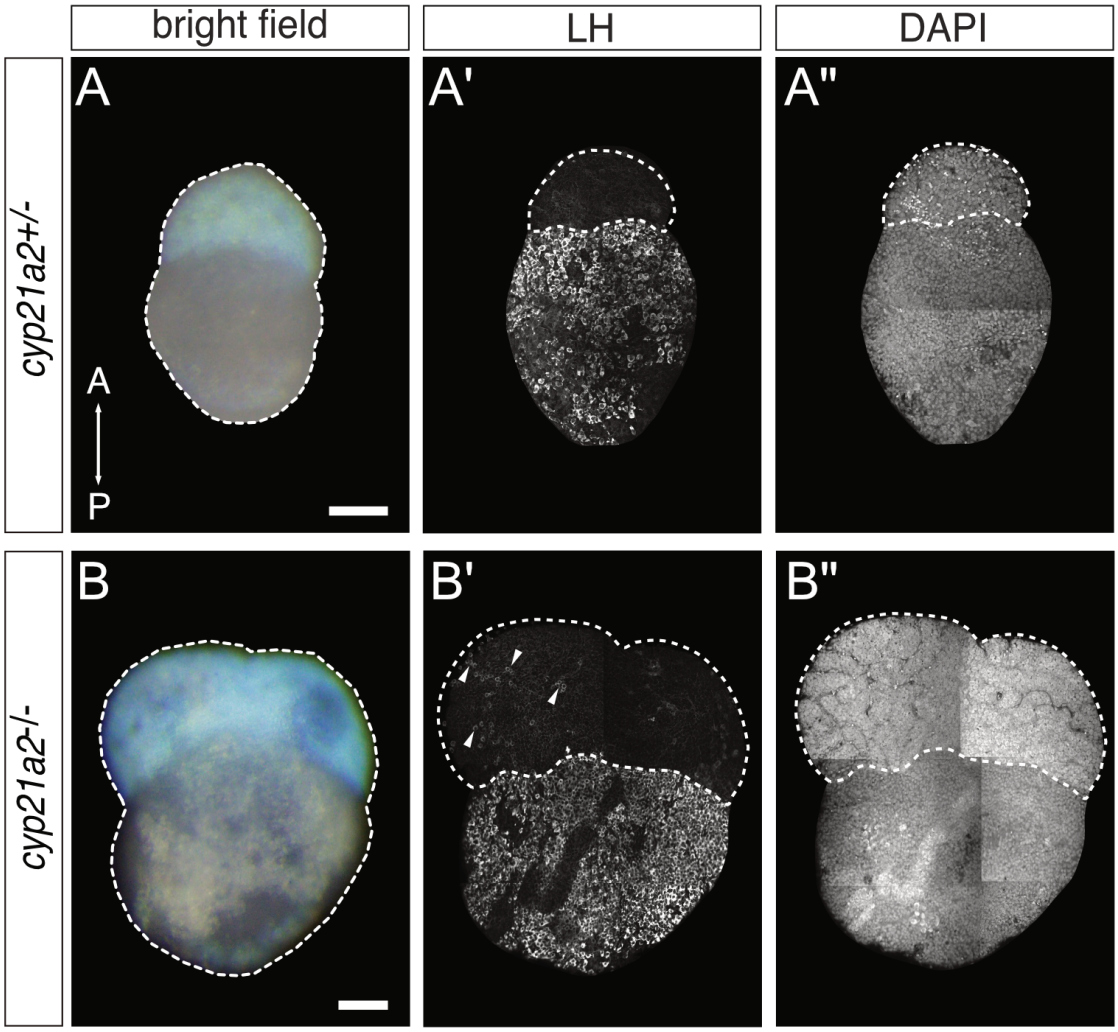

Figure A.2 Pituitary hyperplasia in homozygous mutants

Pituitaries from **(A)** heterozygous and **(B)** homozygous adult female mutants. White arrowheads indicate LH positive cells in the *prolactin*-expressing region. Scale bar, 100 μm.

Table A.1 Steroid hormones measured by LC-MS/MS

Sex	Genotype	Chol (μg/mg)	Preg	21-deoxyB	21-deoxyF	17a-OH-Prog	11-deoxyF	F	E
XX	+/-	8.712886117	97.38003898	230.9681223	NA	4.623107385	12.520175	477.8093017	66.82789296
XX	+/-	8.982906714	156.5660878	255.2932358	NA	1.35372189	15.65894205	459.2107026	61.76025228
XX	+/-	12.20898283	95.93198703	59.57483755	NA	5.869316508	16.23524577	416.7414627	81.76600025
XX	-/-	16.27158994	219.8076381	994.8704019	140.8050231	793.1418446	9.183293139	NA	NA
XX	-/-	12.72304331	160.5921206	441.9276111	42.87407546	320.8590594	3.125907964	NA	NA
XX	-/-	11.72429016	142.1684532	500.2848606	112.7280674	634.6937631	7.308104823	NA	NA
XY	+/-	12.21346177	122.482039	215.1623215	NA	0.581621054	20.69109379	573.0061833	107.9253832
XY	+/-	11.00172501	130.2686351	451.4290362	NA	2.828658808	11.68166413	369.5238465	46.26748065
XY	+/-	12.0693773	66.28650952	228.0965259	NA	3.499964391	18.22209388	556.5359513	91.69350122
XY	-/-	14.95967064	166.2596136	718.549437	100.9387902	430.0295327	6.46211205	NA	NA
XY	-/-	11.5074085	134.2427648	645.971475	117.1789991	794.0398873	4.392890683	NA	NA
XY	-/-	8.8908836	101.4114687	337.2943146	45.79876012	226.2522376	0.21906156	NA	NA

Chol : cholesterol
Preg : Pregnenolone
21-deoxyB : 21-deoxycorticosterone
21-deoxyF : 21-deoxycortisol
17a-OH-Prog : 17a-hydroxyprogesterone
11-deoxyF : 11-deoxycortisol
F : cortisol
E : cortisone

Table A.2 Quantification of *pomca* WISH area (pixels)

wild-type		*cyp21a2+/-*		*cyp21a2-/-*	
XX	XY	XX	XY	XX	XY
3516	3211	3870	3309	5146	5007
3281	2837	3227	2803	3747	4772
4084	2806	3450	3210	4980	4975
2779	3539	3392	3103	5014	4155
2983	3293	2789	3298	6282	4099
3064	2552	3096	2813	5516	6284
2806	3845	3016	3241	4906	5395

Table A.3 Quantification of *cyp17a2* WISH area (pixels)

wild-type		*cyp21a2+/-*		*cyp21a2-/-*	
XX	XY	XX	XY	XX	XY
9061	5030	6870	8425	11912	10848
6169	5197	7693	7226	10571	12972
5234	4957	7027	7883	13578	13030
6407	5113	6637	5745	14056	10673
4876	4492	6919	7471	13478	12526

Table A.4 Quantification of *pomca* FISH area (pixels) related to cortisol rescue experiment

Cortisol (-)				**Cortisol (+)**			
cyp21a2+/-		*cyp21a2-/-*		*cyp21a2+/-*		*cyp21a2-/-*	
XX	XY	XX	XY	XX	XY	XX	XY
39063	50460	77407	91870	54806	62853	57658	57794
67533	58933	81919	88335	51441	59507	64166	62853
54551	71746	81903	79378	50988	58923	50206	65823
57919	60060	85693	88464	52507	58002	56877	52088
53677	66845	88645	82490	51441	58561	54786	55770
78760	73748	92197	77912	58177	64726	48547	54307
68701	83207	87500	64216	53881	44601	67805	51558

Table A.5 Quantification of *cyp17a2* WISH area (pixels) related to cortisol rescue experiment

Cortisol (-)				**Cortisol (+)**			
cyp21a2+/-		*cyp21a2-/-*		*cyp21a2+/-*		*cyp21a2-/-*	
XX	XY	XX	XY	XX	XY	XX	XY
5079	4060	13601	9993	5778	6237	5047	5365
5859	6692	9812	11993	4615	5036	4927	5546
5976	7479	10910	9519	4459	4354	5123	5464
6722	9369	9516	11113	5720	5299	5795	5802
4323	7570	11671	8249	6258	5288	7369	6746
5125	4931	13336	9468	5485	5791	4923	5956
5323	6961	10501	13697	5864	5061	6646	6990
4458	4873	10182	13250	5424	3954	7273	7100

Table A.6 Quantification of total pituitary area in pixels (from *pomca* FISH images)

cyp21a2+/-		*cyp21a2-/-*	
XX	XY	XX	XY
176392	94328	118797	116659
115960	96151	114166	110005
96353	114369	94836	105431
112515	108299	113322	117267
92045	122485	134859	95259
117369	160950	122699	111928
118854	145809	116473	87866

Table A.7 Number of *pomca*-expressing cells in the medaka pituitary

	Cortisol (-)											
	cyp21a2+/-						*cyp21a2-/-*					
	XX			XY			XX			XY		
Sample	RPD	PI	Total	RPD	PI	Total	RPD	PI	Total	RPD	PI	Total
1	9	40	49	33	43	76	50	44	94	69	54	123
2	17	38	55	30	48	78	40	23	63	59	42	101
3	20	37	57	30	37	67	56	45	101	63	45	108
4	26	35	61	32	48	80	76	33	109	53	41	94
5	30	42	72	32	58	90	73	26	99	75	48	123
6	30	44	74	29	49	78	82	36	118	73	50	123
7	17	34	51	38	43	81	75	38	113	89	51	140
Total	149	270	419	224	326	550	452	245	697	481	331	812

	Cortisol (+)											
	cyp21a2+/-						*cyp21a2-/-*					
	XX			XY			XX			XY		
Sample	RPD	PI	Total	RPD	PI	Total	RPD	PI	Total	RPD	PI	Total
1	13	35	48	37	32	69	19	57	76	40	51	91
2	20	42	62	27	46	73	36	44	80	22	54	76
3	20	40	60	43	45	88	43	47	90	27	56	83
4	12	41	53	54	47	101	10	48	58	37	42	79
5	19	39	58	44	46	90	27	46	73	44	40	84
6	8	47	55	33	52	85	42	45	87	43	46	89
7	8	43	51	40	47	87	13	56	69	44	50	94
Total	100	287	387	278	315	593	190	343	533	257	339	596

Table A.8 Mean intensity of *pomca* (from *pomca* FISH images)

RPD								PI							
Cortisol (-)				Cortisol (+)				Cortisol (-)				Cortisol (+)			
cyp21a2+/-		*cyp21a2-/-*		*cyp21a2+/-*		*cyp21a2-/-*		*cyp21a2+/-*		*cyp21a2-/-*		*cyp21a2+/-*		*cyp21a2-/-*	
XX	XY	XX	XY	XX	XY	XX	XY	XX	XY	XX	XY	XX	XY	XX	XY
62	145	208	229	51	131	66	171	145	220	173	176	190	210	204	230
115	123	170	193	128	135	121	96	209	212	128	132	233	226	185	198
140	96	166	209	80	152	95	80	217	161	105	163	181	224	181	199
135	153	144	198	86	121	90	114	226	220	98	122	207	191	192	205
155	155	124	195	113	134	175	167	235	211	73	159	210	196	230	199
122	119	159	208	119	107	73	109	217	227	110	174	137	217	206	215
90	187	198	211	92	124	58	86	204	225	175	179	174	225	179	216

APPENDIX B. Chapter 2 Supplementary Materials

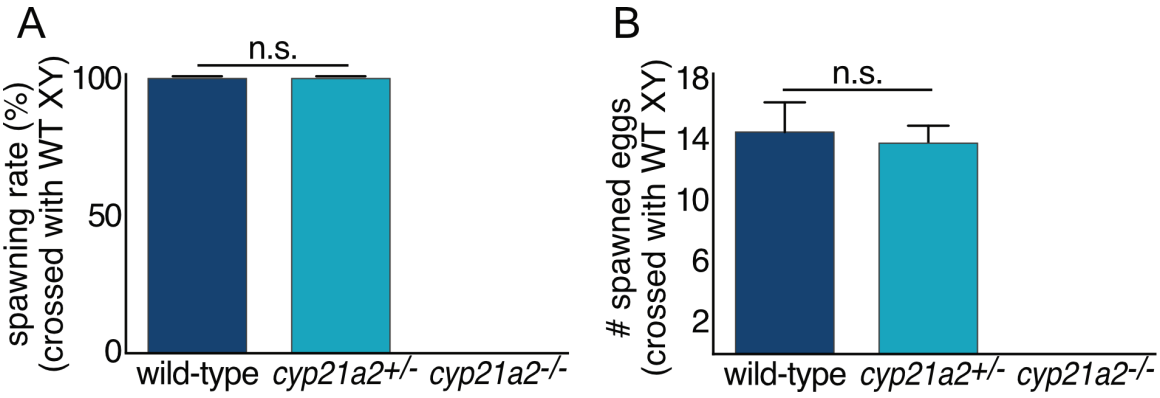

Figure B.1 Fertility in homozygous mutant females

(A) Spawning rate and **(B)** Number of eggs spawned per female. n=3 females per genotype, data collected during 5 days. Graphs are presented with bar, mean; error bar, S.E; n.s. non-significant by Student's *t*-test.

A

F0 **WT XX (3mph)** X  **WT XY (4mph)**

GC: XY_*cyp21a2*$^{-/-}$,tg[*olvasp*:EGFP]

F1 (morula stage)

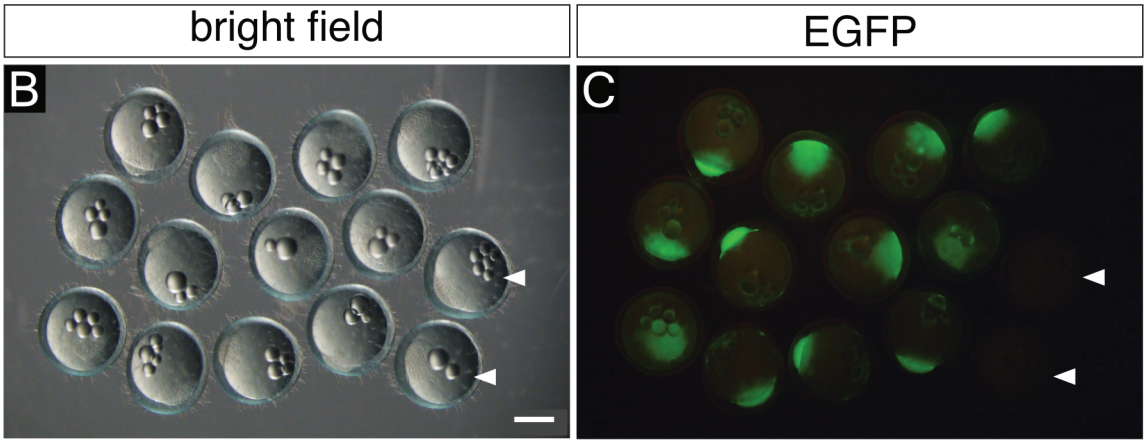

D

F1	EGFP+		EGFP-	
	XX	XY	XX	XY
WT	0	0	14	10
cyp21a2$^{+/-}$	6	30	0	0

EGFP+: 1:3 (XX/XY)
EGFP- : 1:1 (XX/XY)

Figure B.2 Genotyping of the F1 from chimera medaka (XY) cells

(A) Mating strategy of chimera medaka (XY germ cells) with wild-type (XY) medaka. **(B-C)** Embryos collected from A (white arrowhead; EGFP- embryos). **(D)** Genotype and EGFP screening of the embryos from B. Scale bar, 500 µm.

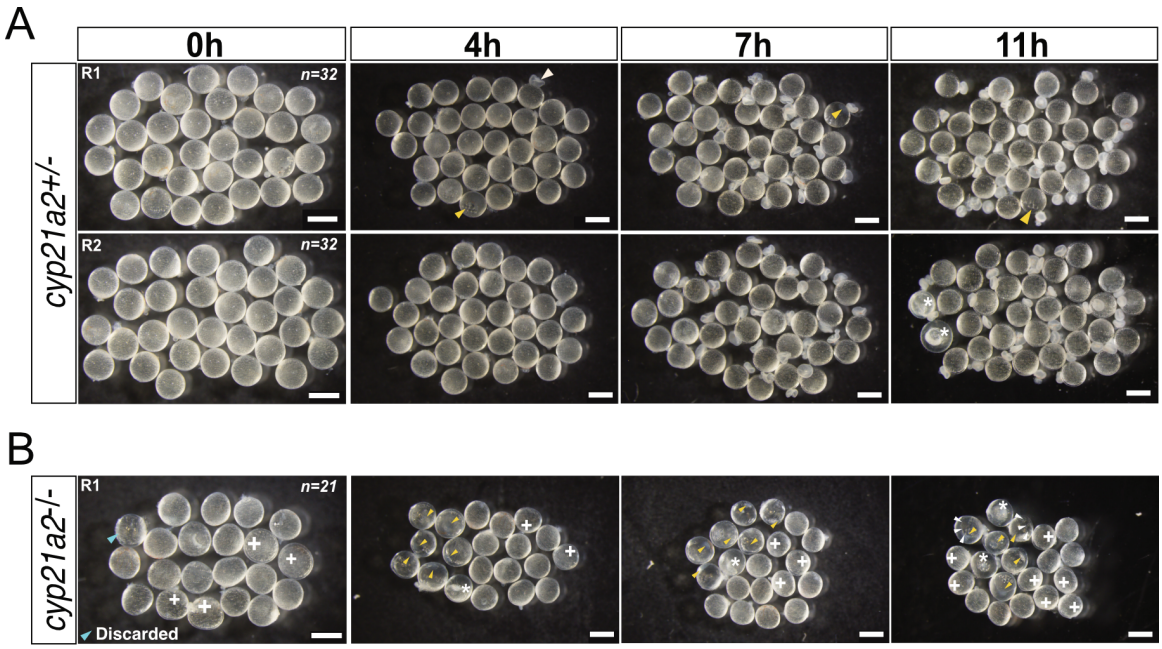

Figure B.3 In vitro ovulation of mutant follicles

In vitro ovulation of **(A)** heterozygous (control group) and **(B)** homozygous mutant follicles. Scale bar, 1 mm.

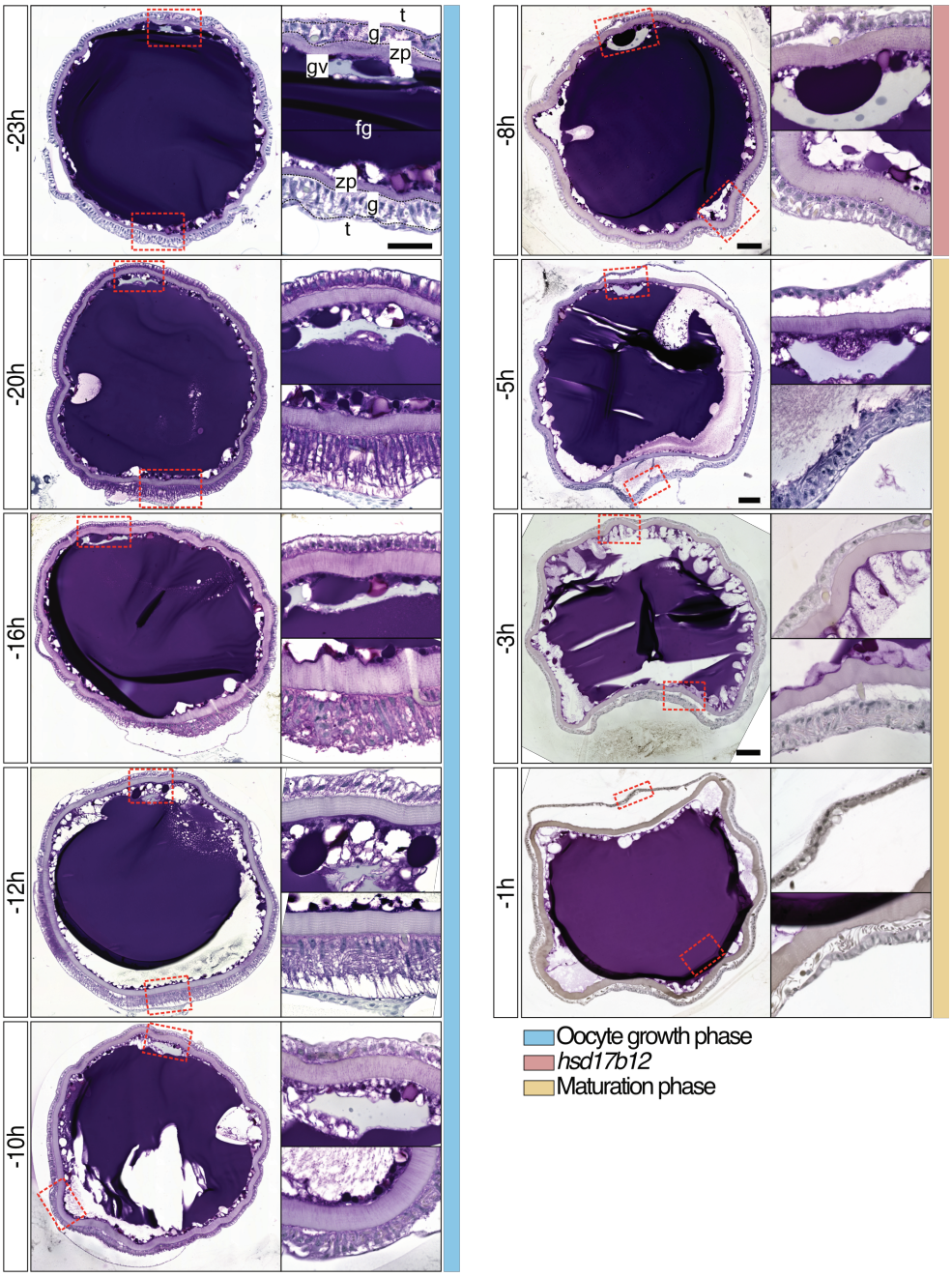

Figure B.4 Morphological changes in granulose cells of wild-type follicles during maturation stage

Histological sections of wild-type follicles isolated at 10 different time points. Insets show a magnify view of the black dashed lines box in follicles cross sections. Scale bar, 100 µmm, 50µm (insets).

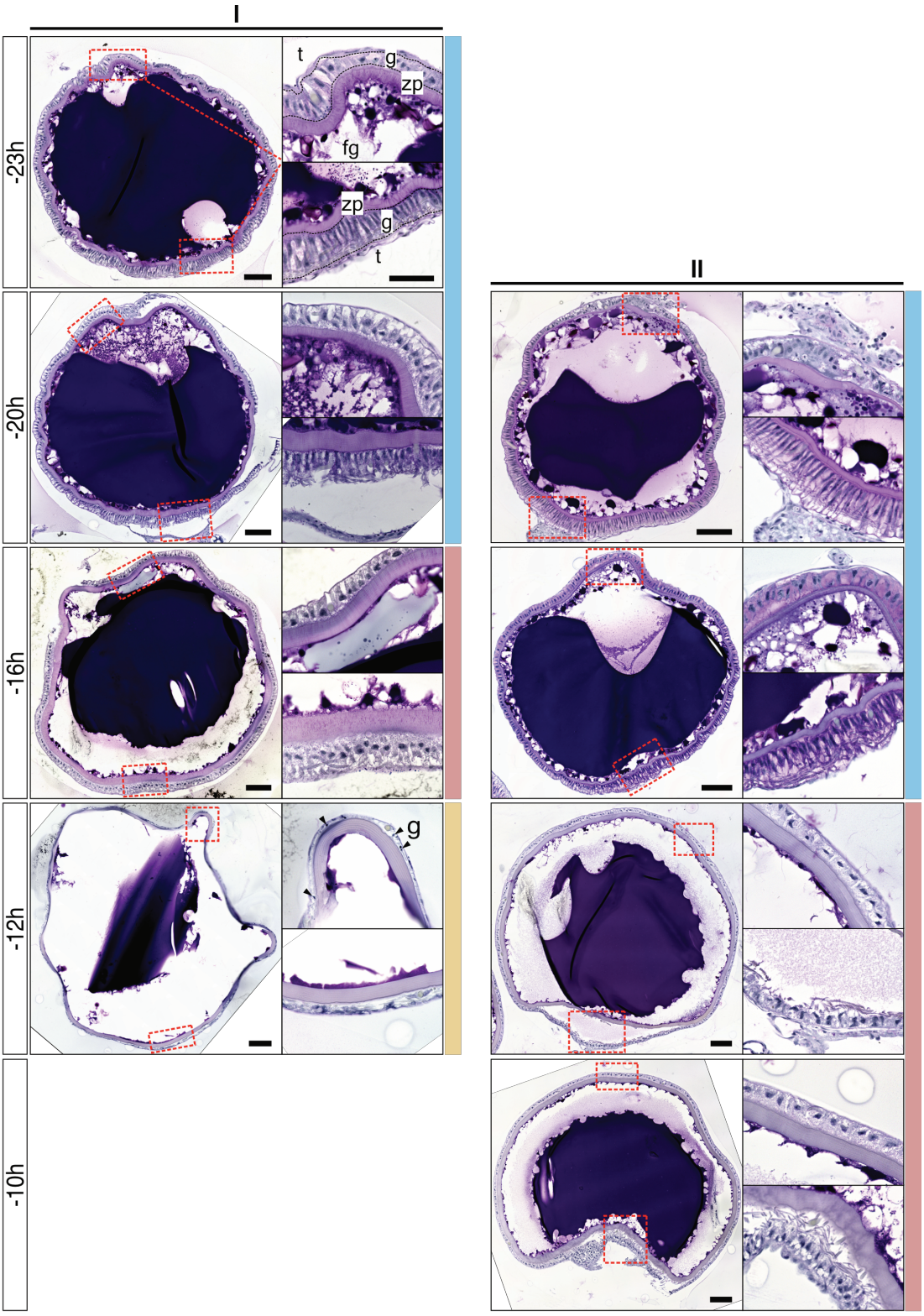
I
II
-23h
-20h
-16h
-12h
-10h
t
g
zp
fg
zp
g
t
g

Figure B.5 Continued

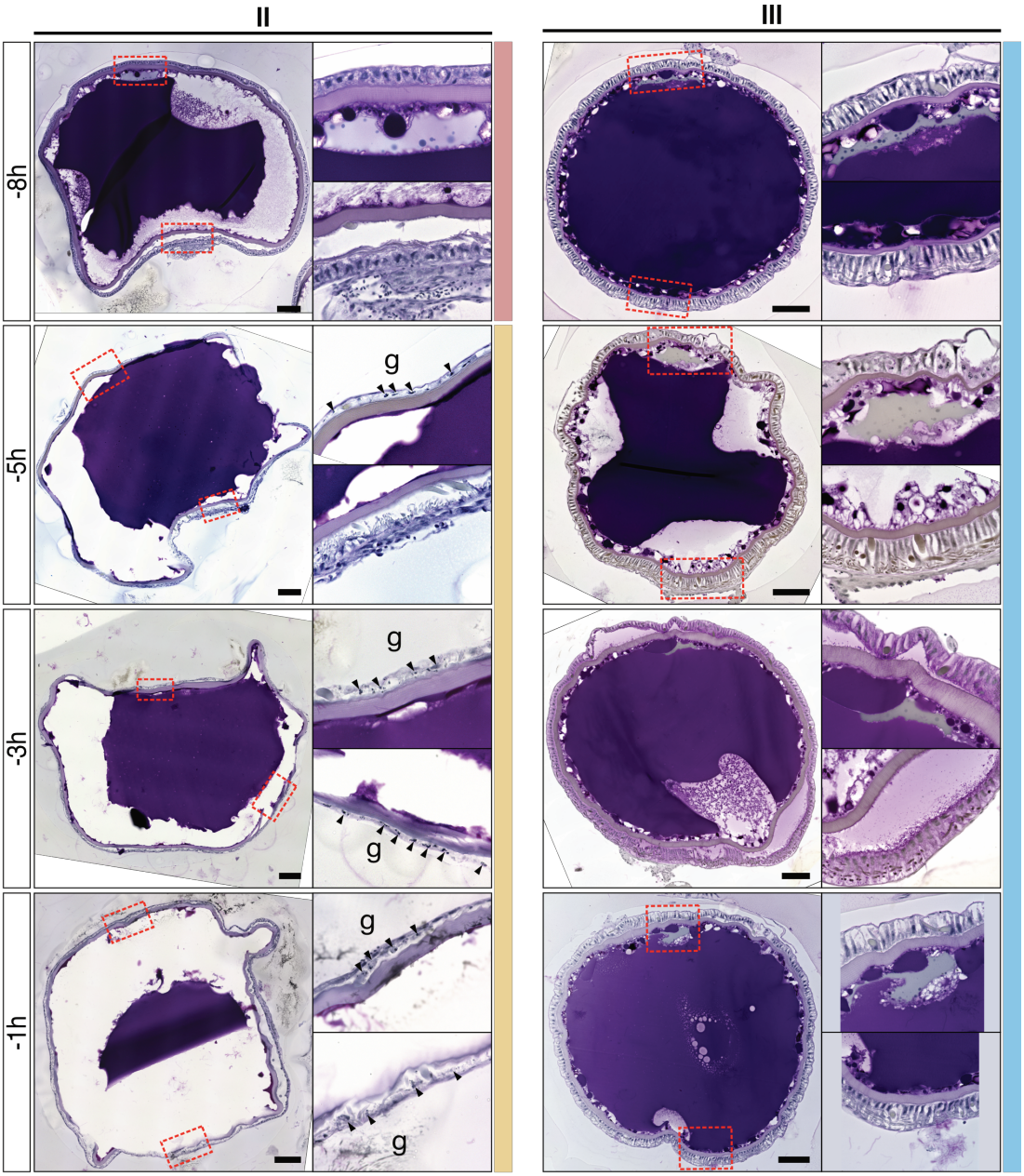

Figure B.5 Morphological changes in granulose cells of mutant follicles during maturation stage

Histological sections of homozygous mutant follicles isolated at 10 different time points. Insets show a magnify view of the red lines box in follicles cross sections. Scale bar, 100 µmm, 50µm (insets).

APPENDIX C. Chapter 3 Supplementary Materials

Table C.1 Mapping summary of RNAseq reads

Genotype	Total raw reads (single)	Unpaired-reads (%)	Total single mapped-reads/ Overal alignment rate	Single-reads; aligned exactly 1 time	Single-reads; aligned >1 times	Unmapped single reads
(wt)_-3h_rep1	12 349 691	100	11 594 709 (93.89%)	10 766 307 (87.18%)	828 402 (6.71%)	754 982 (6.11%)
(wt)_-3h_rep2	11 062 706	100	10 391 741 (93.93%)	9 599 746 (86.78%)	791 995 (7.16%)	670 965 (6.07%)
(wt)_-3h_rep3	9 844 458	100	9 210 461 (93.56%)	8 500 463 (86.35%)	709 998 (7.21%)	633 997 (6.44%)
(-/-)_-3h_rep1	12 050 138	100	11 177 238 (92.76%)	10 524 647 (87.34%)	652 591 (5.42%)	872 900 (7.24%)
(-/-)_-3h_rep2	10 190 267	100	9 537 285 (93.59%)	8 945 351 (87.78%)	591 934 (5.81%)	652 982 (6.41%)
(-/-)_-3h_rep3	12 311 477	100	11 535 702 (93.70%)	10 922 304 (88.72%)	613 398 (4.98%)	775 775 (6.30%)
(wt)_-23h_rep1	10 879 964	100	10 137 698 (93.18%)	9 614 802 (88.37%)	522 896 (4.81%)	742 266 (6.82%)
(wt)_-23h_rep2	22 755 642	100	21 280 665 (93.52%)	20 268 506 (89.07%)	1 012 159 (4.45%)	1 474 977 (6.48%)
(wt)_-23h_rep3	7 127 445	100	6 678 780 (93.71%)	6 339 813 (88.95%)	338 967 (4.76%)	448 665 (6.29%)
(-/-)_-23h_rep1	12 022 965	100	11 204 788 (93.19%)	10 613 874 (88.28%)	590 914 (4.91%)	818 177 (6.81%)
(-/-)_-23h_rep2	9 933 483	100	9 331 758 (93.94%)	8 831 049 (88.90%)	500 709 (5.04%)	601 725 (6.06%)
(-/-)_-23h_rep3	14 668 757	100	13 774 708 (93.91%)	13 025 840 (88.80%)	748 868 (5.11%)	894 049 (6.09%)

Total raw reads (MT1-12):	**145 196 993**
Total single mapped-reads:	**135 855 533**
Overal alignment rate:	**93.57%**

REFERENCES

Adolfi MC, Fischer P, Herpin A, Regensburger M, Kikuchi M, et al. Increase of cortisol levels after temperature stress activates *dmrt1a* causing female-to-male sex reversal and reduced germ cell number in medaka. *Mol. Reprod. Dev.* **86(10)**: 1405-1417 (2019)

Aedo J, Zuloaga R, Aravena-canales D, Molina A, Valdés A. Role of glucocorticoid and mineralocorticoid receptors in rainbow trout (*Oncorhynchus mykiss*) skeletal muscle: A transcriptomic perspective of cortisol action. *Front. Physiol.* **13:** 1048008 (2022)

Aflatounian A, Edwards M, Rodriguez Paris V, Bertoldo M, Desai R, et al. Androgen signaling pathway driving reproductive and metabolic phenotypes in a PCOS mouse model. *Journal of Endocrinology.* **245(3):** 381-395 (2020)

Aluru N, Vijayan M. Stress transcriptomics in fish: a role for genomic cortisol signaling. *Gen. Comp. Endocrinol.* **164 (2-3):** 142-150 (2009)

Araújo RS, Mendonca BB, Barbosa AS, Lin CJ, Marcondes JA, et al. Microconversion between CYP21A2 and CYP21A1P promoter regions causes the nonclassical form of 21-hydroxylase deficiency. *J. Clin. Endocrinol. Metab.* **92:** 4028-34 (2007)

Arterbery A, Fergus D, Fogarty E, Mayberry J, Deitcher D, et al. Evolution of ligand specifity in vertebrate corticosteroid receptors. *BMC Evol. Biol.* **11(14):** 1-15 (2011)

Auer M, Nordenström A, Lajic S, Reisch N. Congenital adrenal hyperplasia. *Lancet*. **401**, 227-44 (2023)

Awaji M, Hanyu I. Annual reproductive cycle of the wild type medaka. *Nippon Suisan Gakkaishi* **53(6):** 959-965 (1987)

Eachus H, Zaucker A, Oakes JA, Griffin A, Weger M, et al. Genetic Disruption of 21-Hydroxylase in Zebrafish Causes Interrenal Hyperplasia. *Endocrinology.* **158:** 4165-4173 (2017)

Engels M, Gehrmann K, Falhammar H, Webb E, Nordenström A, et al. Gonadal function in adult male patients with congenital adrenal hyperplasia. *Eur. J. Endocrinol.* **178(3): 285-294** (2018)

Faught E, Vijayan, MM. Maternal stress and fish reproduction: The role of cortisol revisited. *Fish and Fisheries* **19:** 1016-1030 (2018)

Fukami M, Homma K, Hasegawa T, Ogata T. Backdoor pathway for dihydrotestosterone biosynthesis: implications for normal and abnormal human sex development. *Dev. Dyn.* **242(4):** 320-329 (2013)

Ge S, Son E, Yao R. iDEP: an integrated web application for differential expression and pathway analysis of RNA-Seq data. *BMC Bioinformatics* **19:** 1-24 (2018)

Gennotte V, Sawadogo P, Milla S, Kestemont P, Mélard C, et al. Cortisol is responsible for positive and negative effects in the ovarian maturation induced by the exposure to acute stressors in Nile tilapia, *Oreochromis niloticus*. *Fish Physiol. Biochem.* **38**: 1619–1626 (2012)

Ghayee H, Auchus R. Basic concepts and recent developments in human steroid hormone biosynthesis. *Rev. Endocr. Metab. Disord*. **8:** 289-300 (2007)

Gotoh H, Kusakabe M, Shiroishi T, Moriwaki K. Survival of steroid 21-hydroxylase-deficient mice without endogenous corticosteroids after neonatal treatment and genetic rescue by transgenesis as a model system for treatment of congenital adrenal hyperplasia in humans. *Endocrinology.* **135(4):** 1470-6 (1994)

Greenwood A, Butler P, White R, DeMarco U, Pearce D, et al. Multiple corticosteroid receptors in a teleost fish: distinct sequences, expression patterns, and transcriptional activities. *Endocrinology* **144(10):** 4226-4236 (2003)

Han S, Baba T, Yanai S, Byun DJ, Morohashi KI, Kim JH, Choi MH. GC-MS-based metabolic signatures reveal comparative steroidogenic pathways between fetal and adult mouse testes. *Andrology*. **9**: 400-406 (2020)

Hayasaka O, Takeuchi Y, Shiozaki K, Anraku K, Kotani T. Green-light irradiation during sex differentiation induces female-to-male sex reversal in the medaka *Oryzias latipes*. *Sci. rep.* **9:** 2383 (2019)

Hillier S, Whitelaw P, Smyth C. Follicular oestrogen synthesis: the "two-cell, two-gonadotropin" model revisited. *Mol. Cell Endocrinol.* **100:** 51-54 (1994)

Hirose, K. Biological study on ovulation in vitro of fish - VI effects of metopirone (SU4885) on Salmon gonadotropin - and cortisol-induced in vitro ovulation in *oryzias latipes*. *Bulletin of the Japanese Society of Scientific Fisheries*, **39**: 765–769. (1973)

Hornstein SR, Tajima T, Eisenhofer G, Haidan A, Aguilera G. Adrenomedullary function is severely impaired in 21-hydroxylase-deficient mice. *FASEB J.* **13(10):** 1185-94 (1999)

Iwamatsu T, Ohta T, Oshima E, Sakai N. Oogenesis in the medaka *Oryzias latipes* – stages of oocyte development. *Zool. Sci.* **5:** 353-373 (1988)

Kikuchi M, Nishimura T, Ishishita S, Matsuda Y, Tanaka M. *foxl3*, a sexual switch in germ cells, initiates two independent molecular pathways for commitment to oogenesis in medaka. *Proc. Natl. Acad. Sci. USA* **117(22):** 12174-12181 (2020)

Lee C, Kim JH, Moon SJ, Shim J, Kim HI, Choi MH. Selective LC-MRM/SIM-MS based profiling of adrenal steroids reveals metabolic signatures of 17α-hydroxylase deficiency. *J. Steroid. Biochem. Mol. Biol.* **198**, 105615 (2020)

Liang X, Potter J, Kumar S, Zou Y, Quintanilla R, et al. Rapid and highly efficient mammalian cell engineering via Cas9 protein transfection. *J. Biotechnology.* **208**: 44-53 (2015)

McCormick S. Endocrine control of osmoregulation in teleost fish. *Amer. Zool.* **41:** 781-794 (2001)

Merke D, Auchus R. Congenital adrenal hyperplasia due to 21-hydroxylase deficiency. *N. Engl. J. Med.* **383:** 1248-61 (2020)

Miller W. Mechanisms in endocrinology: Rare defects in adrenal steroidogenesis. *Eur. J. Endocrinol.* **179(3):** R125-R141 (2018)

Milla S, Jalabert B, Rime H, Prunet P, Bobe J. Hydration of rainbow trout oocyte during meiotic maturation and in vitro regulation by 17,20{beta}-dihydroxy-4-pregnen-3-one and cortisol. *J. Exp. Biol.* **209**: 1147–1156 (2006)

Mommsen TP, Vijayan MM, Moon TW. Cortisol in teleosts: dynamics, mechanisms of action, and metabolic regulation. *Rev. Fish. Biol. Fish*. **9:** 211-268 (1999)

Mullins L, Peter A, Wrobel N, McNeilly J, McNeilly A, et al. Cyp11b1 null mouse, a model of congenital adrenal hyperplasia. *JBC* **284(6):** 3925-3934 (2009)

Murata K, Kinoshita M, Naruse K, Tanaka M, Kamei Y (Eds). Medaka: Biology, Management, and Experimental Protocols. 2nd ed, Wiley-Blackwell, Hoboken, USA. (2020)

Nagahama Y, Yamashita M. Regulation of oocyte maturation in fish. *DGD* **50**: S195–S219 (2008)

Nesan D, Vijayan M. Role of glucocorticoid in developmental programming: evidence from zebrafish. *Gen. Comp. Endocrinol.* **181:** 35-44 (2013)

Nesan D, Vijayan M. Maternal cortisol mediates hypothalamus-pituitary-interrenal axis development in zebrafish. *Sci. Rep.* **6:** 22582 (2016)

Nishimura T, Sato T, Yamamoto Y, Watakabe I, Ohkawa Y, et al. *foxl3* is a germ cell intrinsic factor involved in sperm-egg fate decision in medaka. *Science* **349(6245):** 328-31 (2015)

Nishimura T, Yamada K, Fujimori C, Kikuchi M, Kawasaki T, et al. Germ cells in the teleost fish medaka have an inherent feminizing effect. *PLoS Genet.* **14:** e1007259 (2018)

Ogiwara K, Fujimori C, Rajapakse S, Takahashi T. Characterization of luteinizing hormone and luteinizing hormone receptor and their indispensable role in the ovulatory process of the medaka. *PLoS One* **8(1):** e54482 (2013)

Pallan P, Nagy L, Lei L, Gonzalez E, Kramlinger V et al. Structural and kinetic basis of steroid 17α,20-lyase activity in teleost fish cytochrome P450 17a1 and its absence in cytochrome P450 17a2. *J. Biol. Chem.* **290(6):** 3248-3268 (2015)

Papadakis G, Kandaraki E, Tseniklidi E, Papalou O, Diamanti-Kandarakis E. Polycystic ovary síndrome and NC-CAH: distinct characteristics and common findings. A systematic review. *Front. Endocrinol.* **10:** 388 (2019)

Pignatelli D, Pereira S and Pasquali R. Androgens in congenital adrenal hyperplasia. In Hyperandrogenism in women: beyond polycystic ovary syndrome. *Frontiers of hormone research.* **53:** 65-76 (2019)

Quintero-Hunter I, Grier H, Muscato M. Enhancement of histological detail using metanil yellow as counterstain in periodic acid Schiff's hematoxylin staining of glycol methacrylate tissue sections. *Biotech. Histochem.* **66:** 169-172 (1991)

Rahmad Royan M, Siddique K, Csucs G, Puchades M, Nourizadeh-Lillabadi R, et al. 3D atlas of the pituitary gland of the model fish medaka (*Oryzias latipes*). *Front. Endocrinol.* **12**: 719843 (2021)

Reichman D, White P, New M, Rosenwaks Z. Fertility in patients with congenital adrenal hyperplasia. *Fertil. Steril.* **101(2):** 301-309 (2014)

Reisch N, Taylor A, Nogueira E, Asby D, Dhir V, et al. Alternative pathway androgen biosynthesis and human fetal female virilization. *Proc. Natl. Acad. Sci. USA* **116(44):** 22294-22299 (2019)

Riepe FG, Tatzel S, Sippell WG, Pleiss J, Krone N. Congenital adrenal hyperplasia: the molecular basis of 21-hydroxylase deficiency in H-2(aw18) mice. *Endocrinology.* **146:** 2563-74 (2005)

Russell G, Lightman S. The human stress response. *Nat. Rev. Endocrinol.* **15(9):** 525-534 (2019)

Sasagawa Y, Nikaido I, Hayashi T, Danno H, Uno K. Quartz-Seq: a highly reproducible and sensitive single-cell RNA sequencing method, reveals non-genetic gene-expression heterogeneity. *Genome Biol.* **14:** 3097 (2013)

Sakamoto T, Kozaka T, Takahashi A, Kawauchi H, Ando M. Medaka (*Oryzias latipes*) as a model for hypoosmoregulation of euryhaline fihes. *Aquaculture.* **193(3-4):** 347-354 (2001)

Simonetti L, Bruque CD, Fernández CS, Benavides-Mori B, Delea M, et al. CYP21A2 mutation update: Comprehensive analysis of databases and published genetic variants. *Hum. Mutat.* **39(1):** 5-22 (2018)

Shi S, Shu T, Li X, Lou Q, Jin X, et al. Characterization of the interrenal gland and sexual traits development in *cyp17a2*-deficient zebrafish. *Front. Endocrinol.* **13:** 910639 (2022)

Speiser PW, Arlt W, Auchus RJ, Baskin LS, Conway GS, et al. Congenital Adrenal Hyperplasia Due to Steroid 21-Hydroxylase Deficiency: An Endocrine Society Clinical Practice Guideline. *J. Clin. Endocrinol. Metab.* **103**: 4043-4088 (2018)

Stemmer M, Thumberger T, del Sol Keyer M, Wittbrodt J, Mateo JL. CCTop: an intuitive, flexible and reliable CRISPR/Cas9 target prediction tool. *PLoS ONE*. **10(4)**: e0124633 (2015)

Storbeck KH, Schiffer L, Baranowski E, Chortis V, Prete A, et al. Steroid metabolome analysis in disorders of adrenal steroid biosynthesis and metabolism. *Endocr. Rev.* **40(6):** 1605-1625 (2019)

Sun L, Xu W, He J, Yin Z. In vivo alternative assessment of the chemicals that interfere with anterior pituitary POMC expression and interrenal steroidogenesis in POMC: EGFP transgenic zebrafish. *Toxicol. Appl. Pharmacol.* **248:** 217-25 (2010)

Takahashi A, Kanda S, Abe T, Oka Y. Evolution of the hypothalamic-pituitary-gonadal axis regulation in vertebrates revealed by knockout medaka. *Endocrinology.* **157(10):** 3994-4002 (2016)

Tagawa M, Suzuki K, Specker J. Incorporation and metabolism of cortisol in oocytes of tilapia (*Oreochromis mossambicus*). *J. Exp. Zool.* **287:** 485-492 (2000)

To TT, Hahner S, Nica G, Rohr KB, Hammerschmidt M, et al. Pituitary-interrenal interaction in zebrafish interrenal organ development. *Mol. Endocrinol.* **21:** 472-85 (2007)

Trayer V, Hwang PP, Prunet P, Thermes V. Assessment of the role of cortisol and corticosteroid receptors in epidermal ionocyte development in the medaka (*Oryzias latipes*) embryos. *Gen. Comp. Endocrinol*. **194:** 152-161 (2013)

White PC, Speiser PW. Congenital adrenal hyperplasia due to 21-hydroxylase deficiency. *Endrocr. Rev.* **21(3)**: 245-91 (2000)

Xiao H, Xu Z, Zhu X, Wang J, Zheng Q, et al. Cortisol safeguards oogenesis by promoting folicular cell survival. *Sci. China Life Sci.* **65(8):** 1563-1577 (2022)

Yogi A, Kashimada K. Current and future perspectives on clinical management of classic 21-hydroxylase deficiency. *Endocr. J.* **10:** 945-957 (2023)

Zhao B, Lei L, Kagawa N, Sundaramoorthy M, Banerjee S, et al. Three-dimensional structure of steroid 21-hydroxylase (cytochrome P450 21A2) with two substrates reveals locations of disease-associated variants. *J. Biol. Chem.* **287:** 10613-10622 (2012)

Zhou LY, Wang DS, Shibata Y, Paul-Prasanth B, Suzuki A, Nagahama Y. Characterization, expression and transcriptional regulation of P450c17-I and –II in the medaka, *Oryzias latipes. Biochem. Biophys. Res. Commun.* **320**: 83-89 (2007)